EXPLORING HOW ANTIBIOTICS IMPAIR ANTIFUNGAL IMMUNITY

by

Ebrima Bojang

A thesis submitted to the University of Birmingham for the degree of
DOCTOR OF PHILOSOPHY

Institute of Microbiology and Infection
School of Biosciences
College of Life and Environmental Sciences
University of Birmingham
November 2023

ABSTRACT

Prolonged antibiotic use is a controllable risk factor for systemic candidiasis. In recent years, antibiotics have been shown to have off-target detrimental effects on immune cells, but whether antibiotics disrupt antifungal immunity is unknown. Drummond and colleagues recently found that the antibiotic vancomycin enhanced mortality from invasive candidiasis in mice, whereas other antibiotics (e.g., metronidazole) did not affect susceptibility. To examine the mechanisms by which vancomycin impairs anti-*Candida* immunity, I explored how vancomycin pre-treatment of bone-marrow derived macrophages (BMDMs) impacted their responses to *C. albicans* challenge. Vancomycin-treated macrophages had reduced fungal killing, although phagocytosis of yeast cells was unaffected. Instead, vancomycin causes macrophage mitochondrial dysfunction which is accompanied with increased reactive oxygen species (ROS) production. ROS seemingly contributes to early inflammasome priming thus accelerating inflammasome activation and pyroptosis during *C. albicans* infections. Early inflammasome activation and pyroptosis potentially causes macrophages to have reduced time to exert all their antifungal properties on *C. albicans* thus causing reduced killing. Taken together, these results improve our understanding of the pathways regulating antifungal immunity in macrophages and suggest that antibiotic-induced susceptibility to *C. albicans* may be partly driven by disrupted macrophage function.

ACKNOWLEDGEMENTS

Completing a PhD at any time must be challenging but completing it while dealing with a global pandemic and a change of laboratory has made this PhD an enriching journey that has brought out the resilience in me. Personally, I welcomed my second child into this world during this period and this has made the journey both challenging and exciting in equal measure.

I would like to thank my supervisors, Rebecca Drummond, Rebecca Hall, and Robin May for their unwavering support throughout this journey – this would not have been possible without you guys by my side, and I am truly grateful for that. Thank you to everyone past and present in the Drummond and Hall labs for contributing to a positive, friendly, and supportive environment. Special thanks also go to David Bending, Sarah Dimeloe and Kendle Maslowski for their support and guidance during laboratory meetings. Thank you also to everyone involved with the Wellcome Trust MIDAS programme, for funding my PhD and making sure I have an enriching experience throughout. It has been a real privilege working and interact with everyone there.

Thank you to my wife, Bakoto, for everything she does for me to make this journey successful. Thank you for taking care of the kids single-handedly at times while I stay late in the lab to do my experiments. You are my rock, and this would not have been possible without your unconditional love and support. Thank you to my boys, Ibrahim, and Muhammed. Their warm welcome every time I get home makes me immediately forget my stress and fatigue. I am forever grateful to God for these two.

Thank you to all my six siblings for always believing in me and for their kind words and unwavering support. Words cannot express how much I love you all.

Special thanks go to Mum and my late Dad, from whom I learnt the value of education. Mum dropped out of school at a young age and that has been her biggest regret. As your only child to get a university degree, I remember how proud you were back then, and I hope this one makes you even prouder.

TABLE OF CONTENTS

List of Figures

List of Tables

List of Abbreviations

AID Acquired Immune Deficiency Syndrome

AIRE autoimmune regulator gene

ALS agglutinin like sequence

APECED autoimmune polyendocrinopathy-candidiasis-ectodermal dystrophy

ANOVA analysis of variance

ATP adenosine triphosphate

CA^{2+} calcium ion

CARD9 caspase recruitment domain-containing protein 9

CLR C-type lectin receptors

CR complement receptor

DEG(s) differentially expressed gene(s)

DMEM Dulbecco's Modified Eagle Medium

DNA deoxyribonucleic acid

Ece extent of cell elongation

Egfr epithelial growth factor receptor

GI gastrointestinal

HIV Human immunodeficiency Virus

IFN-γ interferon-γ

IL interleukin

ITAM	immunoreceptor tyrosine-based activation motif
KEGG	Kyoto Encyclopaedia of Genes and Genomes
LPS	lipopolysaccharide
MFI	mean fluorescent intensity
MRSA	methicillin-resistant *Staphylococcus aureus*
OPC	Oropharyngeal candidiasis
Padj	adjusted P-value
PAMP(s)	pathogen associated molecular pattern(s)
PFA	Paraformaldehyde
PCR	polymerase chain reaction
PCA	principal component analysis
PKC	protein kinase C
PRR	pattern recognition receptor
RHE	reconstituted human epithelium
RNA	ribonucleic acid
RNA-Seq	ribonucleic acid sequencing
ROS	reactive oxygen species
Rpm	revolutions per minute
RPMI	Roswell Park Memorial Institute Medium
SAP(s)	secreted aspartyl proteinase(s)
SEM	standard error of the mean
SOD(s)	Superoxide dismutase(s)
Syk	spleen tyrosine kinase
TCA	tricarboxylic acid cycle

TLR toll-like receptor

VVC vulvovaginal candidiasis

YPD yeast extract peptone dextrose

1 INTRODUCTION

Parts of this chapter have been previously published:

Bojang E, Ghuman H, Kumwenda P, Hall RA. Immune Sensing of *Candida albicans*. J Fungi (Basel). 2021 Feb 6;7(2):119. doi: 10.3390/jof7020119. PMID: 33562068; PMCID: PMC7914548.

1.1 FUNGAL INFECTIONS

The kingdom of fungi comprises of millions of species but only a few are implicated in human infections, with the most common being *C. albicans*, *Cryptococcus neoformans* and *Aspergillus fumigatus* [Fig. 1.1] (Lionakis et al., 2023, Strickland and Shi, 2021). Fungal infections cause significant morbidity and more than 1 million deaths per annum worldwide (Lionakis et al., 2023, Strickland and Shi, 2021). Fungal infections are prevalent in immunodeficient patients such as patients with HIV/AIDS, however, in recent years there has been a global increase in the number of vulnerable patients. These includes patients receiving transplantations of either solid organ or haematopoietic stem cells, and patients that received myeloablative chemotherapy (Lionakis et al., 2023). The filamentous mould *Aspergillus fumigatus* causes a range of infections including allergic bronchopulmonary aspergillosis, which is an allergic reaction due to colonisation of *A. fumigatus* in the lung and affects approximately 10% of people with cystic fibrosis (Poore et al., 2021) as well as pulmonary and disseminated aspergillosis (Lionakis et al., 2023, Poore et al., 2021, Düesberg et al., 2020). *Cryptococcus neoformans* is the most prevalent *Cryptococcus species* in human disease. It exists as a yeast and causes several infections including pneumonia, disseminated cryptococcosis and is associated to high mortality rates in HIV/AIDS patients when it causes cryptococcal meningitis (Lionakis et al., 2023, Köhler et al., 2017). Furthermore, *Pneumocystis jirovecii* is another human pathogen that exists as cysts and trophozoites that cause pneumonia and disseminated infections mainly in HIV/AIDS patients and patients on corticosteroids (Lionakis et al., 2023). Together these opportunistic pathogens pose significant global infection burden in immunocompromised populations.

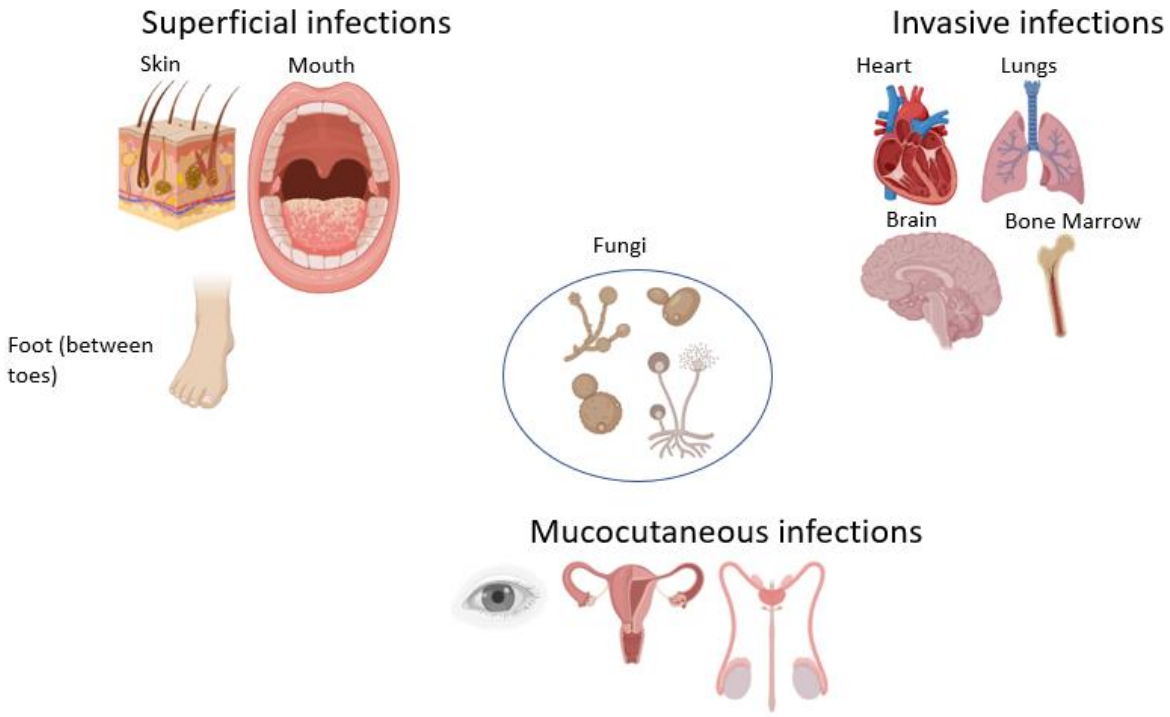

Figure 1.1. **Fungal Infections.** Fungi can infect almost every tissue and organ in the human body. This is a cartoon of the main infection sites and the fungi mostly associated with human infections

1.2 CANDIDA ALBICANS INFECTIONS IN HUMANS

The infections caused by *Candida* species are collectively called candidiasis. They are the most common causes of fungal infections and although at least 36 (Table 1) of these have been implicated in human disease about 90% of candidiasis are caused by only 5 species: *C. albicans, C. glabrata, C. krusei, C. parapsilosis* and *C. tropicalis* (Turner and Butler, 2014, Lionakis et al., 2023, Pappas et al., 2018, Pfaller et al., 2010). Recently, there has been a global emergence of a multidrug-resistant species, called *C. auris,* which can cause hospital outbreaks (Lionakis et al., 2023, Maione et al., 2022).

Table 1.1. Distribution of *Candida species* over a 10-year period in 142 sites in 41 countries.

Species	**Distribution in Candidiasis (% of total) (Pfaller et al., 2010)**
C. albicans	65.3
C. glabrata	11.3
C. tropicalis	7.2
C. parapsilosis	6.0
C. krusei	2.4
C. guilliermondii	0.7
C. lusitaniae	0.6
C. kefyr	0.5
C. famata	0.3
C. inconspicua	0.2
C. rugosa	0.2
C. dubliniensis	0.1
C. norvegensis	0.1
C. lipolytica	0.05
C. sake	0.03
C. pelliculosa	0.03
C. zeylanoides	0.03
C. apicola	0.02
C. valida	<0.01
C. intermedia	<0.01
C. pulcherrima	<0.01
C. haemulonii (pansusceptible)	<0.01
C. stellatoidea	<0.01
C. utilis	<0.01
C. humicola	<0.01
C. lambica	<0.01
C. ciferrii	<0.01
C. collicolosa	<0.01
C. holmii	<0.01
C. marina	<0.01
C. sphaerica	<0.01
C. spp	4.8
C. magnoliae	*ND*
C. orthopsilosis	*ND*
C. paratropicalis	*ND*
C. pseudotropicalis	*ND*
C. auris	*ND*

For fungi to infect humans, they must possess certain attributes including (i) ability to grow at or above 37 °C (ii) being able to breach host physical barriers, (iii) digest and absorb host tissues and (iv) evade and/or withstand immune responses (Lopes and Lionakis, 2022, Köhler et al., 2017). Most fungal infections are opportunistic infections, but these infections are on the rise since the turn of the twentieth century. This increase is attributed to many factors that often result in immunosuppression

in individuals and could be infection related (i.e. HIV/AIDS), medical interventions or inherent disorders of the immune system (Lionakis et al., 2023, Limper et al., 2017). Advances in medical interventions have improved the prognosis of many diseases such as cancers and organ failures but these interventions often require procedures that are immunosuppressive and/or cause dysbiosis of host microbiota. Also, patients with inborn immune defects such as caspase recruitment domain-containing protein 9 (CARD9) deficiency have increased susceptibility to candidiasis (Drummond et al., 2015, Drummond et al., 2018, Lionakis et al., 2023, Lopes and Lionakis, 2022). In these patients, *C. albicans* can breach host defences and cause various infections ranging from superficial infections (oral and genital thrush) to invasive disease (systemic candidemia). Superficial infections pose high morbidity rates, are expensive to treat and affect quality of life but they are not life-threatening (Lionakis et al., 2023). Contrarily, invasive fungal infections are associated with more than 50% mortality rates in most studies but can be as high as 95% in some patient populations such as bone-marrow transplant patients (Romani, 2004, Lionakis et al., 2023). Unlike bacteria, which are prokaryotes, fungi are eukaryotes and therefore share many biological processes with humans. Although the current antifungals are effective, increased antifungal resistance and the challenges of developing new ones due to the shared biochemistry between human and fungi is a public health concern (Odds et al., 2003). Several strategies are being explored to develop fungal vaccines including the use of cell wall proteins (i.e. ALS3 in *Candida* and Crf1 in *A. fumigatus*) but these developments are complicated by the fact that these infections mostly affect immunocompromised individuals (Medici and Del Poeta, 2015). Targeting of cell wall proteins can also be difficult in polymorphic fungi. For instance, *C. albicans* differentially expresses cell wall pathogen associated molecular patterns (PAMPs) between the yeast and hyphae which acts as a moving target for immune cells (Bojang et al., 2021). Therefore, a vaccine targeting only one cell wall protein might only be effective against a specific morphotype of *C. albicans*.

C. albicans is a polymorphic opportunistic fungal pathogen that colonises up to 70% of the human population and has evolved strategies to survive within the human host as a commensal organism (Lopes and Lionakis, 2022). The host immune cells and resident microbiota help restrict *C. albicans* growth to prevent infection (Koh et al., 2008, Azevedo et al., 2015). *C. albicans* colonises most tissues in the body including the skin, vagina and gastrointestinal (GI) tract. Skin and GI tract colonisation is believed to occur early in life as the child passes through the birth canal, which is colonised by *C. albicans* (Ward et al., 2017).

1.2.1 Superficial infections

C. albicans causes a plethora of superficial mucosal infections which affect the quality of life without being life-threatening. These include infections of the vulvo-vaginal area, mouth, throat, and oesophageal infections as well as skin and nail infections (Kisand et al., 2010).

1.2.1.1 Oropharyngeal candidiasis (OPC)

C. albicans is a commensal of the oral mucosa, but during periods of immune suppression, the balance between commensalism and pathogenesis is lost, leading to *Candida* overgrowth and infection. *C. albicans* is the most common cause of oral candidiasis and accounts for about 60% of infections in dentures in over 60 year olds but up to seven non-*albicans Candida* species including *C. glabrata, C. guillermondii, C, krusei, C. stellatoidea, C. parapsilosis, C. tropicalis* and *C. pseudotropicalis* have also been implicated in this infection (Singh et al., 2014). These infections are commonly associated with biofilm formation, and a host of factors can predispose individuals to oral candidiasis. Some of these factors are local such as the use of dentures, immunosuppressive inhalers, and xerostomia, whereas the factors leading to systemic immunosuppression such as HIV/AIDS, malnutrition,

leukaemia, radiation therapy, diabetes, and broad-spectrum antimicrobials also increase susceptibility to oral candidiasis (Millsop and Fazel, 2016). Limited data exists regarding oral candidiasis, but it is estimated that 20–50% of HIV patients develop oral candidiasis (Ambe et al., 2020, Kirti, 2019). This increased prevalence indicates the importance of $CD4^+$ cells in combating oral colonisation, which is reduced in this patient group. Additionally, mice lacking $CD4^+$ T cells are also highly susceptible to oropharyngeal candidiasis (Farah et al., 2002), which is not the case with other *Candida* infections.

Autoimmune polyendocrinopathy-candidiasis-ectodermal dystrophy (APECED) patients (patients with mutation to the autoimmune regulator gene (AIRE)), also have increased susceptibility to mucocutaneous candidiasis, but in about 10% of cases, rather than this being because of immunodeficiency, OPC is driven by a hyperactive type 1 response (Break et al., 2021). CD4+ and CD8+ T cells in this condition produce excess amounts of interferon-γ (IFN-γ) in the oral mucosa that compromise oral epithelial barrier function thus promoting candidiasis (Break et al., 2021). Majority of APECED patients have autoantibodies against interleukin-17F (IL-17F), IL-17A and IL-22, which are important for mucosal anti-fungal immunity (Kisand et al., 2010). However, it is yet to be determined if these result to defective type 17 and/or local immune responses in mucosal candidiasis. Furthermore, detection of these autoantibodies does not always result to candidiasis and interestingly patients without detectable levels of these autoantibodies still develop chronic mucocutaneous candidiasis (Kisand et al., 2010, Orlova et al., 2017, Puel et al., 2011). Together, these indicate that several factors including both autoimmune induce immunodeficiency and T cell mediated immunopathology contribute to the increased susceptibility to mucosal candidiasis in APECED patients.

Oral candidiasis presents in various forms, but the most common presentations include pseudomembranous (thrush), erythematous, hyperplastic, median rhomboid glossitis, angular cheilitis, and linear gingival erythema (Millsop and Fazel, 2016). Pseudomembranous candidiasis is the most common presentation accounting for more than a third of oral candidiasis (Singh et al., 2014). It presents as a confluent white plaque on the tongue, hard-palate, oral pharynx, soft palate, and buccal mucosa. Although most patients are asymptomatic, others may experience changes in taste perception, bleed easily at affected sites, and experience burning sensation which are caused by fungal overgrowth, epithelial cell desquamation and necrotic tissues (Millsop and Fazel, 2016).

1.2.1.2 Cutaneous (Skin) and Onychomycosis (Nail) Candidiasis

Warm and moist environments promote the expansion of *C. albicans* on the skin, leading to superficial skin infections including nail infections. Consequently, cutaneous candidiasis often occurs in least dry areas such as under the breast, groin (nappy rash), foreskin of uncircumcised penis, between toes (athlete's foot) and armpits (Bojang et al., 2021, Prevention, 2021). Nail infections typically lead to brittle and splitting nails with accompanying brown, white or yellow discolouration. Although general immunosuppression is key for establishing these infections, patients with diabetes, obese people and people on long-term antibiotics, steroids, and chemotherapy are particularly susceptible to these infections (Elewski and Tosti, 2015). *C. albicans* uses hydrolytic enzymes, such as secreted aspartyl proteinases (SAPs), which are important in tissue invasion to establish nail and other superficial infections (Mohammadi et al., 2020, Naglik et al., 2004, Schaller et al., 2005). These infections are potentiated by increased phospholipase activity, which also correlates with biofilm formation, particularly in nail infections (Mohammadi et al., 2020, Schaller et al., 2005).

1.2.1.3 Vaginal candidiasis

Vulvovaginal candidiasis (VVC) is the most common *Candida* infection, infecting 75% of the female population at least once in their lives, and up to 9% of these women will go on to develop recurrent infections (RVVC), defined as three or more episodes in a twelve-month period (Foxman et al., 2013, Denning et al., 2018, Sobel, 2007). Unlike for oral candidiasis, immune suppression is not a prerequisite for infection, and HIV-positive women are not more prone to the development of VVC (White, 1996). Instead, the predisposing factors include vaginal dysbiosis after antimicrobial therapy, elevated oestrogen levels (due to pregnancy, oral contraceptive use, or hormone-replacement therapy) and uncontrolled diabetes (Gonçalves et al., 2016). Genetic polymorphisms such as the codon 54 variant allele in *MBL2* exon 1, carrying a variable number tandem repeat in *NLRP3* gene, polymorphisms to SIGLEC15 and IDO1 and non-synonymous mutation to TLR2, (rs5743704, Pro631His) are also enriched in women with RVVC indicating genetic predisposition (Giraldo et al., 2007, Gonçalves et al., 2016, Hammad et al., 2018, Jaeger et al., 2016, Rosentul et al., 2014, Lionakis et al., 2023). Although neutrophil recruitment is increased in VVC (driven by both *Candida* virulence factors and sex hormones), their anti-*Candida* functions are impaired in the vaginal microenvironment (Salinas-Muñoz et al., 2018, Yano et al., 2017, Yano et al., 2018). This is driven by vaginal heparin sulphate, which competes for binding to complement receptor 3 (CR3) on neutrophils thus impairing their binding to, and killing of, *C. albicans* (Yano et al., 2017, Yano et al., 2018). The accumulated neutrophils are hyper inflammatory manifested by the increased NLRP3 inflammasome activation and increased IL-1β production by these cells (Bruno et al., 2015, Roselletti et al., 2017). Consistently, mice deficient in *Nlrp3*$^{-/-}$ have reduced neutrophils, alarmins and inflammatory cytokines in their vaginal lavage fluid during VVC (Bruno et al., 2015). Also, the main source of carbon within the vaginal microenvironment is lactate (due to the presence of lactobacilli) and *C. albicans* growth in lactate promotes concealment of β-glucan. This will reduce recognition by

innate immune cells and potentially contribute to the reduced killing by neutrophils (Ballou et al., 2016, Ene et al., 2013). Furthermore, growth in oestrogen as experienced in the vaginal environment helps *C. albicans* evade the innate immune system. Oestrogen adapted *C. albicans* recruits more Factor H, which binds to Gpd2 on their cell wall. Factor H inactivates C3b to iC3b thus abolishing its opsonic properties and enhancing *C. albicans* immune evasion (Kumwenda et al., 2022). Together, these indicate that modulating the immunopathology or enhancing immune recognition of *C. albicans* may be the best practice to curb the effects of VVC in susceptible patients.

1.2.2 Invasive/systemic infections

Invasive candidiasis is a serious life-threatening infection that can affect the kidneys, liver, spleen, brain, heart and other organs (Pappas et al., 2018). These infections often lead to death or have significant impact on one's quality of life. Candidemia, which is the bloodstream infection, is very prevalent in hospital settings and is the 3rd or 4th most common hospital acquired invasive infection (Lionakis et al., 2023, Wisplinghoff et al., 2004). Risk factors include prolonged antibiotic use, long stays in intensive care units, immunosuppression and use of central venous catheter (Ricotta et al., 2021) *C. albicans* colonises the GI tract of most individuals and the gut is the major source of most cases of invasive candidiasis (Lopes and Lionakis, 2022). Interventions that perturb gut microbiota play a key role in this phenomenon. For instance, prolonged antibiotic treatment reduces bacterial populations in the gut thus leading to a fungal bloom, which then increases their chances of traversing the gut barrier and causing disseminated infection and candidemia (Drummond et al., 2022, Lopes and Lionakis, 2022). Other interventions, which compromise the gut barrier such as chemotherapy, gastrointestinal surgery, and parenteral nutrition all increase the risk of disseminated candidiasis often starting as candidemia but can infect almost all tissues and organs (Koh et al., 2008, Perlroth et al., 2007). Although hospital acquired invasive candidiasis is also associated with antibiotics use, it is

mostly skin derived with candidaemia developing within 2 days of using a central venous catheter in about 85% of patients in one study (Strollo et al., 2016, Ricotta et al., 2021). Intravenous infection also differs from GI derived candidiasis as it is associated with increased kidney damage (Jae-Chen et al., 2015). Together these invasive syndromes result to death in approximately 50% of cases, which increases with delayed antifungal treatment (Koh et al., 2008, Perlroth et al., 2007). Notably, this mortality rate is significantly higher than other causes of bloodstream infections (Gudlaugsson et al., 2003). Together these make the surveillance of candidiasis very important as early detection is often lifesaving.

1.3 CANDIDA ALBICANS VIRULENCE FACTORS

For successful colonisation and infection, microorganisms must possess certain virulence factors to enable them to adapt to the host microenvironment, avoid host immune surveillance, and breach host barriers when the opportunity arises. Below are some of the virulence factors that make *C. albicans* unique in its ability to infect almost every tissue in the human body.

1.3.1 Cell wall remodelling

The *C. albicans* cell wall is a dynamic organelle composed of polysaccharides organised in a multi-layered structure (Fig. 1.2). It has an innermost layer comprised of chitin and β1-3-glucan and β1-6 glucan, which provides strength and structural support. It also serves to anchor glycosylated mannoproteins that make the outer layer. These proteins play a vital role in adhesion and virulence. All the cell wall components act as PAMPs and are recognised by pattern recognition receptor (PRR) on innate immune cells. For instance, β1,3-glucan, which is the major PAMP of the cell wall is

recognised by Dectin-1 on phagocytic cells and is essential for effective immune responses against *Candida* (Brown and Gordon, 2001, LeibundGut-Landmann et al., 2007). Complement receptor 3 also recognises β1,3-glucan and is especially important in neutrophil recognition (Baert et al., 2015). However, β1,3-glucan is often masked by outer mannan and mannoproteins and thus its exposure is restricted to bud scars at the resting stage, which partly contributes towards *C. albicans* immune evasion.

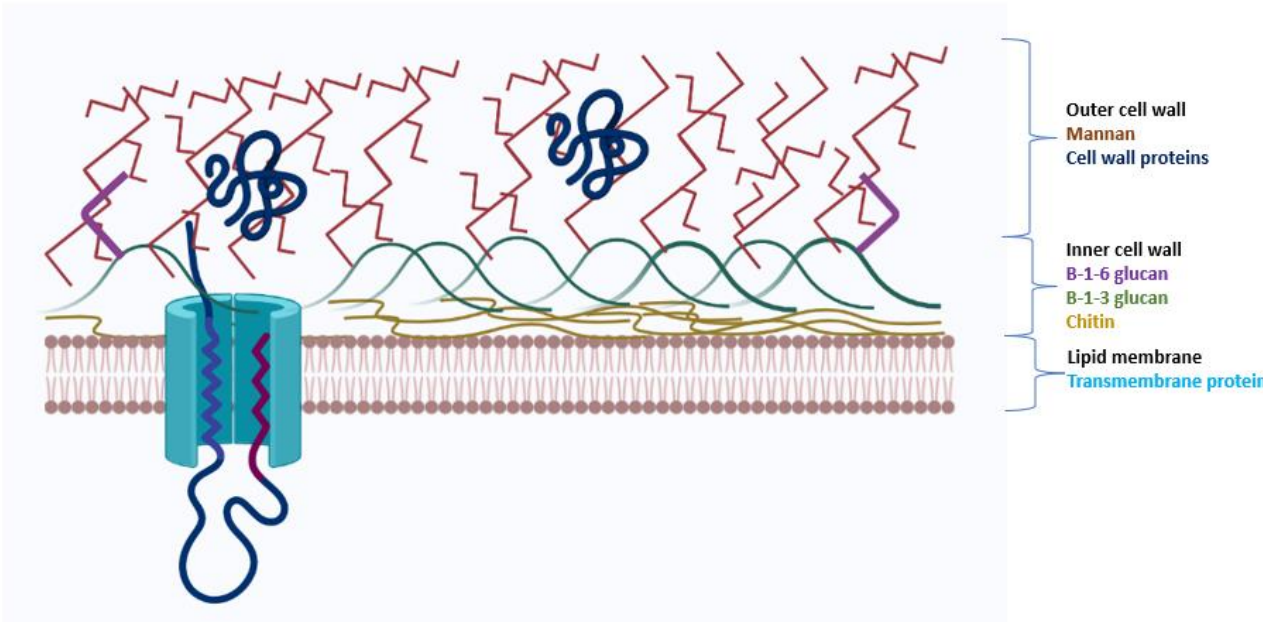

Figure 1.2. **Cartoon of *C. albicans* cell wall structure** adapted from (Gow and Hube, 2012). The cell wall is made up of an innermost and outmost layer. The innermost layer consists of the chitin and β-1-3 and β-1-6 glucan and the outermost layer consists of mannan and cell wall proteins. The cell wall is a dynamic organelle that changes the composition of its components. Growth phase *C. albicans* for example has reduced terminal α1,2-mannose and growth in acidic environments reduces expression of a cell wall chitinase Cht2, which hydrolyses chitin into short fragments to be incorporated into the inner layer of the cell wall. The reduced expression or absence of this chitinase in acidic environments leads to incorporation of long chitin polymers into the cell wall and increased chitin exposure.

Nonetheless, the *C. albicans* cell wall constantly undergoes remodelling to permit adaptation to the host environment. So far, changes in pH, iron levels, carbon source, hypoxia, serum, and use of antifungal agents have all been shown to alter the structure and composition of the cell wall (Ballou

et al., 2016, Hall, 2015, Sherrington et al., 2017). These changes have significant consequences in their interaction with host immune cells during both colonisation and disease as the cell wall is the first point of contact between the fungus and immune cells. Interestingly, cell wall remodelling occurs differentially according to the environmental stimuli with some stimuli promoting increased exposure of certain PAMPs, while others promote masking of these PAMPs (Ballou et al., 2016, Sherrington et al., 2017). For instance, growth in lactate promotes increased β1,3-glucan masking. The vaginal environment is a rich source of lactate, which is the main source of energy during *C. albicans* adaptation during both colonisation and disease. As such, there is increased β1,3-glucan masking and immune evasion in the vagina (Ballou et al., 2016). Conversely, during *C. albicans* growth in acidic conditions, likely encountered within the vaginal mucosa, there is increased exposure of chitin and β-glucan, and the exposed β1,3-glucan invokes a strong pro-inflammatory innate immune response (Sherrington et al., 2017). Additionally, *C. albicans* cell wall chitin and to a lesser extent β1,3-glucan undergo increased exposures within macrophage phagosomes, which may be partly driven by the acidic pH encountered within this compartment (Wagener et al., 2017). This would likely have an impact on subsequent immune responses as *C. albicans* escapes from the phagocytes and disseminate to other tissues.

1.3.2 Morphological switching in *C. albicans*

Aside from exposure of certain cell wall PAMPs, other factors such as the morphology of *C. albicans* influence phagocytosis rates as hyphae can reach lengths that preclude full internalisation thus resulting in frustrated phagocytosis (only partial hyphal engulfment) (Lewis et al., 2012, Maxson et al., 2018). *C. albicans* is a polymorphic organism with the ability to switch reversibly between the yeast and hyphae form during infection, which is essential for its virulence (Fig. 1.3) but other forms

have since been described including pseudohyphae, chlamydospores, grey, opaque, and gastrointestinally induced transition (GUT) cells (Lo et al., 1997, Murad et al., 2001). Several pathways have been characterised in modulating morphological switching in *C. albicans* depending on the stimuli. The Hog1 Mitogen-Activated Protein Kinase pathway (MAPK) drives hyphal formation when activated by osmotic and oxidative stresses through either Sln1 or Sho1 (Noble et al., 2017). The Cek1 MAPK pathway is activated by several stimuli including cell wall damage, low nitrogen, and osmotic stress and drives filamentation by phosphorylating the transcription factor, Cph1 but also this pathway activates mating genes in opaque cells when Cek2 is also phosphorylated (Noble et al., 2017). The protein kinase A (PKA) pathway is involved in both filamentation and white to opaque switching. This signalling cascade can be activated by stimuli including serum, low nitrogen, 37 °C, and CO_2 leading to synthesis of c-AMP downstream of Ras1 signalling. c-AMP then activates Tpk1 and Tpk2, which then phosphorylate enhanced filamentous growth protein 1 (Efg1), a central transcription factor in *C. albicans* morphogenesis, biofilm formation and metabolism (Noble et al., 2017). Similarly, the Rim101 pathway, which is activated by alkaline pH also converges to the Efg1 gene albeit via Dfg1 and Rim21 and the ESCRT complex (ESCRTI and two ESCRTII) (Noble et al., 2017).

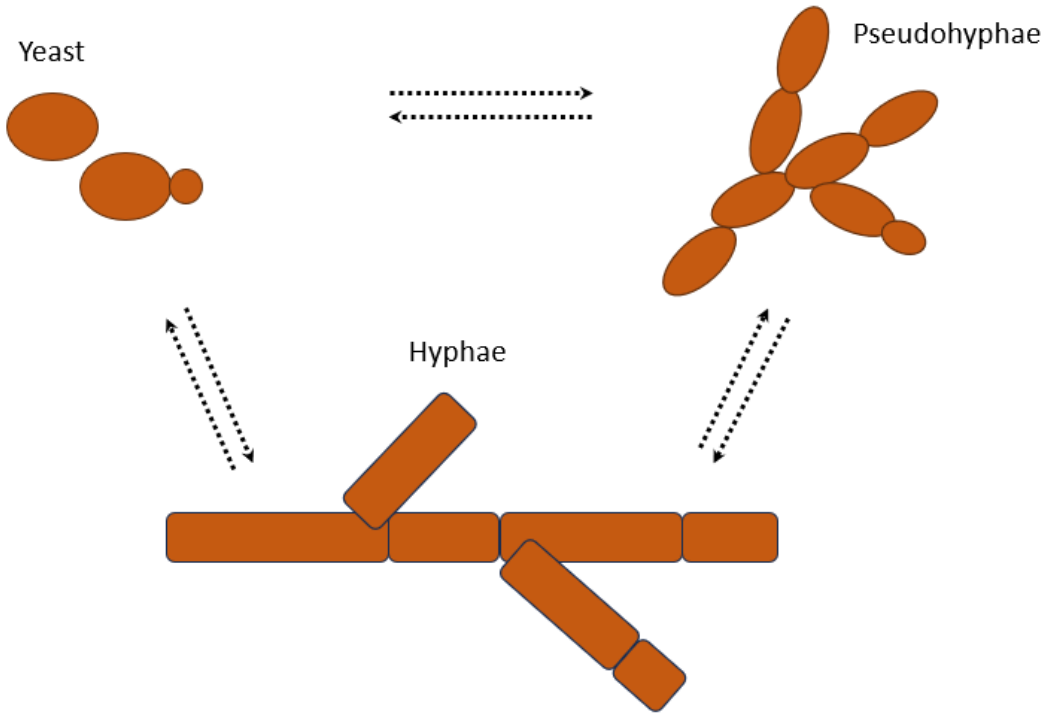

Figure 1.3. ***C. albicans*** **can switch reversibly between yeast, pseudohyphae and hyphae.** Asexual division occurs when new cell material appears on the side of the yeast, continues to grow before the daughter cell separates from the parent by forming a partition (budding). Pseudohyphae are characterised by synchronous unipolar cell division, resulting in chains of elongated yeast cells. True hyphae are tubular cells that are branched and have no narrowing at the site of septation. A new cell material can appear and bud off forming new yeast cells from both pseudohyphae and hyphae and depending on the environmental cues such as temperature, yeast cells can transition into pseudohyphae or hyphae. Importantly the ability to switch between these morphotypes are important for its virulence and dissemination.

Different *C. albicans* morphotypes are important for different stages of infection as yeast cells are more important for dissemination but they lack the ability to invade tissues and are avirulent without filamentation (Lo et al., 1997, Saville et al., 2003). Double mutants of *efg1/efg1 cph1/cph1* do not form hyphae and are avirulent in mouse models of infection (Lo et al., 1997). Similarly, hyphae-locked mutants express diminished virulence (Chow et al., 2021, Mukaremera et al., 2017). Therefore, both are important elements of *C. albicans* pathogenicity. *Candida* cell wall components such as chitin and β-glucan are also differentially exposed in yeast and hyphae therefore resulting to

different immune recognition and response (Talapko et al., 2021, Gow and Hube, 2012). For example, hyphal cells contain higher levels of chitin and the major PAMP, β-glucan but are better at masking these PAMPs at the resting stage to evade immune recognition (Hall, 2015, Staniszewska et al., 2013). *In vivo* mouse models of invasive candidiasis have also shown more functional damage to the kidneys than other organs and intriguingly *C. albicans* hyphae was present in the kidneys but absent in spleen and liver further confirming the importance of hyphae in virulence (Lionakis et al., 2011). Additionally, hyphae are associated with the increased expression of adhesins, invasins, secreted hydrolases, and candidalysin that allow it to attach, invade and damage tissues (Bojang et al., 2021, Talapko et al., 2021, Zhu and Filler, 2010, Moyes et al., 2016).

1.3.3 Adhesins and Invasins

To establish colonisation and tissue invasion, *C. albicans* cells must adhere first to the host epithelium. Consequently, *C. albicans* has evolved several adhesins that mediate adhesion in unique ways and are differentially expressed in yeast and hyphae (Zhu and Filler, 2010). The agglutinin-like sequence (ALS) family is an 8-member family of glycosylphosphatidylinositol (GPI)-linked adhesins that are surface expressed and differ in their binding to host cells. For instance, Als1, Als3, and Als4 bind more cell types (i.e., epithelial cells, and endothelial cells) and host substrates (i.e., gelatin) than other Als proteins (Naglik et al., 2011, Talapko et al., 2021, Zhu and Filler, 2010). Hyphal wall protein 1 (Hwp1) is also a key adhesin that mimics host proteins to adhere covalently to epithelial cell-associated transglutaminases (Ponniah et al., 2007) and plays an important role in biofilm formation by mediating *C. albicans* hypha-hypha interactions through its ability to bind both Als1 and Als3 (Nobile et al., 2008). Interestingly, Als1 is differentially expressed in biofilms compared to planktonic cells (García-Sánchez et al., 2004) and an Als3 double mutant lacked biofilm formation (Nobile et

al., 2006). Other less defined adhesins include enhanced adherence to polystyrene 1 (Eap1) and Iff4 family proteins (Zhu and Filler, 2010).

Furthermore, the ability to invade host tissues is essential for *C. albicans* virulence as mutants with reduced invasive potential (i.e., *rim101*) have reduced virulence (Nobile et al., 2008). Invasion of host tissues is achieved either by active penetration of epithelial cells, hyphal growth through intercellular junctions or passively through endocytosis, which is driven by *C. albicans* invasins (secreted or expressed on hyphae) that interact with epithelial cells to initiate their uptake by epithelial cells (Phan et al., 2007, Zhu and Filler, 2010). Interestingly, adhesin related proteins Als1 and Als3 (hyphae specific proteins) have been shown to act as invasins to drive endocytosis (Hoyer et al., 2008, Phan et al., 2007, Sheppard et al., 2004). Furthermore, Als3 and Ssa1 promotes *C. albicans* hyphal endocytosis by engaging the epithelial growth factor receptor (Egfr) and Her2 (Lopes and Lionakis, 2022).

1.3.4 Secreted effectors

Although mechanical force plays a role in active penetration of epithelial cells and cell junctions, some studies have shown the role of secreted hydrolases in this process (Naglik et al., 2008, Naglik et al., 2011, Schaller et al., 2003, Wächtler et al., 2011). Epithelial invasion is accompanied by E-cadherin degradation in *in-vitro* studies (Zhu et al., 2012, McNulty et al., 2005). Interestingly, HIV-positive patients with OPC also express reduced levels of E-cadherin suggesting that degradation of E-cadherin is essential for invasion (McNulty et al., 2005). It is believed that secreted aspartyl proteinases (SAPs), a family of 10 play a role in degrading E-cadherin (abundant in intraepithelial junctions and required for their integrity) and therefore may be involved in penetration through intracellular junctions (Frank and Hostetter, 2007). *C. albicans* also secretes Sap2, which indirectly

impairs macrophage responses by inactivating complement proteins and factor H, and thus increasing its chances of evading the immune system (Svoboda et al., 2015). SAPs are expressed during infection in a temporal manner, and this is different between infection models. For instance, using a reconstituted human epithelium (RHE) model of candidiasis, *SAP1 and SAP3*, were the first to be upregulated, followed by *SAP6*, and finally *SAP2* and *SAP8* during late infection. Contrarily, a vaginal model of candidiasis induced early expression of *SAP2, SAP9* and *SAP10*, which was followed by *SAP1, SAP4* and *SAP5* before upregulation of *SAP6* and *SAP7* (Naglik et al., 2008, Schaller et al., 2003). In an *in-vivo* vaginitis model in mice, *SAP5* expression was increased early during infection with *SAP4* expression seen in fewer cells late during infection (Naglik et al., 2008, Staib et al., 2000). Ultimately, blocking SAPs with protease inhibitor pepstatin A reduces *C. albicans* epithelial damage *in-vitro* indicating their role in infection (Naglik et al., 2008).

C. albicans possesses other secreted hydrolases such as the lipases, a family of ten that play a role in cellular metabolism and phospholipases such as phospholipase A-D, but there is little evidence as to their role in either active penetration or endocytosis (Hube et al., 2001, Niewerth and Korting, 2001, Dalle et al., 2010, Naglik et al., 2011). Still, reduced host cell penetration was observed in phospholipase 1 mutants (Niewerth and Korting, 2001).

Hyphal formation in *C. albicans* has long been associated with epithelial cell invasion and damage, but in 2016 a *ece1* (extent of cell elongation 1)-deficient strain that can still form hyphae was shown to attach and invade epithelial cells but could not initiate damage, induce danger signals or cytokine secretion (Moyes et al., 2016). This gene is a hyphae specific gene that was confirmed to encode 8 peptides including the first known human fungal cytolytic toxin, candidalysin (Ece1-peptide III) (Moyes et al., 2016). Candidalysin is processed to its mature form through processing of the Ece1

protein by Kex2 and Kex1 proteases into eight peptides (Richardson et al., 2018). The secreted toxin plays a key role in tissue invasion and can cause damage to several cell types including red blood cells by intercalating into membranes, forming pores and calcium influx in a dose dependent manner (Moyes et al., 2016, Richardson et al., 2018, Naglik et al., 2019). Consequently, early during infection, low concentrations of candidalysin trigger immune responses (driving neutrophil recruitment and Th17 immunity) until it reaches a threshold whereby damage to host cells is more prevalent (Moyes et al., 2016, Naglik et al., 2019). In systemic infections, candidalysin aids the recruitment of neutrophils. For instance, in the kidneys, it activates the inflammasome leading to secretion of IL-1β which then helps to recruit neutrophils (Lopes and Lionakis, 2022, Swidergall et al., 2019). In the CNS, candidalysin acts on CARD9+ microglia cells to secrete IL-1β and CXCL1, which are required for recruiting protective CXCR2+ neutrophil (Drummond et al., 2019, Drummond et al., 2015, Lopes and Lionakis, 2022). These indicate the differential roles candidalysin plays in different infection niches.

1.3.5 *Candida* and biofilms.

C. albicans yeast-hyphae transition is also essential for biofilm formation - communities of microbes forming 3D structures surrounded by an extracellular polysaccharide matrix (Tsui et al., 2016). The polysaccharide structures provide protective cover for the microbes from immune cells and antimicrobial therapies making them difficult to treat (Ghannoum et al., 2015, Lewis, 2001, O'Toole et al., 2000). Biofilms can form on both host tissues and abiotic surfaces such as catheters (Ghannoum et al., 2015). Studies performed *in-vitro* to understand biofilm formation suggest four distinct steps; (1) an adherence step whereby yeast cells attach to the surface/substrate to form a basal layer, (2) an initiation step involving the formation of filamentous hyphae, (3) a maturation step whereby an extracellular polysaccharide (mainly of α-mannan, β-1,6 glucan, and β-1,3 glucan) is formed and (4)

the dispersal step, involving the breaking off of mainly yeast cells from these biofilms which can disseminate to the blood and other organs causing life-threatening systemic infections (Finkel and Mitchell, 2011, Hall and Gow, 2013, Mitchell et al., 2015, Uppuluri et al., 2010, Mathé and Van Dijck, 2013). Recently, implanted medical devices and catheters play a key role in medical care, however, this comes with a caveat with up to 60% of these devices getting infected. *Candida* accounts for about 20% of these infections making it a very important microorganism in these settings (Ramage et al., 2006). Unfortunately, these infections are associated with very high mortalities and thus safety measures must be observed to minimise their occurrence (Ramage et al., 2006, Williams and Lewis, 2011).

1.4 SPECIFIC CONTRIBUTION OF INNATE IMMUNE CELLS TO C. ALBICANS CONTROL

Nutritional immunity, phagocytosis and intact physical barriers all play a role in controlling *C. albicans* and preventing infection. Below is a summary of some of the host cells' contribution during *C. albicans* commensalism and disease.

1.4.1 Epithelial cells

C. albicans is a commensal at mucosal sites and epithelial cells serve as the first point of contact during both commensalism and disease (Naglik et al., 2017). Consequently, epithelial cells must recognise when *C. albicans* has become pathogenic and respond accordingly. *C. albicans* has evolved several ways to induce endocytosis but its secretion of candidalysin at high concentrations is what triggers cell damage (Lopes and Lionakis, 2022). Therefore, candidalysin is a major determinant of pathogenicity. Candidalysin intercalates to cell membranes forming pores and calcium influx, which

plays a major role in activating immune responses. Candidalysin also indirectly activates epidermal growth factor receptor (EGFR) through the release of EGFR ligands (i.e., epiregulin and epigen) in a process involving matrix metalloproteinases (MMPs) even though how candidalysin induces cleavage of these ligands by MMPs is not completely understood (Ho et al., 2019). Nonetheless, epiregulin and epigen are part of the ErbB family of surface bound endogenous ligands that can be cleaved to release functional ectodomains that can induce autocrine and paracrine signalling through EGFR {Ho, 2019 #82}. This leads to downstream signalling of MAPK through p38 to activate cFos, which augments immune cell recruitment (i.e., Th17 cells and neutrophils) via chemokine and cytokine secretion (Gaviria et al., 1999, Ho et al., 2019, Liles et al., 1997). EGFR activation also leads to activation of ERK1/2 and MPK1 with the latter regulating epithelial immune cell response via dephosphorylation of p38 (Ho et al., 2019).

Interestingly, endocytosis of *C. albicans* can be achieved via Als3-Her2 interaction, which leads to Als3-Her2-EGFR heterodimerisation, but this does not result to strong immune response via the MAPK signalling pathway. The different strengths in immune responses are further evidence of the central role candidalysin plays in epithelial cell differentiation of commensal and pathogenic *C. albicans* (Ho et al., 2019, Murciano et al., 2012, Zhu et al., 2012, Naglik et al., 2019).

1.4.2 Phagocytes and *C. albicans*

Myeloid cells (i.e., macrophages, neutrophils, and dendritic cells) of the innate immune system play a vital role in immunity against *C. albicans* infections [Fig. 1.4] These cells can recognise, engulf *C. albicans* yeast through phagocytosis and secrete cytokines to recruit other immune cells. Phagocytosis is a multi-step process initiated by pathogen recognition. This leads to the engulfment of the pathogen, phagosome maturation to eliminate the pathogen and then the resolution of the phagolysosome

(Bojang et al., 2021, Canton et al., 2014). Innate immune cells interact differently with the yeast and hyphal morphologies of *C. albicans* as detailed above (Mukaremera et al., 2017). Immune cells recognise *C. albicans* via their PRRs such as Toll-like receptors (TLRs) and C-type lectin receptors (CLRs). CLRs including Dectin-1, Dectin 2 and MINCLE are key to recognising various *C. albicans* PAMPs (Lionakis et al., 2023). Engagement of these CLRs by their corresponding fungal PAMP causes phosphorylation of their immunoreceptor tyrosine-based activation motifs (ITAM) or hemITAM leading to recruitment and activation of spleen tyrosine kinase (Syk). Activation of Syk leads to signalling through the adapter protein CARD9, which forms a complex with B-cell lymphoma/leukaemia 10 (BCL10) and mucosa associated lymphoid tissue (Malt1) and subsequently activates NFκB and ERK leading to innate (i.e. phagocytosis and production of reactive oxygen species (ROS)) and adaptive immune responses and cytokine production (Drummond et al., 2018, Hardison and Brown, 2012, Lionakis and Levitz, 2018, Lopes and Lionakis, 2022). Accordingly, mice deficient in Syk have increased susceptibility to fungal infections and especially systemic candidiasis (Negoro et al., 2020, Whitney et al., 2014). Furthermore, Syk deficient neutrophils have impaired netosis, phagocytosis, neutrophil swarming, cytokine, and ROS production against various *Candida* species (Negoro et al., 2020). Since CARD9 acts downstream of several CLRs and Syk activation, it must be vital for anti-fungal immunity. In fact, it is the only known inherited immunodeficiency in humans that predisposes to fungal infections without having any impact on viral, bacterial, or parasitic infections or even non-infectious sequelae (Glocker et al., 2009, Lopes and Lionakis, 2022, Wang et al., 2018). CARD9 deficiency is also unique in that it increases susceptibility to both mucosal and systemic infections - especially CNS infections (Glocker et al., 2009). Interestingly, neutrophils from CARD9 deficient patients have a selective killing defect for unopsonised *C. albicans* yeast but not the hyphae (Drewniak et al., 2013, Drummond et al., 2015). This is partly explained by the two distinct fungal killing pathways of unopsonised and opsonised

Candida in human neutrophils (Gazendam et al., 2014). Unopsonised *Candida* killing is mediated through the CR3-Syk- phosphatidylinositol-3-kinase (PI3K)- CARD9 signalling pathway, while opsonised *Candida* killing takes place through a CARD9-independent pathway involving Fcγ receptor, protein kinase C (PKC) and ROS (Gazendam et al., 2014). Moreover, CARD9 deficient patients have a high propensity for CNS candidiasis and although opsonisation levels are low in the CNS and therefore may play a role, crucially, neutrophil recruitment is severely impaired in these individuals due to reduced or inefficient upregulation of chemokine production by microglia and glial cells (Drummond et al., 2015, Drummond et al., 2019). Below, the contribution of the different phagocytes in sensing and immune response to *C. albicans* is dissected.

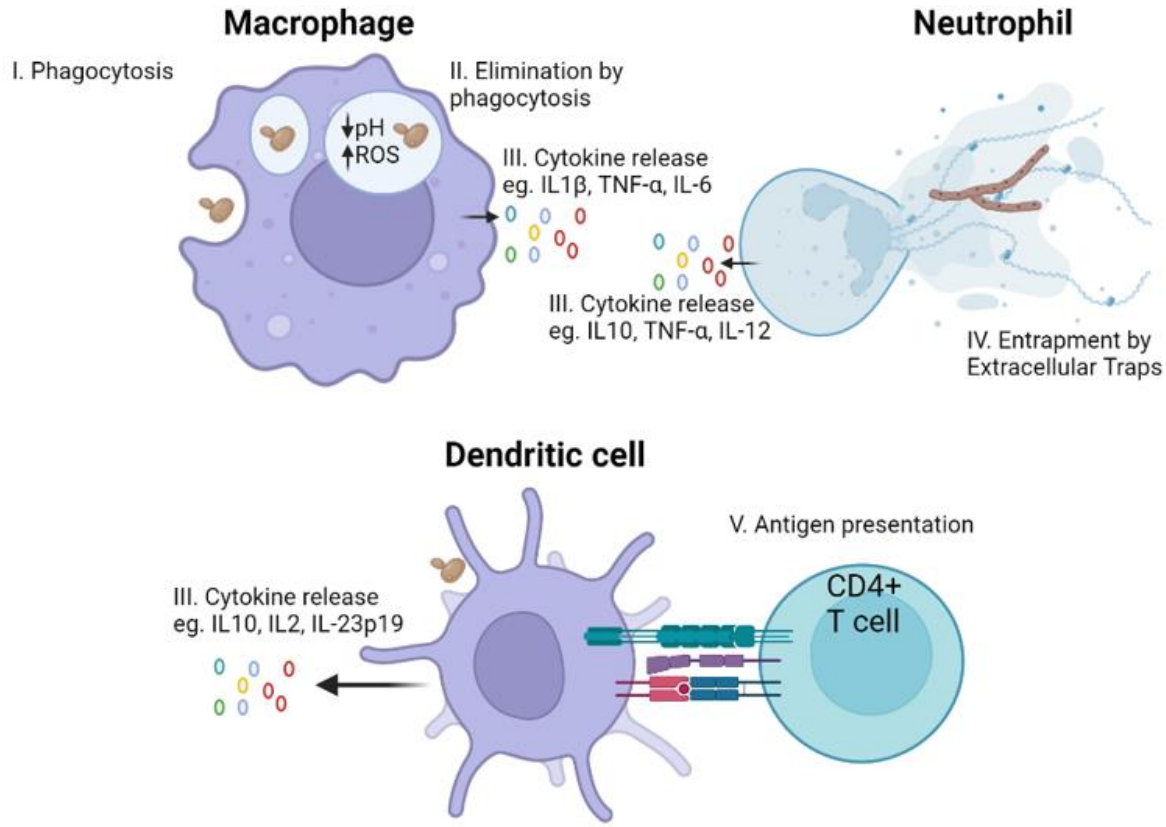

Figure 1.4. **Phagocytic cell responses to *C. albicans*.** Macrophages, neutrophils, and dendritic cells respond differentially to *C. albicans*, and these responses are shaped by the fungal morphotype encountered. Different cytokines are secreted to these immune cells to activate similar or different pathways. Neutrophils respond to hyphae by releasing extracellular traps and dendritic cells have the added responsibility of activating the adaptive immune system.

1.4.2.1 Macrophages

Although macrophages can be derived from recruited monocytes to tissues, long-lived tissue resident macrophages are seeded early after birth and are present for most of the host's life and are often the primary immune cells in these naïve tissues (Austermeier et al., 2020, Gray and Farber, 2022). Several studies have described the contribution of tissue resident macrophages in anti-*Candida* immunity. Intestinal resident CX3CR1+ mononuclear phagocytes are crucial for maintaining gut fungal levels by phagocytosis and induction of T_H17 responses (Leonardi et al., 2018). Furthermore, Kupffer cells, that are resident to the liver prevent *C. albicans* hyphal formation and, together with splenic

macrophages, help to prevent fungal dissemination by eliminating circulating fungi (Qian et al., 1994, Sun et al., 2019). Also, CARD+ microglia, which are resident to the brain are vital for neutrophil recruitment during *C. albicans* meningitis. Detection of candidalysin by these brain resident macrophages triggers the production of IL-1β and CXCL1, essential for neutrophil recruitment (Drummond et al., 2015, Drummond et al., 2019). Macrophages assert their immunity mainly by elimination after phagocytosis and cytokine secretion to recruit other immune cells. Phagocytosis is initiated by PRR-PAMP interaction and involves two main stages: (i) phagosome formation and (ii) maturation. When phagocytic receptors such as CR3, Fcγ receptors (FcγRs) and Dectin-1 bind to their target PAMP, receptor clustering occurs and subsequently phosphorylation of their ITAMs and the activation of Rho-family GTPases occurs. Rho-GTPases then activate nucleation-promoting factors (NPFs), which cause actin-driven protrusions from the plasma membrane to advance around the target forming a phagosome (Gold et al., 1999, Marie-Anaïs et al., 2016). Hydrolysis of phosphoinositide $(4,5)P_2$ then leads to both clearance of F-actin at the base of the phagocytic cup and the release of IP_3, which drives signalling pathways that promote Ca^{2+} efflux from the endoplasmic reticulum (ER) to the cytosol (Austermeier et al., 2020). Cytosolic Ca^{2+} activates myosin and this is thought to be important in phagocytic cup formation and sealing, to form the phagosome (Campellone and Welch, 2010, Levin et al., 2016).

Phagosomes undergo maturation, whereby they gradually progress into a highly hostile and degradative environment, which is necessary to achieve pathogen elimination. This occurs slightly differently between different immune cells. For instance, macrophages undergo rapid recruitment and fusion of endosomes, which is driven by Rab5 and subsequently Rab7 as the phagosome transitions into its late phase (Levin et al., 2016). Lysosomes then fuse with late phagosomes to form a phagolysosome, which is armed with lytic enzymes and is highly acidic (i.e., in M2 macrophages,

which are involved in tissue repair and the resolution of inflammation) and oxidative, to provide an extremely degradative environment for pathogens (Levin et al., 2016, Roberts et al., 2000, Vieira et al., 2003, Vylkova and Lorenz, 2014). Notably, proinflammatory macrophages (i.e., M1 macrophages) and neutrophils, which mainly eliminate pathogens, have slightly alkaline phagosomes during the maturation process. This phenomenon is thought to be driven by the increased proton consumption during superoxide dismutation, reduced granule fusion observed during ROS production, and the increased leakiness of H^+ caused by the oxidative effect of ROS (Canton et al., 2014, Jankowski et al., 2002). Together, these stresses help eliminate and dispose of *C. albicans*.

However, achieving this end goal is made difficult through various mechanisms employed by *C. albicans* to consolidate its survival and escape from phagosomes. Hyphal growth within phagosomes exerts mechanical stress on the phagosome and may lead to phagosomal rupture. *C. albicans* also initiates macrophage death by competing for glucose, attacking membranes through candidalysin secretion, and triggering inflammasome-dependent pyroptotic cell death (Austermeier et al., 2020, Kasper et al., 2018, Olivier et al., 2022, Wellington et al., 2014, Westman et al., 2020). To limit phagosomal rupture by growing hyphae, macrophages increase lysosome production upon the recognition and engulfment of *C. albicans.* As hyphae grow within phagosomes, this causes mechanical stress to the phagosomal membrane, causing transient Ca^{2+} releases into the cytosol. These Ca^{2+} releases act as triggers to increase lysosomal fusion to the phagolysosomes to increase their surface area and prevent phagosomal rupture. Together, these increase the chance of *Candida* remaining confined within intact phagolysosomes long enough to effect killing (Westman et al., 2020).

Innate immune cells also contribute to the control and elimination of *C. albicans* by releasing inflammatory and chemotactic cytokines to recruit more immune cells to the site of infection. Macrophages upon recognition of *C. albicans* release proinflammatory cytokines such as IL-1β, IL-6 and TNF- α (Fig. 1.4) that contribute to neutrophil recruitment (Aybay and Imir, 1996, Chin et al., 2014, Ganesan et al., 2014, Yamamoto et al., 1997). CARD9+ brain resident macrophages (microglia) also play a crucial role in neutrophil recruitment in response to the *C. albicans* toxin, candidalysin during infection of the brain by producing IL-1β and CXCL1 (Drummond et al., 2019).

1.4.2.2 Neutrophils

Neutrophils play a crucial role in anti-*Candida* responses in most niches and neutropenic patients have increased susceptibility to systemic candidiasis and suffer worst outcomes when they get infected (Fradin et al., 2005, Hope et al., 2007, Ramy et al., 2017, Desai and Lionakis, 2018, Pappas et al., 2018). Neutrophils act as the first line of defense in most systemic infections and their rapid recruitment to the site of infection is critical for effective fungal control but delayed hyper-recruitment could lead to immunopathology (Lionakis et al., 2011). Consequently, the liver and spleen, which can rapidly recruit neutrophils within the first 24 hours during systemic candidiasis, have less fungal burden and damage. Conversely, the kidneys recruit less neutrophils in the first 24 hours but robust recruitment follows driven by the chemokine receptor, Ccr1, but this delayed recruitment does not alleviate the fungal burden or prevent organ damage thus highlighting the benefits and detrimental effects of neutrophils depending on time of recruitment (Lionakis et al., 2011, Lionakis et al., 2012). When neutrophils encounter *C. albicans* they exert their antifungal effects depending on the morphology of *Candida* (Branzk et al., 2014). Detection of *C. albicans* through Dectin-1 leads to the activation of the integrin, Mac-1 (CR3) and this is essential for fungal engulfment and elimination

(Lee et al., 2003, Nordenfelt and Tapper, 2011, Li et al., 2011). Phagocytosis in neutrophils differs from that of macrophages. For instance, neutrophils undergo much quicker phagosome maturation, which involves phagosomal fusion with lysosomes and neutrophil granules containing antimicrobial peptides and proteolytic enzymes (Lee et al., 2003, Nauclér et al., 2002, Nordenfelt and Tapper, 2011). Like macrophages, *C. albicans* is exposed to ROS within neutrophil phagosomes to potentiate its killing (Chauhan et al., 2006, Netea et al., 2008, Thompson and Wilton, 1992, Warris and Ballou, 2019). Also, nicotinamide adenine dinucleotide phosphate (NADPH) is produced by two separate, glucose-dependent pathways: glycolysis and the pentose phosphate pathway (Azevedo et al., 2015). Patients with kidney disease that have reduced expression of the glucose transporter, GLUT1, and patients with chronic granulomatous disease have reduced ROS production and increased susceptibility to candidiasis, demonstrating the importance of NADPH oxidase in ROS production (Henriet et al., 2013, Jawale et al., 2020). While phagocytosis and phagosomal killing is efficient against yeast cells, extracellular containment and killing tactics such as neutrophil extracellular trap (NET) release are employed against hyphae (Fig. 1.4) (Branzk et al., 2014). NET (decondensed chromatin fibres) release is driven through Dectin-1 and is the main extracellular antimicrobial mechanism used by neutrophils on large microbes such as *C. albicans* hyphae (Branzk et al., 2014, Urban and Backman, 2020). NETs are decorated with granules, histones and cytoplasmic proteins (i.e. calprotectin – the major antifungal NET associated protein) (Urban and Backman, 2020) and its release is mediated by serine protease, neutrophil elastase and a myeloperoxidase-containing complex (Metzler et al., 2014, Papayannopoulos et al., 2010, Urban and Backman, 2020). Depending on the PRR engaged and whether *C. albicans* is opsonised or not, NET release can proceed in both a ROS-dependent and independent way (de Bont et al., 2018, Wu et al., 2019). NET release is a crucial component of the neutrophil's arsenal against fungal infections, but its regulation is also essential to prevent immunopathology. While mutations that cause a lack of NET formation predispose patients

to fungal infections (Brinkmann and Zychlinsky, 2012), uncontrolled NET release and inefficient NET degradation is linked to several diseases such as vascular disease and Cystic Fibrosis (Kessenbrock et al., 2009, Papayannopoulos et al., 2011). Neutrophils also play a key role in fungal clearance, by releasing proinflammatory cytokines such as TNF-α and IL-12, extracellular vesicles, and degranulation, which releases antimicrobial factors (Fig. 1.4) (Endo et al., 2017, Lehman and Segal, 2020, Romani et al., 1997, Shopova et al., 2020). Also, during *C. albicans* infection in the CNS, recruited neutrophils are major producers of chemotactic chemokines like CXCL2 to drive a positive feedback loop (Drummond et al., 2015). Taken together, neutrophils contribute to both direct killing of *C. albicans* and regulating inflammation by recruiting more immune cells to help eliminate and dispose of *C. albicans*.

1.4.2.3 Dendritic cells

Dendritic cells (DCs) are myeloid cells renowned for their antigen presentation and activation of T cells thus serving as the bridge between innate and adaptive immunity (Whitney et al., 2014). They play a non-redundant role in innate resistance against systemic candidiasis. This was elegantly shown in Whitney *et al.*, (Whitney et al., 2014) that signalling through the Syk-CARD9 axis is vital for resistance against systemic candidiasis. During systemic candidiasis, signalling of the Syk-CARD9 axis in DCs leads to the production of cytokines such as IL-10, IL-2 and IL-23p19 (Whitney et al., 2014, LeibundGut-Landmann et al., 2007). The latter acts on NK cells to enhance GM-CSF secretion which helps to sustain neutrophil anti-*Candida* activity within the kidneys to initiate clearance. Furthermore, DCs also discriminate between the different *C. albicans* morphologies, and this differentially stimulates adaptive immunity, with yeast cells provoking a Th1 response, while hyphae initiate a Th2 response (d'Ostiani et al., 2000). Their activation through Dectin-1 and Dectin-2 also promotes T_H-17 differentiation and IL-17 production by regulatory T cells (T_{reg} cells) thus confirming

their importance in modulating both innate and adaptive antifungal responses (LeibundGut-Landmann et al., 2007, Robinson et al., 2009).

1.4.2.4 Natural killer cells

The only lymphoid cell that contributes to anti-*Candida* responses during systemic candidiasis are natural killer (NK) cells. These cells sustain the antimicrobial activities of neutrophils through secretion of GM-CSF and have also been shown to promote the phagocytic activity of splenic macrophages in mice (Algarra et al., 2002, Voigt et al., 2013, Whitney et al., 2014). They can also recognise and phagocytose *C. albicans* yeast through detection of β-glucan by NKp30 receptors and can exert cytotoxic effects mainly through secreted perforin against hyphae (Li et al., 2018, Voigt et al., 2013). In humans, low NK levels increase the risk of fungal infections and are a good predictive measure for transplant patients who would go on to develop invasive fungal infections (Orange and Ballas, 2006, Schmidt et al., 2017, Stuehler et al., 2015). Furthermore, in a yet to be determined mechanism, IL-17ra deficient mice have NK cells that are intrinsically hyporesponsive, which increased their susceptibility to invasive fungal infections (Bär et al., 2014). Taken together, these findings suggest a particularly important role for NK cells in anti-*Candida* immunity although the exact mechanisms are not fully understood.

1.5 PROLONGED ANTIBIOTIC USE

Success of antibiotics to human health cannot be overstated. However, resistance to existing antibiotics is threatening to send us back to the pre-antibiotic era and its associated challenges. Efforts to identify and rapidly develop new potent candidates is well underway (David et al., 2021). However, prolonged antibiotic use is a known risk factor for candidiasis (Drummond et al., 2022). When

patients are on long-term antibiotics use such as hospitalised patients and post-surgery patients, this disrupts their gut microbiota, reducing the bacterial population and causing a fungal bloom (Fan et al., 2015). The most abundant fungus in the human gut is *C. albicans* and thus it has increased odds of disseminating to the blood and other organs when fungal bloom is coupled with phagocyte depletion or gut barrier disruption thus causing systemic infections (Fan et al., 2015, Ifrim et al., 2016, Netea et al., 2008). Furthermore, antibiotics have been shown to have detrimental off-target effects on immune cells (Scott et al., 2018, Erny et al., 2015) but the exact mechanisms by which antibiotics confer their effects on immune cells to predispose the host to candidiasis are not fully understood. Nonetheless, studies have shown several classes of antibiotics to affect mitochondrial function of other mammalian cells (Miller and Singer, 2022). β-lactams have been shown to affect both the tricarboxylic acid cycle (TCA) and anionic substrate transport in renal cell mitochondria (Miller and Singer, 2022). Moreover, some antibiotics can also have an indirect effect on immune cells. For example, when β-lactams act on bacteria such as *Escherichia coli*, they cause the release of endotoxins that have detrimental effects on neutrophils (Matsuda et al., 2002). Low levels of endotoxin release when imipenem was incubated with *E. coli* caused neutrophil apoptosis, while ampicillin and cephalosporins that induce release of higher endotoxin levels caused neutrophil necrosis (Matsuda et al., 2002). Conflicting results exist on β-lactam effects on immune cell function. While some studies reported defects in phagocytosis, others observed the opposite and the same is true for functions like neutrophil chemotaxis and superoxide production thus making it very difficult to draw any solid conclusions from these findings (Miller and Singer, 2022). Macrolides are also reported to have anti-inflammatory effects and have been used to treat hypersecretory conditions such as Cystic Fibrosis and panbrochiolitis (Nau and Tauber, 2008). Although the mechanisms by which they exert these immunomodulatory effects to improve health are poorly understood, the fact that erythromycin and azithromycin have been shown to reduce neutrophil chemotaxis, neutrophil elastase

(essential for NET formation) and oxidative burst may help to explain these effects (Lin et al., 2000, Nau and Tauber, 2008, Saiman et al., 2003, Pasquale and Tan, 2005). Similarly, tetracyclines also causes decrease production of TNF-α, nitric oxide, neutrophil elastase, and IL-1β (Pasquale and Tan, 2005). Fluoroquinolones mainly exert anti-inflammatory effects by blocking pro-inflammatory cytokines but alatrofloxacin was shown to have a short-term pro-inflammatory effect during bacterial phagocytosis by THP-1 cells (Nau and Tauber, 2008). Together, these findings suggest that antibiotics can have both immuno-stimulatory and immunosuppressive effects on immune cells through direct and indirectly mechanisms thus warranting proper monitoring to prevent immunopathology or development of opportunistic infections.

In efforts to elucidate how antibiotics might be affecting antifungal immunity Drummond *et al*., (Drummond et al., 2022) treated mice with an antibiotic cocktail consisting of ampicillin, metronidazole, neomycin and vancomycin through their drinking water for 28 days and then challenged them intravenously with *C. albicans* yeast [Fig. 1.5] and found increased death in the antibiotic treated mice. These mice had increased fungal growth in the gut and bacterial and fungal co-infection in the blood. Furthermore, they observed reduced Th17 cells in the intestine of antibiotic treated mice which was attributed to reduced microbial diversity within the gut exemplified by reduced segmented filamentous bacteria, known for stimulating Th17 cell differentiation (Drummond et al., 2022). Segmented filamentous bacteria including *Bacteroides thetaiotamicron* and *Blautia producta* have also been shown to be critical for resistance to *C. albicans* colonisation by modulating the immune system (GI epithelial cells) to produce antimicrobial agents such as cathelicidin-related antimicrobial peptide (*Cramp*), which is orthologous to human LL-37 and has anti-*C. albicans* properties. This is induced through the hypoxia-inducible factor-1α (*HIF-1α*) – *Camp* axis (Fan et al.,

2015). Other studies have also reported the importance of both gut barrier integrity and phagocytes in *Candida* dissemination to the blood (Koh et al., 2008, Zhai et al., 2020).

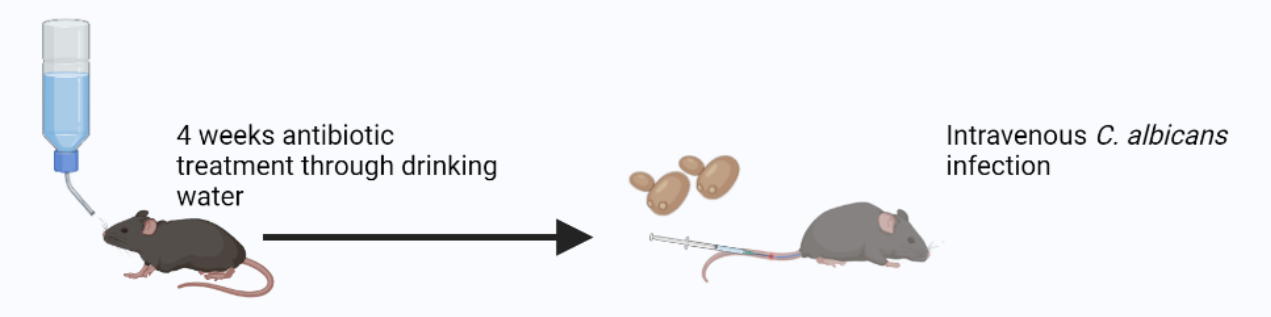

Figure 1.5. ***In-vivo* mouse experimental model**. Mice were treated with vancomycin in their drinking water for 28 days and challenged intravenously with *C. albicans* through their tail vein.

Interestingly, when mice were treated with the individual antibiotics in their study, vancomycin treatment was able to replicate this phenotype (Drummond et al., 2022). Vancomycin is a glycopeptide that is used within the clinic to treat severe Gram-positive infections such as those caused by *Staphylococcus aureus*, *Enterococcus faecium* and *Clostridium difficile* (Bode et al., 2015, Ingram et al., 2008, van Opstal et al., 2016). Vancomycin exerts its antibacterial effects in two ways; (i) It inhibits second stage cell wall synthesis by binding $_{D}$-alanyl-$_{D}$-alanine (found in peptidoglycan precursors) containing peptides at the free carboxyl end and therefore inhibiting polymerisation of the phosphodisaccharide-pentapeptide lipid complex and (ii) it alters cell membrane permeability and selectively inhibits ribonucleic acid (RNA) synthesis (Watanakunakorn, 1984). Earlier studies have also shown vancomycin to significantly disrupt the gut microbiota causing relapse during *C. difficile* treatment in aged mice (van Opstal et al., 2016) and impaired immune cell development and intestinal mucosal damage in neonatal mice (Cheng et al., 2017).

Although vancomycin clearly affects gut microbiota and Th17 numbers, it did not have any direct effects on CD4+ T cell function (as measured by cytokine production) (Drummond et al., 2022) thus

it is unclear from these studies if it affected the function of other immune cells such as macrophages. Nonetheless, vancomycin treatment was shown to cause increased oxidative stress and apoptosis in renal tubular cells (Arimura et al., 2012) and at high concentrations (2000 mg/L), vancomycin causes reduced adherence and phagocytosis of polymorphonuclear cells (Capodicasa et al., 1991) but this was lost at therapeutic concentrations (Morán et al., 1991). Vancomycin also reduces both the levels and biological activities of TNF-α secreted by LPS activated monocytes *in-vitro,* thus, potentially explaining its beneficial role in treating sepsis (Siedlar et al., 1997). However, a more recent study has shown vancomycin treatment of LPS stimulated monocytes to increase pro-inflammatory cytokines including TNF-α, IL-6 and IL-1β (Bode et al., 2015). These results suggest that vancomycin's effect on immune cells may be context dependent and studies to understand the mechanisms by which it suppresses or enhances immune responses are necessary to understand when to use vancomycin alongside immune response enhancers or suppressors.

Conflicting results exist regarding the role of macrophages in disseminated candidiasis, however, these differences could be explained by the site of depletion and/or the degree of macrophage depletion achieved as higher depletion rates or reduced function of splenic macrophages (Algarra et al., 2002, Qian et al., 1994) showed greater importance of these immune cells than a study that had only modest depletion of macrophages (intestinal macrophages) (Koh et al., 2008). Even less is known about the role of macrophages in antibiotic induced susceptibility to candidiasis. However, depletion of gut macrophages was recently shown to lead to increased fungal burden and reduced gut integrity leading to bacterial and fungal dissemination to the blood (Hiengrach et al., 2022b). This is like the observations made by Drummond *et al* in vancomycin pre-treated mice thus suggesting a potential effect of vancomycin on macrophages (Drummond et al., 2022). Furthermore, macrophages are a major source of GM-CSF, and these levels were reduced in vancomycin treated mice and

reconstitution with recombinant GM-CSF, an FDA approved therapy for accelerating myeloid reconstitution partially rescued the phenotype (Dignani et al., 2005, Drummond et al., 2022, Gavino et al., 2014). Together, these observations suggest a role for macrophages in anti-*Candida* immunity which may be disrupted by vancomycin pre-treatment. Therefore, to understand the specific effects of vancomycin on macrophage anti-*Candida* immunity the aims of my research were to:

1. Determine the direct impact of vancomycin on phagocytosis and killing of *C. albicans* by macrophages and how it affects activation of the inflammasome.
2. Assess the effects of vancomycin on mitochondrial function.
3. Determine how vancomycin pre-treatment affects fungal cell wall remodelling within phagosomes and its potential consequences on subsequent immune responses.

2 MATERIALS AND METHODS

Parts of this chapter have been previously published:

Bojang E, Drummond RA, Hall RA. Molecular and Microscopic Methods of Quantifying *Candida albicans* Cell Wall PAMP Exposure. Methods Mol Biol. 2022; 2542:309-321. doi: 10.1007/978-1-0716-2549-1_23. PMID: 36008675.

2.1 ETHICAL STATEMENT

This study involving the use of animals was carried out under the Project Licence PBE275C33 and was approved by the Animal Welfare and Ethical Review Board and UK Home Office. Wild-type (C57BL/6 Taconic) used in this study were purchased from Charles River. 8–12-week-old C57BL/6 mice (males and females) were housed in individually ventilated cages under specific pathogen free conditions at the Biomedical Services Unit at the University of Birmingham. Mice were housed in groups of 2-5 per cage and had access to standard chow and drinking water *ad libitum*. Mice were euthanised by cervical dislocation to collect bones for BMDM differentiation.

2.2 TISSUE CULTURE OF CELL LINES

RAW 264.7 (Gift from Julie Rayes) and J774.1A (Sigma-Aldrich, UK) macrophages were grown from liquid nitrogen stocks in Dulbecco's Modified Eagle Media (DMEM, ThermoFisher) supplemented with 10% heat-inactivated Foetal Bovine Serum (FBS), 1% L-glutamine and 1% penicillin-streptomycin in T75 tissue culture flasks incubated at 37 °C with 5% CO_2. Macrophages were passaged whenever they have reached 80% confluence and were used for experiments at passages 3 through 15. Prior to phagocytosis, macrophages were serum starved in DMEM for 1 hour with PMA (1.5 μg/ml) activation.

2.3 DIFFERENTIATION OF PRIMARY MOUSE BONE MARROW DERIVED MACROPHAGES (BMDMS)

Hind-limbs of mice were collected from 8–12-week-old (C57BL/6Ncrl) mice (males and females) and submerged in fresh Roswell Park Memorial Institute (RPMI) media containing GlutaMax and HEPES and kept on ice. Bones were then placed in a sterile petri-dish and sprayed with 70% ethanol to keep them sterile. Muscles were removed from the bones as previously described (Toda et al., 2021). Briefly, muscles were cut near the base of the femur and the Achilles tendon and muscle around the femur and tibia removed respectively. The bones were cut at the knee joint before removing the epiphyses of the femur and tibia by cutting both ends to get access to the bone marrow. Bone marrow was slowly flushed into a petri-dish with ice cold PBS with 2 mM EDTA using a 1 mL syringe fitted to a 23G needle. Bone marrow was then passed through a 70 μm cell strainer into a 50 ml falcon tube. The plunger of the syringe was used to smash the bone marrow further and the strainer washed with PBS with 2 mM EDTA. The cell suspension was centrifuged at 1500 rpm for 5 minutes at 4 °C. The supernatant was discarded, and cells were resuspended in 12 mL of 100% heat inactivated FBS. Cell suspension was then split in half by transferring 6 mL to a fresh 50 mL falcon tube. To each half, we added 24 mL of fresh RPMI to make a 20% FBS in RPMI. Premium grade M-CSF (Miltenyi Biotec) was added to each tube to make a final concentration of 40 ng/mL. We then added vancomycin (Fresenius Kabi) to the treatment group to a final concentration of 20 μg/mL (Fig. 2.1). Cells were aliquoted (10 ml) into three T75 tissue culture flasks per condition and incubated at 37 °C with 5% CO_2. On day 3, 80-90% of old media was replaced with fresh 10 mL of media prepared as described above and re-incubated under the same conditions. Fully differentiated cells were harvested on day 5 of incubation.

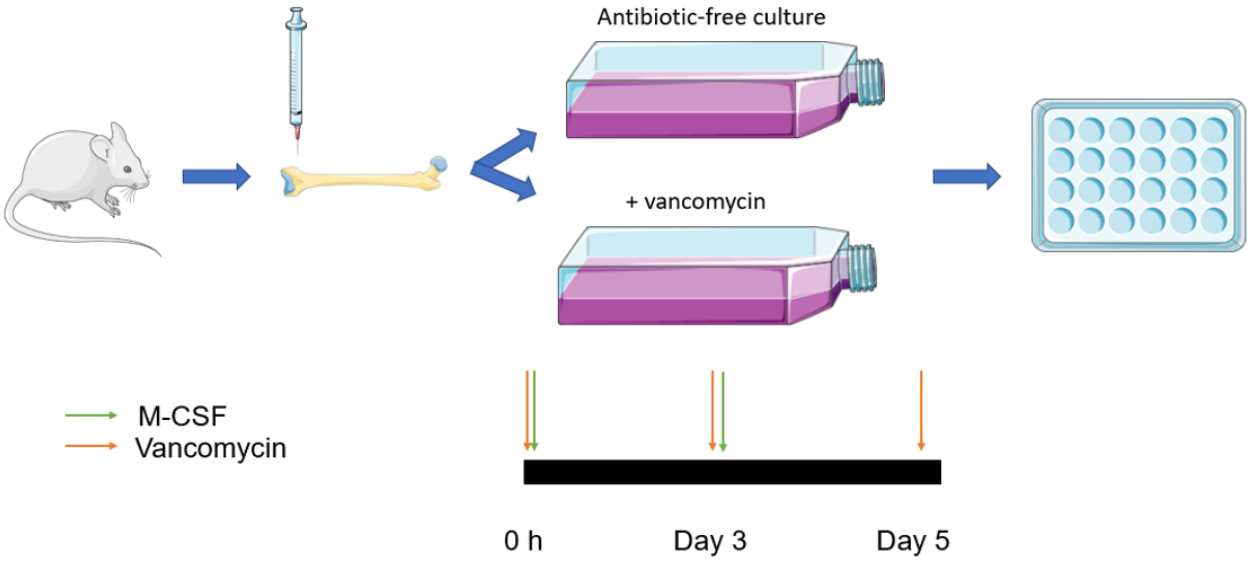

Figure 2.1. **Graphical workflow of bone marrow derived macrophage differentiation.** Bone marrow is flushed from the tibia and femur of the hind limbs of mice. These cells are resuspended in 20% heat-inactivated foetal bovine serum in RMPI with Glutamax. M-CSF is added at a final concentration of 40 ng/ml and cells are treated with vancomycin at 20 µ g/ml or left untreated. After 3 days of incubation at 37 °C with 5% CO_2, 70-80% of old media is replaced with fresh media and cells are harvested on day 5 and set up for the different assays.

2.4 HARVESTING FULLY DIFFERENTIATED BMDMS

Fully differentiated macrophages were harvested on day 5 for experiments. Media was removed and replaced with 12 mL of ice-cold PBS with 2 mM EDTA. The flasks were incubated on ice for 5-10 minutes and cells gently lifted using a cell scraper (Corning). Cells of the same condition were pooled in a 50 mL falcon and centrifuged at 1500 rpm for 5 minutes at 4 °C. Cells were resuspended in 10 mL of 10% FBS in RPMI with GlutaMax. In addition, 20 µg/mL of vancomycin was added to the treatment group. To count cells and assess viability, 5 µL of cell suspension was diluted 1:20 in 45 µL trypan blue and 50 µL media. A 10 µL aliquot was added to a haemocytometer to fill the chambers by capillary action and viable cells (cells that excluded the stain) were counted under a microscope

(Motic). Cells that were within the 16 big squares including cells that were on the right-hand and bottom boundary lines were counted. Another 16 squares diagonal to the counted squares were counted and total divided by 2. All four corners of 16 squares can also be counted and divided by four. The final count was multiplied by 10^4 and the dilution factor (20) to get the total number of cells/mL.

2.5 CD4 T CELL ISOLATION

Major lymph nodes (inguinal, axillary, branchial, mesenteric, and cervical) and spleens were collected from 6-8 weeks old wild-type mice and kept separately in ice-cold RPMI. Organs were then smashed through a 70 μm filter with a sterile plunger and collected in a 6-well plate (Corning). Cell suspensions were then passed through the filter 2-3 more times using RPMI to wash the filter each time. Then suspensions were passed through a 40 μm filter and collected in a 50 mL falcon tube (Corning). Cells were centrifuged at 1500 rpm for 5 minutes at 4 °C and red blood cells from spleen samples lysed using Pharmlyse (BD Biosciences) prior to resuspending cells in 5 mL of RPMI. Lymphocytes were counted using a haemocytometer with dead cells discriminated by trypan blue. Cells were centrifuged, supernatant aspirated and cell pellet resuspended in 40 μL of Miltenyi buffer per 10 x 10^6 cells. Cells were then filtered through a 70 μm cell strainer before adding biotin-antibody cocktail at 10 μL per 10 x 10^6 cells and incubating for 5 minutes at 4 °C. An LS column was securely placed in a MACS separator (Miltenyi Biotec) and cell suspension passed through the column and the flow through was collected in a 15 mL falcon placed on ice. This flow through was enriched for CD4 T cells and were counted using a haemocytometer and used for subsequent experiments.

2.6 CANDIDA ALBICANS CULTURE

The *C. albicans* strains used in this study are listed in Table 2.1 below. A single colony *of C. albicans* was inoculated in 10 mL of yeast extract peptone dextrose (YPD) (1% Yeast extract, 2% Peptone and 2% Glucose (All from Sigma-Aldrich) and incubated overnight at 30 °C with aeration at 200 rpm. Cells were then washed trice in PBS, counted using a Neubauer chamber and diluted to the desired concentration, and used for subsequent experiments. In earlier experiments (i.e., phagosome induced cell wall remodelling experiments) *C. albicans* was grown overnight at 37 °C with aeration at 200 rpm. Overnight cultures were then diluted 1:100 in 10 mL of YPD and incubated for 4 hours under the same conditions to reach mid-log exponential phase. A 1.5 mL aliquot of the culture was then transferred into Eppendorf tubes and centrifuged (1650g) for 3 minutes. Cells were washed trice in PBS by centrifugation, counted, and used for subsequent experiments.

Table 2.1. *Candida albicans* strains used in this study.

Strain	Parental strain	Description	Genotype	Reference
SC5314		*Candida albicans* standard wild-type strain	Wild type	(Gillum et al., 1984)
CAF2-dTomato	CAF2.1	*dTomato fluorescing strain*	Δ*ura3::imm434/URA3 with ENO1-dTom-NAT^r plasmid*	Kind gift of Rob Wheeler

2.7 C. ALBICANS INACTIVATION

C. albicans yeast were inactivated by heat killing, UV exposure or PFA fixing. Overnight cultures of *C. albicans* were washed in PBS and diluted to 2 x 10^6/mL in 1.5 mL tubes (Eppendorf). For heat-killing, cells were incubated at 70 °C for 30 minutes on a heating block. UV inactivation was achieved

by exposing cells to UV light in a hood for 1 hour. *C. albicans* yeast were also incubated with 4% PFA for 30 minutes at room temperature to inactivate the cells.

2.8 PHAGOCYTOSIS ASSAY

The ability of vancomycin pre-treated macrophages to phagocytose *C. albicans* was tested. BMDMs were infected with td-tomato fluorescing *C. albicans* at a multiplicity of infection (MOI) of 2 and incubated at 37 °C for 30 minutes and 1 hour. Cells were placed on ice to stop phagocytosis and cells stained with an anti-*Candida* FITC stain to stain extracellular *Candida* (non-phagocytosed *Candida*) [Fig. 2.2]. Macrophages were also stained with macrophage markers in the wells, gently scraped off the wells and analysed by flow cytometry. We defined macrophage populations that had interacted with *C. albicans* as populations positive for macrophage surface markers and td-Tomato [Fig. 2.3]. Given that surface attached *Candid*a would stain for anti-*Candida*-FITC, macrophage populations were separated based on surface staining into macrophages with fully engulfed *Candida* (F480+, td-Tomato+ and anti-*Candida*-FITC-) and macrophages with surface attached *Candida* (F480+, td-Tomato+ and anti-*Candida*-FITC+). To evaluate phagocytosis of opsonised and un-opsonised *C. albicans*, cells were either opsonised in 10% mouse serum for 10 minutes on ice prior to infection or left un-opsonised.

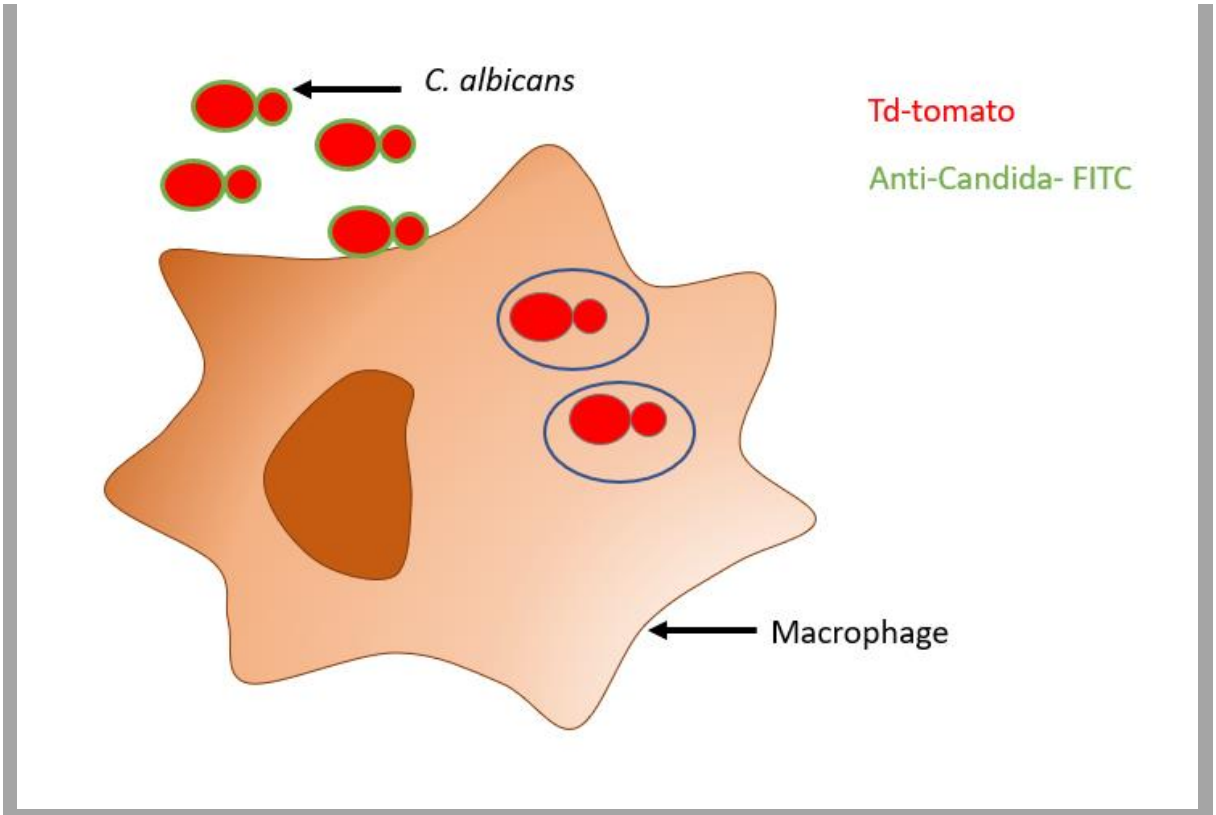

Figure 2.2. Phagocytosis of *C. albicans* by BMDMs. Macrophages were incubated with td-Tomato fluorescing *C. albicans* for 30 minutes and 1 hour and extracellular *C. albicans* was stained with anti-*Candida*-FITC. Macrophages were stained for macrophage markers and analysed using flow cytometry.

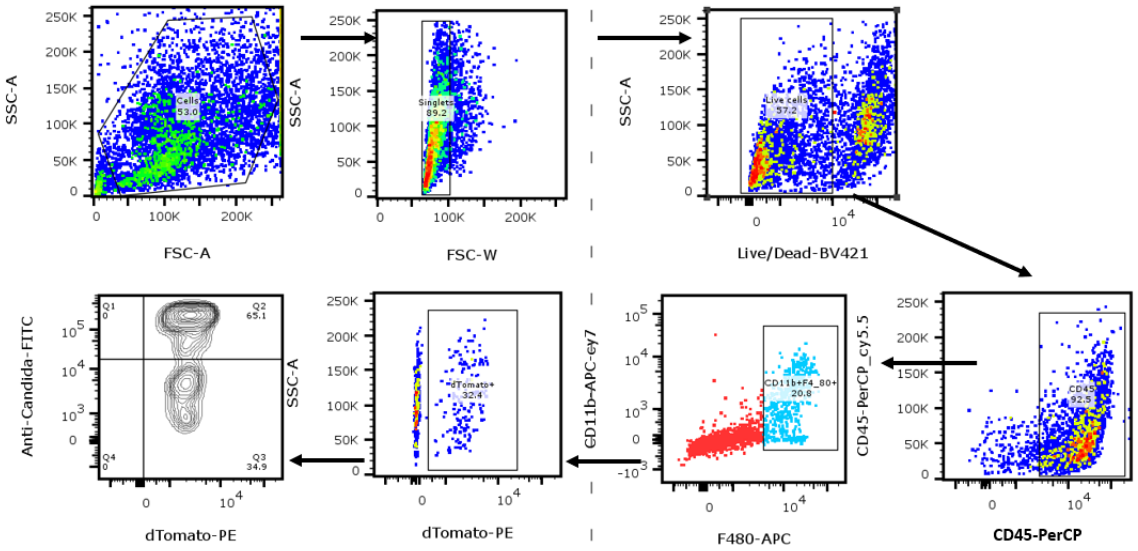

Figure 2.3. **Gating strategy for *C. albicans* phagocytosis.** Gating was first made on cells excluding debris, then singlets were gated for before gating for live cells using the live/dead discriminating dye. We then gated for macrophages using the myeloid marker, CD45 and then CD11b+ F480+ cells were gated. We then quantified the proportion of these cells that are associated with *C. albicans* using the PE gate. This population was further separated based on whether *C. albicans* was engulfed (FITC negative) or surface attached (FITC positive).

2.9 VYBRANT PHAGOCYTOSIS ASSAY

To assess if vancomycin treatment affected phagocytosis of bacteria macrophages were challenged with fluorescent *E. coli* beads using the Vybrant phagocytosis assay (ThermoFisher). Briefly, $1x10^5$ BMDMs were seeded overnight in 96-well plates. *E. coli* mix was added to cells at 100 µL/well and incubated at 37 °C for 2 hours. Trypan blue solution was then added to wells at 100 µL/well and incubated at room temperature for 1 minute to quench fluorescence of extracellular *E. coli*. Trypan blue was then washed off and fluorescence of intracellular *E. coli* was read at an Excitation/Emission of 480/520 nm.

2.10 MACROPHAGE LYSIS

2.11 TO LYSE MACROPHAGES, THEY WERE INCUBATED FOR 5 MINUTES AT ROOM TEMPERATURE IN ULTRA-PURE WATER WITH 0.02% TRITON X-100.CELL WALL STAINING AND QUANTIFICATION (BOOK CHAPTER)

All stains used to quantify *C. albicans* cell wall components in this project are diluted as outlined in Table 2.2 below.

Table 2.2. Concentration of cell wall stains used in this study.

Stain	Final working concentration	Solvent
Fc-Dectin-1	3 μg/mL	PBS with 2% BSA
Concanavalin A	25 μg/mL	PBS with 2% BSA
Wheat Germ Agglutinin	10 μg/mL	PBS with 2% BSA
Calcofluor White	3.5 μg/mL	PBS
Human anti-mouse conjugated to Alexa Fluor 488	1:200	PBS with 2% BSA

Briefly, cells were blocked in 2% BSA in PBS for 30 minutes on ice. Cells were then washed trice with PBS and stained on ice with prepared stains.

2.11.1 β-glucan staining

Exposed β-glucan was stained for by staining washed cells with 3 μg/mL of Fc-Dectin-1 (Invitrogen) and incubating on ice for 60 minutes. Cells were then washed trice with PBS followed by staining on ice with anti-mouse secondary antibody conjugated to FITC (diluted 1:200 in 2% BSA in PBS) for 30 minutes. Cells were then kept in the dark until analysed by microscopy or flow cytometry.

2.11.2 Mannan and Chitin staining

We assessed cell wall mannan levels by staining washed cells with 25 μg/ml of concanavalin A (conA, Invitrogen) on ice for 30 minutes. Similarly, exposed chitin was assessed by staining cells

with 10 μg/mL of wheat germ agglutinin (WGA, Invitrogen) on ice for 30 minutes. Total cell wall chitin was assessed by staining cells with 3.5 μg/mL of calcofluor white (CFW, Sigma-Aldrich) and incubating on ice for 10-15 minutes.

2.12 FLOW CYTOMETRY

2.12.1 Cell wall components

Staining was performed in tissue culture plates before harvesting the cells by scraping in cold PBS. Washed cells were then resuspended in 500 μL of FACS buffer (0.5% BSA and 0.02% sodium azide in PBS) or PBS. To prepare controls for compensation, single stains for each fluorophore used were prepared. Flow cytometry analysis was performed using the Attune NxT equipped with a 488 nm (FITC filter set), 405 nm (BV421 filter set), 561 nm (PE filter set) and 633 nm (APC filter set) laser lines with at least 5000 events recorded. All other analysis by flow cytometry were performed using the Fortessa (BD). Data analysis was performed on FlowJo Software (FlowJo LLC, USA).

2.13 COMPENSATION

Single stained beads or where appropriate single stained cells were used for compensations. Negative and Positive beads (BD Biosciences) were added to each FACS tube and stained with one of the fluorophores in our panel with one tube left unstained. The stain stains the positive beads and thus producing two peaks on each channel, a negative and positive peak. These peaks are used by the Fortessa to automatically calculate spectral overlap and apply compensation to the samples.

2.14 GATING GENERAL

Debris and doublets were excluded using (SSC-A vs FSC-A) and (SSC-A vs FSC-W) respectively. The live-dead discrimination dye, BV-421 was used to exclude dead cells by gating on BV-421 negative cells.

2.15 FLUORESCENT MICROSCOPY

Macrophages were seeded on cover slips (12 mm) overnight in 24-well plates (Corning) for fluorescent imaging. These were then mounted on glass slides before imaging. For time-lapse imaging of live cells, macrophages were seeded directly in 24-well plates with transparent plastic bottoms.

2.15.1 Time-lapse ROS quantification

To measure reactive oxygen species production by macrophages, 2 x10^5 BMDMs were seeded in 24-well plates and let to adhere overnight. Media was replaced with fresh media containing 5 μM of CellRox Green reagent (ThermoFisher). BMDMs were then infected with live or heat-killed *Candida* at an MOI of 6 and green fluorescence read every 5 minutes for 6 hours using the Zeiss Axio Observer (Carl Zeiss) at 40x magnification. The microscope chamber was kept at 37 °C and cells supplied with 5% CO_2 throughout the experiments.

2.15.2 Mitochondrial membrane potential assessed by JC-1 staining.

The effects of vancomycin on mitochondrial membrane potential were assessed using the JC-1 stain. JC-1 accumulates and forms dimers that fluoresce red in polarised mitochondria. Accumulation is limited in depolarised mitochondria and the dye stays as monomers that fluoresce green. Control and vancomycin pre-treated macrophages were seeded overnight in 24-well tissue culture plates at 2 x 10^5 cells/well. The cells were washed with PBS and incubated with fresh media containing the JC-1

stain (1:10000) (ThermoFisher) for 30 minutes at 37 °C. Cells were washed with PBS and fresh media added to wells. Cells were then imaged using an inverted epifluorescence microscope (Olympus IX71) coupled to Retiga R6 CCD digital camera (QImaging, Teledyne) and images were quantified using imageJ (Fiji).

2.15.3 Phagosome maturation

To assess phagosome maturation, 2 x10^5 BMDMs were seeded in 24-well plates as above. Media was replaced with fresh media containing 50 ng/ml Lysotracker Red DND-99 (ThermoFisher). Cells were infected with live or heat-killed *Candida* at an MOI of 6 and red fluorescence was read every 5 minutes for 6 hours on the Zeiss Axio Observer (Carl Zeiss) at 40x magnification. Cells were kept alive by maintaining microscope chamber at 37 °C with 5% CO_2.

2.15.4 *Candida* cell wall components

To assess phagosome induced *C. albicans* cell wall remodelling, J774.1 and RAW264.7 macrophages were used. Macrophages were seeded overnight in 24-well plates at 2 x 10^5 macrophages/well. Prior to infection, macrophages were activated with PMA (0.15 μg/ml) for 2 hours in serum free DMEM. Macrophages were washed and fresh media added before infecting with *C. albicans* yeast at an MOI of 5. To synchronise phagocytosis, plates were incubated on ice for 30 minutes to initiate attachment of *Candida* to macrophages without phagocytosis. Unbound *Candida* cells were then washed off with PBS and fresh media was added to macrophages before plates were incubated for 1, 2 or 3 hours at 37 °C with 5% CO_2. Macrophages were gently washed with PBS and stained with 10 μg/ml of anti-*Candida*-FITC to stain extracellular *Candida*. Macrophages were then lysed with distilled water containing 0.02% Triton-X100. To stain intracellular *C. albicans*, macrophages were permeabilised in PBS containing 0.02% Triton-X100. Washed *C. albicans* cells were then stained with cell wall

stains as mentioned above and assessed microscopically on the Zeiss Axio Observer at 63X magnification. Images were analysed using the Fiji Software.

2.16 CONFOCAL MICROSCOPY

2.16.1 Mitochondrial morphology

Fully differentiated BMDMs in the treatment and untreated groups were harvested and seeded on cover slips in 24-well plates and allowed to adhere overnight. Media was replaced with fresh pre-warmed media containing 50 ng/mL of the MitoTracker DEEP RED dye (stains mitochondria based on its membrane potential, ThermoFisher) and cells re-incubated for 30 minutes at 37 °C with 5% CO_2. Macrophages were washed with PBS and fixed in 4% paraformaldehyde (PFA) for 30 minutes at room temperature and away from light. Macrophages were then stained with the DNA dye, DAPI (2 μg/mL) for 30 minutes. Coverslips were mounted using PBS or ProLong Gold antifade mountant (ThermoFisher) and imaged using the airy scan function of the Zeiss LSM 880 confocal microscope (Carl Zeiss) equipped with x63 water immersion objective.

2.16.2 Vancomycin binding dynamics

BMDMs differentiated in antibiotic free media were adhered on coverslips overnight as above. Media was replaced with fresh media containing fluorescent vancomycin (concentrations as indicated in figures) and incubated for 4-5 hours at 37 °C with 5% CO_2. In some experiments, macrophages were further stained with MitoTracker red for 30 minutes, washed in PBS and fixed for 30 minutes in 4% PFA. Mouse CD4+ T cells isolated from spleen were also subjected to vancomycin staining. Contrary to BMDMs, these are non-adherent, and staining was performed immediately after isolation in FACS

tubes. CD4+ T cells are also subjected to mitochondrial and nuclear staining just as above. About 3 μL aliquots of the cell suspensions were mounted on glass microscope slides (epredia) and sealed at the edges with nail polish. All samples were imaged using the airy scan function of the Zeiss LSM 880 confocal microscope (Carl Zeiss) equipped with x63 water immersion objective.

2.17 ROS QUANTIFICATION – PLATE READER

Intracellular reactive oxygen species were assessed using H_2DCFDA (ThermoFisher) fluorescent labelling probe. Differentiated BMDMs were seeded overnight in 96-well white opaque plates (Costar) at a concentration of 1 x 10^5 cells/well. Cells were gently washed with pre-warmed PBS and then treated with H_2DCFDA for 30 minutes at 37 ℃. BMDMs were then infected with heat-killed *C. albicans* at the indicated multiplicity of infection in PBS supplemented with 10% FBS and incubated at 37 ℃ with 5% CO2 for the indicated times. Fluorescence intensity of DCF was measured a fluorescence spectrophotometer (FlexStation 3 equipped with SoftMax Pro 7 software) at an excitation and emission wavelengths of 485 nm and 525 nm respectively.

2.18 TLR9-MCHERRY PLASMID TRANSFORMATION

The TLR9-mCherry plasmid was transformed into *E. coli* (DH5 alpha). TLR9-mCherry plasmid of PMSCV vector containing an ampicillin resistant gene. *E. coli* was transformed with the plasmid using the heat shock method. Briefly, the *E. coli* and plasmid mixture were placed on ice for 30 minutes. The mixture was then heated in a water bath at 42 °C for 30 seconds and immediately put back on ice. LB broth was added to tubes at 500 μL/tube and tubes incubated at 37 °C for 30 minutes at 200 rpm. Cells were pelleted by centrifugation at 5000 rpm, supernatant discarded, and pellet

resuspended. The entire cell suspension was put in LB agar with ampicillin and incubated overnight at 37 °C. Single colonies were picked and re-cultured on LB agar with ampicillin.

2.19 PLASMID PURIFICATION

Transformed *E. coli* was grown in 100 ml of LB broth overnight and to an O.D 600 of between 2-4. Cells were pelleted by centrifugation at 5000 rpm for 10 minutes and supernatant discarded. Cells were resuspended in 3 ml of suspension solution. Three millilitres of Cell lysis solution was added to the mixture and mixed by gentle inversion and incubated at room temperature for 3 minutes. Then 5 ml of neutralisation solution was added to the mixture and again mixed gently by inverting the tube between 3-5 times and tube allowed to sit in an upright position to allow a white flocculent precipitate to form. Tube was then centrifuged at 1500 g for 15 minutes to pellet the bulk of cellular debris. The rest of the debris were removed using the PureYield cleaning columns. Briefly, clear lysate was passed through the membrane by vacuuming and DNA bound membrane was washed with 5 ml endotoxin removal wash before washing with 20 ml of column wash solution. Membrane was dried by vacuuming and DNA eluted in 600 μL of nuclease-free water.

2.20 TRANSFECTION INTO RAW 264.7 MACROPHAGES

To transfect macrophages, DNA was diluted to 2 μg per 100 μL of deionised water (H_2O). RAW 264.7 macrophages were transfected at the recommended FuGene HD transfection reagent: DNA ratio of 3.5:1 and incubated for 15 minutes. Mixture was added to each well at 0.5 μg DNA per well and incubated at 37 °C overnight. Cells were then used for experiments.

2.21 SAMPLE PREPARATION FOR WESTERN BLOT, ELISAS AND LDH ASSAYS.

Macrophages were seeded overnight in 24-well or 96-well plates at the indicated concentrations. Prior to infection, macrophages were stimulated with 50 ng/ml lipopolysaccharide (LPS) for 2 hours (except for autophagy proteins, LC3 and p62). Cells were then infected with *C. albicans* at the indicated MOI or with appropriate controls (nigericin (10 μM) or bafilomycin A 50 nM) and incubated for a further 4 hours. Supernatants were collected and stored at -20 °C and cells lysed in RIPA buffer supplemented with protease and phosphatase inhibitor cocktail (Sigma) on ice for 10 minutes.

2.22 BCA PROTEIN QUANTIFICATION ASSAY

Protein content was measured from cell lysates and supernatants using the microplate procedure of the Pierce BCA (bicinchroninic acid) protein assay kit (ThermoFisher scientific). Briefly, protein samples were diluted 1 in 10 in PBS and 25 μL aliquoted in duplicates in 96-well flat bottom plates (Corning). Known concentrations of the protein, albumin was also aliquoted in duplicates and used as standards. Working reagent was prepared by adding reagents A and B of the assay kit at a ratio of 50:1 and 200 μL was then added to each well and mixed thoroughly for 30 seconds. Plates were then incubated at 37 °C for 30 minutes. Plates were then cooled to room temperature and absorbance read at 562 nm using a plate reader (SpectraMax ABS Plus, Molecular Devices). A standard curve was generated using the absorbance from known albumin concentrations. Equation of the curve was used to calculate the concentrations of the unknown samples. The protein concentration of original samples was determined by multiplying by the dilution factor.

2.23 WESTERN BLOTTING

Samples were boiled with Laemmli (Sigma) for 5 minutes at 95 °C and equal amounts of protein were subjected to SDS-PAGE and immunoblot analysis. Briefly, proteins were separated on 10% acrylamide gels and transferred onto 0.45 μM PVDF membranes. Membranes were incubated in blocking buffer (6% non-fat milk in PBS-Tween 20 or 5% BSA in PBS-Tween 20) for 1 hour at room temperature. Blots were then probed with primary antibodies (1:1000) overnight at 4 °C on a shaker platform. Primary and secondary antibodies used in these experiments are listed in Table 2.3 below. Blots were then washed with washing buffer (10 mM Tris, 100 mM sodium chloride and 0.1% Tween20) using three 5-minute cycles. Blots were then probed with secondary antibodies conjugated to HRP for 2 hours at room temperature. This was followed by 5 x 5-minute cycles of washing with washing buffer and an additional wash step with distilled water. Visualisation was then achieved by incubating blots in Clarity Western ECL Substrate (Bio-Rad) for 1 minute in the dark then imaged using a Gel-Doc imager (Bio-Rad). Band intensities were calculated using the Fiji software and graphed in Prism 9.4.1 (GraphPad Software, Inc. USA).

Table 2.3. Antibodies used in this study and their concentrations.

Primary Antibody	Species	Dilution	Secondary Antibody	Species	Dilution
IL-1β	Mouse monoclonal (3A6)	1:1000	Anti-mouse (7076s)	Horse	1:5000
Caspase-1	Mouse (AG-20B-0042-C100)	1:1000	Anti-mouse (7076s)	Horse	1:5000
NLRP3	Rabbit (D4P8t)	1:1000	Anti-rabbit (7074s)	Goat	1:5000

Gasdermin D	Rabbit monoclonal (ERP19828)	1:1000	Anti-rabbit (7074s)	Goat	1:5000
LC3	Rabbit polyclonal (NB100:2220)	1:1000	Anti-rabbit (7074s)	Goat	1:5000
P62	Guinea pig polyclonal (GP62-C)	1:1000	Anti-Guinea pig (ab6908)	Goat	1:5000
β-actin	Mouse (8H10D10)	1:1000	Anti-mouse (7076s)	Horse	1:5000

2.24 ELISA

Control and vancomycin pre-treated macrophages were seeded overnight in 96-well tissue culture plates at 1 x 10^5 cells/well in 4-6 replicates. The next day, macrophages were primed with 50 ng/mL LPS for 2 hours and stimulated with live-*C. albicans* for 4-6 hours at an MOI of 6 or left unstimulated as indicated. Supernatants were collected and IL-1β and TNF-α detected using the mouse IL-1β and TNF-α ELISA kits from R&D (Minneapolis, MN, USA). Briefly, 96-well ELISA plates (ThermoFisher) were coated overnight with capture antibody at RT. Plates were then washed trice with PBS with 0.05% Tween (PBS-T) and blocked for 1 hour in Reagent diluent. The washing step was performed as previously. Standards were prepared by serial dilution according to manufacturer's instructions and used to generate an interpolated standard curve using GraphPad Prism 9.4.1. Samples were diluted in reagent diluent where necessary and added to appropriate wells before incubating for 2 hours at RT. Plates were again washed trice and incubated at RT with detection antibody for 2 hours. Washing was again initiated with PBS-T and Streptavidin-HRP diluted 40-fold in reagent diluent was added to plates and incubated for 20 minutes protected from direct light. Plates were washed trice after incubation and substrate solution added and incubated in the dark for 30 minutes. Stop solution was added to all wells and tapped gently to mix and absorbance read immediately at 450 nm using a Spectrophotometer (SpectraMax ABS Plus, Molecular Devices).

2.25 LDH ASSAY

Macrophage death was measured by quantifying the cytosolic enzyme, LDH in culture supernatants (same as ELISAs) using the CyQUANT LDH Cytotoxicity Assay Kit (Invitrogen). LDH was measured following manufacturer's instructions. Briefly, 50 µL of supernatants were transferred to a fresh 96- well plate in triplicates. We than added 50 µL of reaction mix (prepared by adding 600 µL of assay buffer stock solution to 11.4 mL of substrate stock solution) and mixed by gentle tapping. Plates were incubated for 30 minutes at room temperature protected from light. Fifty microlitres of stop solution (provided) was added to each well and absorbance was read at 490 nm and 680 nm within 1 to 2 hours. LDH activity was calculated by subtracting the 680 nm absorbance value (background signal) from the 490 nm absorbance value.

2.26 LACTATE MEASUREMENT

We measured the level of glycolysis using lactate levels as a proxy. This was performed on culture supernatants using the Lactate-Glo Assay (Promega) following manufacturer's instructions. Briefly, lactate detection reagent was prepared for each reaction by adding 0.13 µL each of Reductase, Reductase substrate, Lactate dehydrogenase and NAD to 25 µL of Luciferin detection solution. This mixture was added to the prepared samples at 1:1 ratio and incubated away from direct light for 1 hour. Luminescence was measured using a Spectrophotometer (FlexStation 3 equipped with SoftMax Pro 7 software)

2.27 SAMPLE PREPARATION FOR METABOLITE SCREEN BY LC-MS

Macrophages were seeded into 24 well plates overnight (as above), and then challenged with heat-killed *C. albicans* for 2 hours (10:1 fungi to macrophage). Macrophage monolayers were washed with 0.9% sodium

chloride solution on ice twice prior to quenching and lifting with 0.5mL 70% acetonitrile. Macrophages were snap-frozen on dry-ice and thawed wet-ice 3 times prior to spinning down; supernatants were collected (approx. 0.5mL per sample) and stored at -80ºC prior to analysis. All samples were collected within 20 minutes of being removed from the 37ºC incubator.

2.28 NEUTROPHIL ISOLATION

To isolate neutrophils from human whole blood, a dual gradient of Percoll was created in universal tubes by layering 6 ml of Percoll at 1.098 density underneath 6 ml of Percoll at 1.079 density. Six ml of undiluted whole blood was then layered on top of the dual gradient and centrifuged for 8 minutes at 150 g, followed by 10 minutes centrifugation at 1200 g with acceleration and brake set at 0. After a nice separation of cells with two bands of white cells, the second band of white cells (neutrophils) was removed into a fresh 50 ml falcon tube. Red blood cell (RBC) lysis buffer (1L – 8.3g NH4Cl, 1g KHCO3, 0.04g Na2 EDTA 2H2O, 2.5g BSA, filter sterilise) was added to the tube at a ratio of 1:3 and gentle mixing by inversion was maintained for 3 minutes. Mixture was centrifuged for 6 minutes at 400 g; buffer was discarded, and cells washed twice with 40 ml PBS followed by centrifuged for 6 minutes at 400 g. Neutrophils were then resuspended in 1 ml of RPMI by gentle pipetting and viable cells counted in a 1:1 trypan blue using a haemocytometer.

2.29 CANDIDA KILLING ASSAY

BMDMs from vancomycin-treated and untreated macrophages were seeded in 96 well plates at 5 x 10^4 cells/well and incubated overnight, 37C, 5% CO_2. Media was removed from cells by flicking and 50 µL of 10% mouse serum in PBS was quickly added to each well. To assess killing efficiency, *C. albicans* only wells with known concentrations were used as standards. A serial dilution of live *C. albicans* was prepared in PBS with concentrations ranging from 4 x 10^6 cells/mL to 0 (PBS) as

illustrated in Fig. 2.4. An aliquot of 50 µL of the standards were added to the allocated wells in duplicates such that the highest standard had 2 x10^5/mL cells and the lowest had 0 cells.

BMDMs were then infected with *C. albicans* SC5314 yeast at a multiplicity of infection of 2 (MOI:2) by adding 50 µL of a 2 x10^6 cells/mL preparation to each well to make a final concentration of 5% mouse serum in PBS and plates incubated for 2 hours at 37 °C with 5% CO_2. After incubation, macrophages were lysed in distilled water containing 0.02% triton-X100. Plates were centrifuged at 2000 rpm for 4 minutes and supernatants discarded. Remaining yeast cells were then washed twice by adding 100 µL of fresh PBS followed by centrifugation at 2000 rpm for 4 minutes and discarding supernatant by flicking each time. 100 µL of 1X alamarBlue (ThermoFisher Scientific) was added to the cells and incubated at 37 °C with 5% CO_2 for 18 hours. Fluorescence was read at excitation/emission wavelength of 560/590nm using a plate reader (FlexStation 3 with SoftMax Pro 7 software).

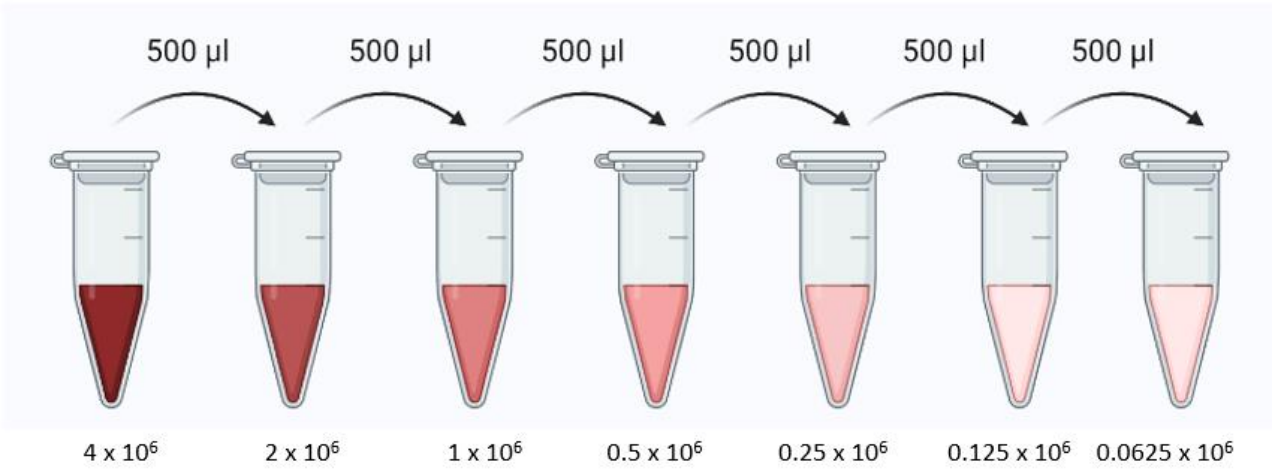

Figure 2.4. **Serial dilution of *C. albicans* standards for alamar blue assay.** *C. albicans* yeast was serially diluted in PBS as above. Fifty microliters of each standard were added to wells in duplicates. Fifty microliters of a 2x10^6 dilution were added to macrophages for a multiplicity of infection of 2.

2.30 SEAHORSE ASSAY

Control and vancomycin treated macrophages were seeded overnight at 37 °C in 5% CO_2 at 2 x 10^5 cells/well in a 96-well Seahorse tissue culture plate (Agilent) in 150 µL of control and vancomycin media respectively. Each condition had 8-10 replicates while avoiding outside wells. On the same day, the cartridge/utility plate was hydrated by immersing probes in 200 µL of distilled water and incubated overnight in a non-CO_2 incubator with adequate humidity. Seahorse calibrant (50 mL) was also incubated in a non-CO_2 overnight. Macrophages were stimulated with heat-killed *C. albicans* at an MOI of 10 and incubated for 4 hours. Seahorse media was prepared by adding sodium pyruvate (final concentration 1 mM), glucose (final 10 mM) and L-glutamine (final 2 mM) to 50 mL of pre-made base solution from Agilent. The distilled water in which the probes were submerged in was discarded and the probes re-submerged in the warm calibrant. The media on cells was replaced with Seahorse media. Drugs were prepared as in Table 2.4 and added to the cartridge/utility plate in a safety cabinet.

Table 2.4. Seahorse reagents used to probe the different mitochondrial parameters.

Drug	Volume of Stock (µL)	Working solution (recipe)	Final concentration (well)	Volume added to port (µL)	Port
Oligomycin	630	2.55 mL media + 450 µL stock solution	1.5 µM	20	A
FCCP	720	2.4 mL media + 600 µL stock solution	2 µM	22	B
Rotenone/ Antimycin A	540	2.7 mL media + 300 µL stock solution	0.5 µM	25	C

The cartridge/ utility plate is placed in the Seahorse machine and the utility plate is replaced with the cell culture plate after the initialisation step. The run is then started with the machine recording oxygen consumption rate and sequentially added the drugs at fixed times. Oligomycin targets ATP synthase and therefore causes reduction in ATP related oxygen consumption. FCCP is an uncoupler

that depolarises the membrane by shuttling protons across the membrane causing the respiratory chain to respond by consuming oxygen at a maximal rate. The combination of rotenone and antimycin A completely shuts mitochondrial respiration by inhibiting complex I and III. The raw data is exported as Excel reports and GraphPad files for further analysis.

2.31 MITOCHONDRIAL STAINING OF LIVE MACROPHAGES

Control and vancomycin pre-treated macrophages were seeded overnight on 15 mm glass coverslips in 24-well tissue culture plates (Corning). Stain with MitoTracker Red at a final concentration of 50 ng/ml and incubate at 37 °C for 30 minutes. Cells were washed 3 times in PBS protected from light and fixed in 4% PFA for 10-15 minutes. For some experiments, cells were then stained with DAPI (2 μg/mL).

2.32 RNA ISOLATION

Control and vancomycin pre-treated macrophages were seeded overnight in 24-well plates at $1x10^6$ cells/well. Macrophages were then stimulated with live-*C. albicans* for 2 hours at an MOI of 2 or left untreated. Media was discarded from wells and 1 ml of TRIZOL (Life Technologies) added to each well. Lysed cells in TRIZOL were immediately stored at -80 °C. Samples were thawed to room temperature on the day of RNA isolation and 200 μL of chloroform was added to each tube, mixed by inverting several times and allowed to settle for 5 minutes. Samples were then centrifuged at 12000 g for 15 minutes at 4 °C. Then, 500 μL of the top and clear portion were carefully transferred to RNAse-free Eppendorf tubes. Equal volume of 70% ethanol was added to each sample and 700 μL of the mixture transferred to a Qiagen column (RNeasy Kit). Samples were pulse spun for 15 seconds and flow through discarded. The remaining 300 μL of samples were transferred to appropriate

columns and spinning repeated. Columns were washed with 350 μL RW1 (RNeasy kit) and flow through discarded. Then 70-80 μL of DNAse was carefully added to the membrane of each column and samples incubated at RT for 30 minutes. Columns were again washed with 350 μL RW1 before transferring to fresh collection tubes. Further washing of the membranes were performed, initially with 350 μL of RPE buffer (RNeasy kit) for 15 seconds and then with 500 μL RPE for 2 minutes at 10,000 g. Columns were then transferred into fresh Eppendorf tubes and RNA was diluted in 30 μL of nuclease-free water, which was added to each sample and spun for 1 minute at 10,000 g. RNA samples in Eppendorfs were stored at -80 °C until needed.

2.33 RNA-SEQ ANALYSIS

Illumina sequencing was performed on the NextSeq 500 sequencing platform using the v2.5 150 cycles mid output flow cell, which produced 75 bp single reads. Reads where mapped to the Mus musculus reference genome. Read counts were quantified using HTSeq-count. Differentially expressed genes between biological conditions were detected using the DESeq2 plugin in R ($p_{adj} < 0.05$). Comparison was performed between *C. albicans* stimulated and unstimulated macrophages in both vancomycin treated and untreated groups.

2.34 QRT-PCR

To reverse transcribe RNA to cDNA, 9 μL of RNA sample was added to 1 μL reverse transcriptase and 10 μL of 2x Buffer (ThermoFisher). The reaction was run for 1 hour at 37 °C and then 95 °C for 5 minutes. The SYBR Green RT Master mix (ThermoFisher) was used for qPCR. For each qPCR, 1 μL of cDNA was 10 μL of 2X SYBR Green Master Mix (ThermoFisher), 1 μL forward/reverse

primers (Table 2.5) and 7 μL water. The PCR was conducted on the ABI PRISM 7900HT Sequence Detection System. Relative expression was calculated relative to expression of GAPDH.

Table 2.5. List of primers used for our qRT-PCR.

Gene	Forward primer 5'-3'	Reverse Primer 5'-3'
Arg2	GATCGGCTGATTGGCAAAAGG	ATGCTGTTGTGAAAGGTGCC
Nlrp3	AGCCAGAGTGGAATGACACG	TCACCTCTCGGCAGTGGATA
Mir155hg	GCTTGCTGAAGGCTGTATGC	CGAGAATGGCCGTCCTGAAT
Gapdh	AACTTTGGCATTGTGGAAGG	ACACATTGGGGGTAGGAACA
Macir	TGGGATTTAGTCTGGCGTG	TGGAGTGAGCCCTCTTACCT
Il-1β	TGGCAACTGTTCCTG	GGAAGCAGCCCTTCATCTTT

2.35 STATISTICS

Statistical analysis was performed on at least three biological replicates using Prism 9.4.1. Data were presented with mean ± stand error of the mean. Differences between two groups was evaluated using Student's t-test and differences between three or more groups was performed using one-way analysis of variance (one-way ANOVA) with Tukey's multiple analysis test using Prism 9 (GraphPad Software, Inc. USA). Specific test details are in figure legends.

3 VANCOMYCIN PRE-TREATMENT OF MACROPHAGES IMPAIRS *C. ALBICANS* KILLING AND ACTIVATION OF INFLAMMATORY PATHWAYS

3.1 INTRODUCTION

Macrophages are mononuclear innate immune cells that provide first line defence against invading microbes and contribute to tissue repair. Tissues are continuously seeded with new macrophages differentiating from circulating monocytes, but there are also long-lived resident macrophages, that are present for most of the organisms' existence (Gray and Farber, 2022). As professional phagocytes, macrophages recognise and engulf their targets by phagocytosis. As the phagosome matures, the phagosomal environment becomes increasingly hostile. Pathogens face among others nutritional, oxidative and nitrosative stresses which all contribute to the antimicrobial potency leading to their elimination (Bojang et al., 2021). Intestinal macrophages for example play an important role in maintaining host-microbe symbiosis thus contributing to maintaining fungal growth to commensal levels in the gut (Chikina et al., 2020, Smith et al., 2011). Also, a macrophage subset found within the distal colon was shown to maintain gut integrity by limiting absorption of fungal toxins and metabolites, which otherwise induce apoptosis in epithelial cells and compromises gut barrier function (Chikina et al., 2020). Consequently, depletion of intestinal macrophages was associated with increased gut fungal burden and leaky gut barrier which led to increased dissemination of *Candida spp*. into the blood and exacerbated sepsis in mice (Hiengrach et al., 2022a). Macrophages also play a key role in recruiting other immune cells to the site of infection through cytokine release.

Inflammasome activation, which leads to the cleavage and release of mature IL-1β and IL-18 from the cells to recruit other inflammatory cells and contribute to the overall inflammation is also a conserved host response to infection (Gross et al., 2009). Inflammasome activation can trigger the activation of pyroptosis, a lytic cell death pathway (He et al., 2015). Gasdermin D cleavage is a key step in this process, and its N-terminal portion, which forms pores in the inner macrophage membrane also has antibacterial properties (He et al., 2015). The released contents of the dying cell also induce inflammation, which contributes to the recruitment of other immune cells that help to clear the infection and initiate homeostasis. Consequently, pyroptosis is a beneficial host response in such instances (Fink and Cookson, 2007). However, *C. albicans* hijacks this pathway to initiate its escape from macrophages to continue disseminating to other cells and organs so it is less favourable to the host in this context (Uwamahoro et al., 2014). These reports highlight the importance of macrophages within the gut.

Antibiotics disrupt host microbiota, reducing bacterial abundance and complexity and this has wide-reaching effects on host immune system (Erny et al., 2015, Drummond et al., 2022). For instance, antibiotic treatment of mice caused reduced microbiota complexity that led to defective maturation, differentiation, and function of microglial cells (Erny et al., 2015). Similarly, limiting microbiota complexity in neonatal mice by treating their pregnant mothers with antibiotics caused impaired production of neutrophils (granulocytosis) and increased their susceptibility to sepsis (Deshmukh et al., 2014). Furthermore, antibiotic treatment of mice has been shown to cause mucosal macrophages to become hyper-responsive to bacteria and polarize CD4+ T cells to become T_H1 cells, which increases susceptibility to infections requiring other T_H type responses for protection (Scott et al., 2018). Together, these studies show the effects of antibiotic treatment on immune cells including macrophages. However, none of these studies examined the effects of antibiotics on macrophage

function in the context of fungal infections even though prolonged antibiotics use is a risk factor for developing fungal infections.

Therefore, the aim of this chapter is to examine the effects of vancomycin on key macrophage functions. Firstly, vancomycin's effect on macrophage killing of *C. albicans* was assessed before broadly assessing phagocytosis of *C. albicans* and other microbes/microbial particles. The chapter then investigated vancomycin's effect on transcriptional changes with or without infection with *C. albicans*. Activation of the inflammasome signalling pathway was also investigated together with macrophage death rates in this chapter.

3.2 RESULTS

3.2.1 Vancomycin does not affect *C. albicans* growth

Vancomycin treatment of mice and subsequent challenge with *C. albicans* caused a fungal bloom in the gut (Drummond et al., 2022). Vancomycin treatment of patients have also been shown to be associated with candidiasis in a hospital setting (Russo et al., 2015). To ascertain that vancomycin had no direct effects on *C. albicans* that may enhance their growth or decreased killing, we first grew different strains of *C. albicans* in different concentrations of vancomycin and monitored their growth rate over 24 hours. There was no defect or enhancement of growth in any of the strains and in all conditions evaluated [Fig 3.1A] suggesting that vancomycin does not directly affect the growth of *C. albicans*.

Next, I investigated if vancomycin binds directly to *C. albicans* by staining with a fluorescently tagged vancomycin and there was no evidence of vancomycin binding to *C. albicans* but rather there was extensive binding to macrophages [Fig. 3.1B].

Finally, we assessed hyphal formation by *C. albicans* in the presence of vancomycin and again observed no differences in hyphal formation at 1 hour [Fig. 3C], 2 hours [Fig. 3D] and 3 hours [Fig. 3E] post co-incubation. Taken together, these data show that vancomycin has no direct effect on *C. albicans* growth or hyphal formation.

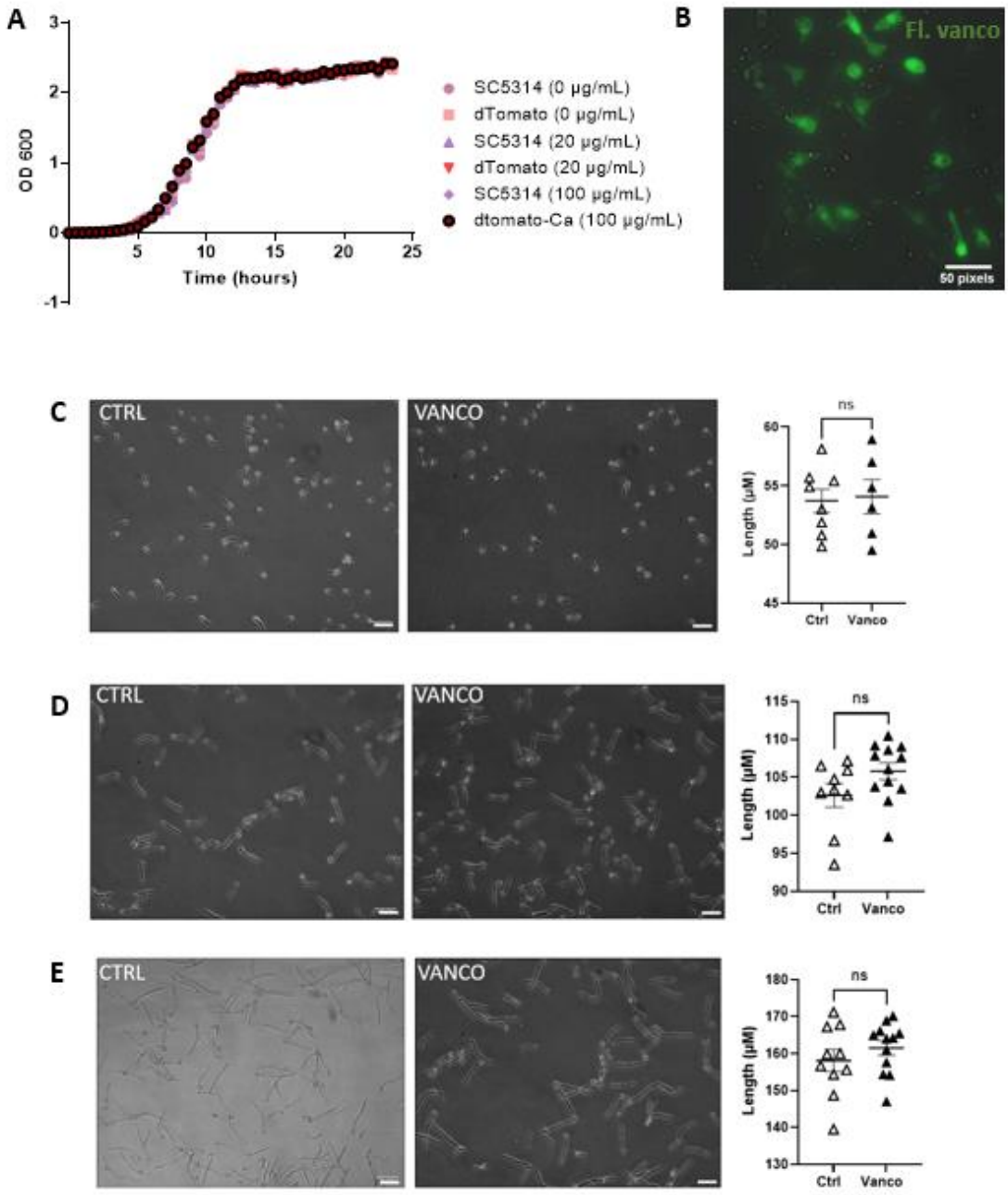

Figure 3.1. Investigating the effects of vancomycin on *C. albicans*. (A) Different strains of *C. albicans* were grown in the presence of a range of vancomycin concentrations or left untreated and growth was measured over 24 hours. (B) Macrophages and *C. albicans* were incubated with a fluorescently tagged vancomycin and binding was assessed using microscopy. *C. albicans* was incubated with 20 µg/ml of vancomycin and hyphal length measured after 1 hour (C), 2 hours (D) and 3 hours (E). Hyphal length was assessed in 3 independent repeats counting more than 50 cells per experiment. Each data point represents the average length in a field of view. Data are means ± SEM. Student's t-test was used to analyse data (ns - not significant).

3.2.2 Vancomycin affects macrophage killing of *C. albicans.*

Having ruled out any direct effects of vancomycin on *C. albicans*, we then investigated if vancomycin affects macrophage anti-fungal responses. Antibiotics have been shown to have immunosuppressive effects on immune cells. Erythromycin and azithromycin exert their immunosuppressive effects on neutrophils by inhibiting chemotaxis, neutrophil elastase (essential for NET formation), and oxidative burst (Pasquale and Tan, 2005, Saiman et al., 2003). Other antibiotics such as tetracycline, macrolides and fluoroquinolones have all been shown to suppress proinflammatory cytokine production to dampen immune responses (Pasquale and Tan, 2005). Additionally, β-lactam antibiotics have also been reported to suppress phagocytosis although there are conflicting reports regarding this effect (Miller and Singer, 2022). To determine if vancomycin pre-treatment affected the killing efficiency of macrophages during *C. albicans* infection, we differentiated macrophages in vancomycin media then challenged them with *C. albicans* yeast for 2 hours. Macrophages were lysed and *C. albicans* viability was quantified using Alamar Blue dye. Vancomycin pre-treated macrophages had 20-25% less killing than control macrophages, thus clearly demonstrating impaired killing [Fig. 3.2A].

To determine if this impaired killing is due solely to prolonged exposure (i.e., 5 days) to vancomycin or whether short-term exposure could induce similar effects, we treated fully differentiated macrophages with high dose of vancomycin (100 μg/ml) for 6 hours and infected them with *C. albicans* as previously. Again, the vancomycin pre-treated macrophages had a killing defect with approximately 40% less killing than controls [Fig. 3.2B]. Together these results demonstrate that vancomycin causes a killing defect to macrophages.

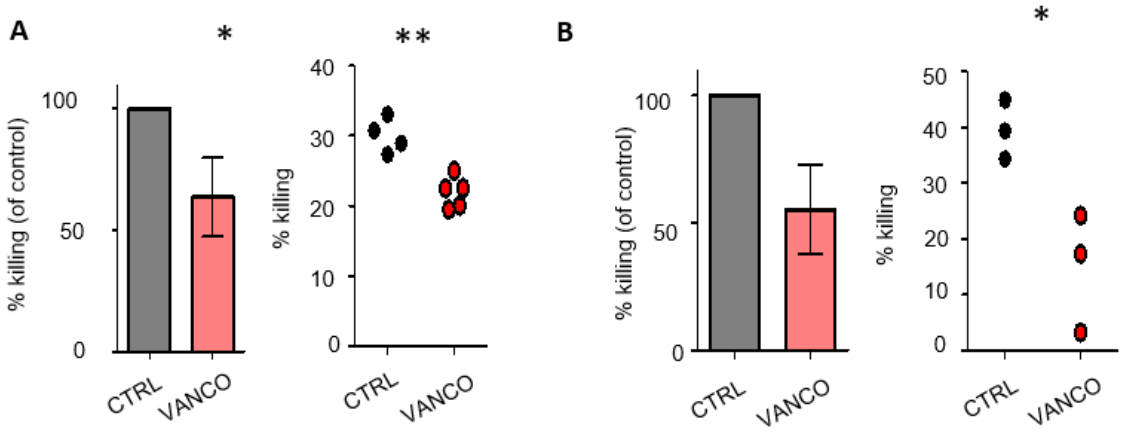

Figure 3.2. Vancomycin treatment caused decreased killing of *C. albicans* by macrophages. (A) Macrophages differentiated in 20 μg/ml of vancomycin for 5 days and challenged with *C. albicans* for 2 hours. Viable cells were quantified and expressed relative to untreated controls. (B) Differentiated macrophages were treated with high dose vancomycin for 6 hours and then challenged with *C. albicans* yeast as before. The bar charts represent percentage killing relative to untreated controls and the dot plots represents percentage killing in both groups. Data are means ± SEM of at least 3 biological replicates. Student's t-test was used to analyse data (* $P < 0.05$; ** $P < 0.005$).

3.2.3 Vancomycin does not affect macrophage differentiation and proliferation.

To investigate if the effects of vancomycin on macrophages was mediated by affecting differentiation and proliferation, bone marrow was flushed from the hind limbs of mice and equal amounts seeded in tissue culture flasks with or without vancomycin treatment. After 5 days of differentiation, macrophages were collected from each condition and viable cells were counted. No difference in numbers was seen between vancomycin treated and untreated macrophages (Fig. 3.3A) suggesting that vancomycin exerts its effect on macrophage function rather than numbers. Although macrophage numbers were unaltered, we wanted to investigate whether macrophages differentiated in the presence of vancomycin had any maturation defects by assessing expression of macrophage maturation markers. Using flow-cytometry, vancomycin pre-treated macrophages had similar expression of CD11b [Fig. 3.3B], MHCII [Fig. 3.3C] and F4/80 [Fig. 3.3D] compared to untreated controls.

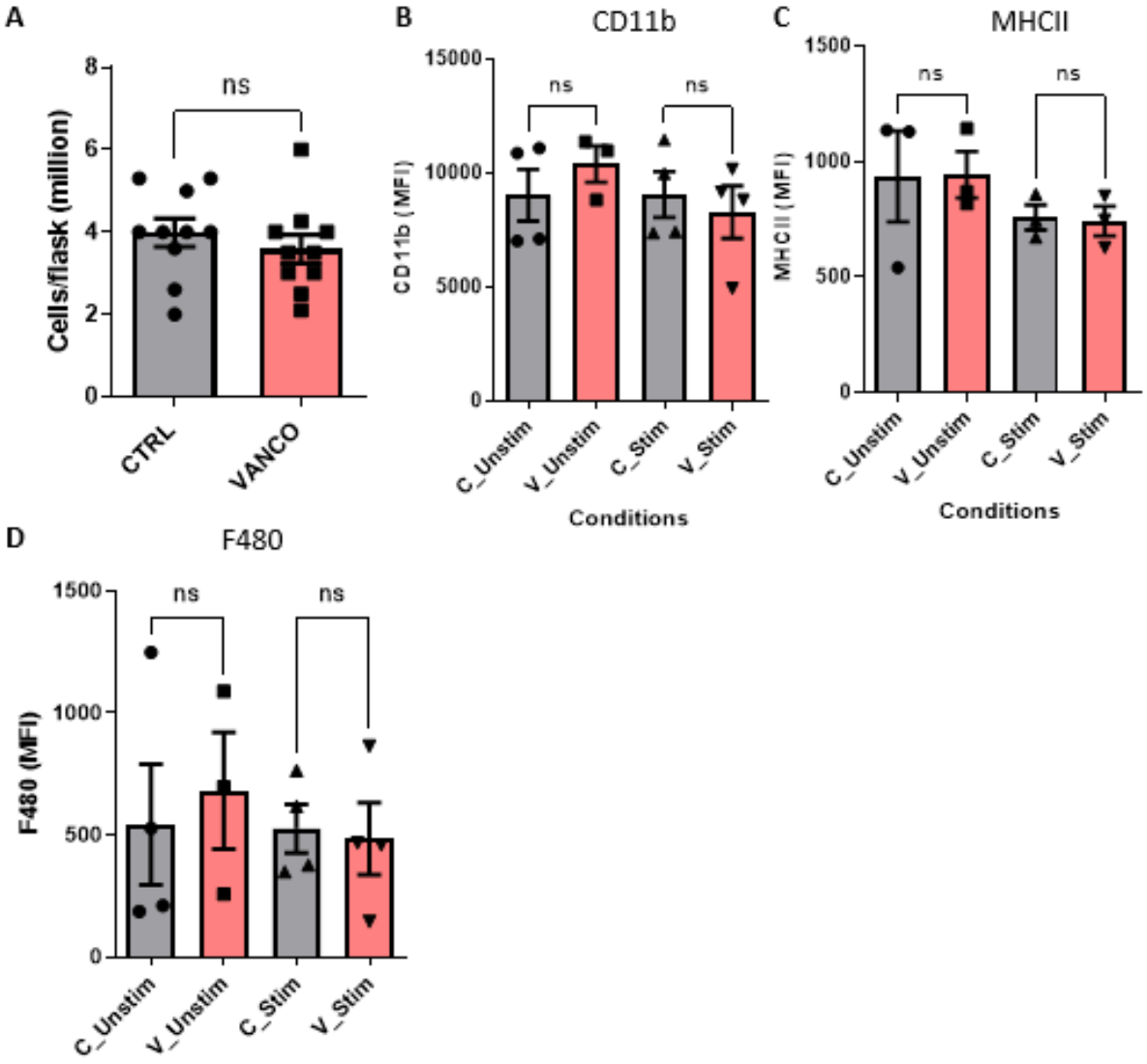

Figure 3.3. Vancomycin did not affect macrophage proliferation or maturation. (A) Macrophages numbers were counted after 5 days of differentiation. (B-D) Macrophage maturation markers were quantified using flow cytometry after 5 days of differentiation. Some macrophages were stimulated with *C. albicans* yeast for 2 hours. Data are means ± SEM of 3-4 biological replicates. Data points in number of cells per flask in 3 independent experiments. Student's t-test was used to analyse data (ns not significant).

3.2.4 Recognition and phagocytosis of *C. albicans* is unaffected by vancomycin pre-treatment

The first step of fungal killing is uptake via phagocytosis and formation of mature phagolysosome. Studies have shown antibiotics do affect phagocytosis (Pasquale and Tan, 2005) and vancomycin has also been shown to disrupt autophagy flux resulting to the accumulation of LC3II and p62 proteins

(Ha et al., 2015). LC3-associated phagocytosis is a novel non-canonical autophagy pathway whereby LC3 is anchored to the phagosome membrane and is important for the clearance of pathogens and apoptotic cells (Heckmann et al., 2017). To determine whether vancomycin influences *C. albicans* recognition and phagocytosis by macrophages, BMDMs were challenged with fluorescent *C. albicans,* and uptake assessed by flow cytometry at the indicated times. The effects of vancomycin on phagocytosis of *E. coli* K-12 bioparticles and live *Salmonella Typhimirium* were also investigated to determine if bacterial phagocytosis was affected by vancomycin treatment and whether being dead or live would influence phagocytosis of bacteria.

3.2.5 Unopsonised *Candida*

To understand if the impaired killing observed is potentially due to reduced phagocytosis, we first probed for the direct effects of vancomycin on *C. albicans* phagocytosis by challenging macrophages with unopsonised *C. albicans* yeast. Macrophage association to *C. albicans* was first quantified using flow cytometry and there was no difference seen between vancomycin treated and untreated controls [Fig. 3.4A]. Attachment of *C. albicans* to macrophages [Fig. 3.4B] and complete phagocytosis [Fig. 3.4C] was then assessed from that population and similar proportions were seen in both vancomycin treated and untreated controls. Phagocytosis of *C. albicans* increased between 30 minutes and 1 hour in both treatment conditions [Fig. 3.4C] suggesting that vancomycin does not affect direct macrophage-*Candida* interaction and engulfment.

3.2.6 Opsonised *Candida*

Next, I wanted to investigate if phagocytosis of opsonised *C. albicans* might be affected since most *C. albicans* that macrophages would encounter *in-vivo* would likely be opsonised. For this,

macrophages were challenged with serum opsonised *C. albicans* yeast. There was a difference observed in overall macrophage association to *C. albicans* at 60 minutes post infection with control macrophages having higher association [Fig. 3.4D]. However, there was no difference in the proportion of that population that had either surface attached *C. albicans* [Fig. 3.4E] or had completely phagocytosed *C. albicans* [Fig. 3.4F] between vancomycin treated and untreated macrophages, suggesting that phagocytosis of opsonised live yeast were largely unaffected in the vancomycin-treated macrophages. Phagocytosis levels were also similar at 30 minutes and 1 hour suggesting that phagocytosis is rapid and reached a plateau at 30 minutes with opsonised *C. albicans*. Together, these results suggest that vancomycin pre-treated macrophages were able to recognise and phagocytose opsonised *C. albicans* as well as controls.

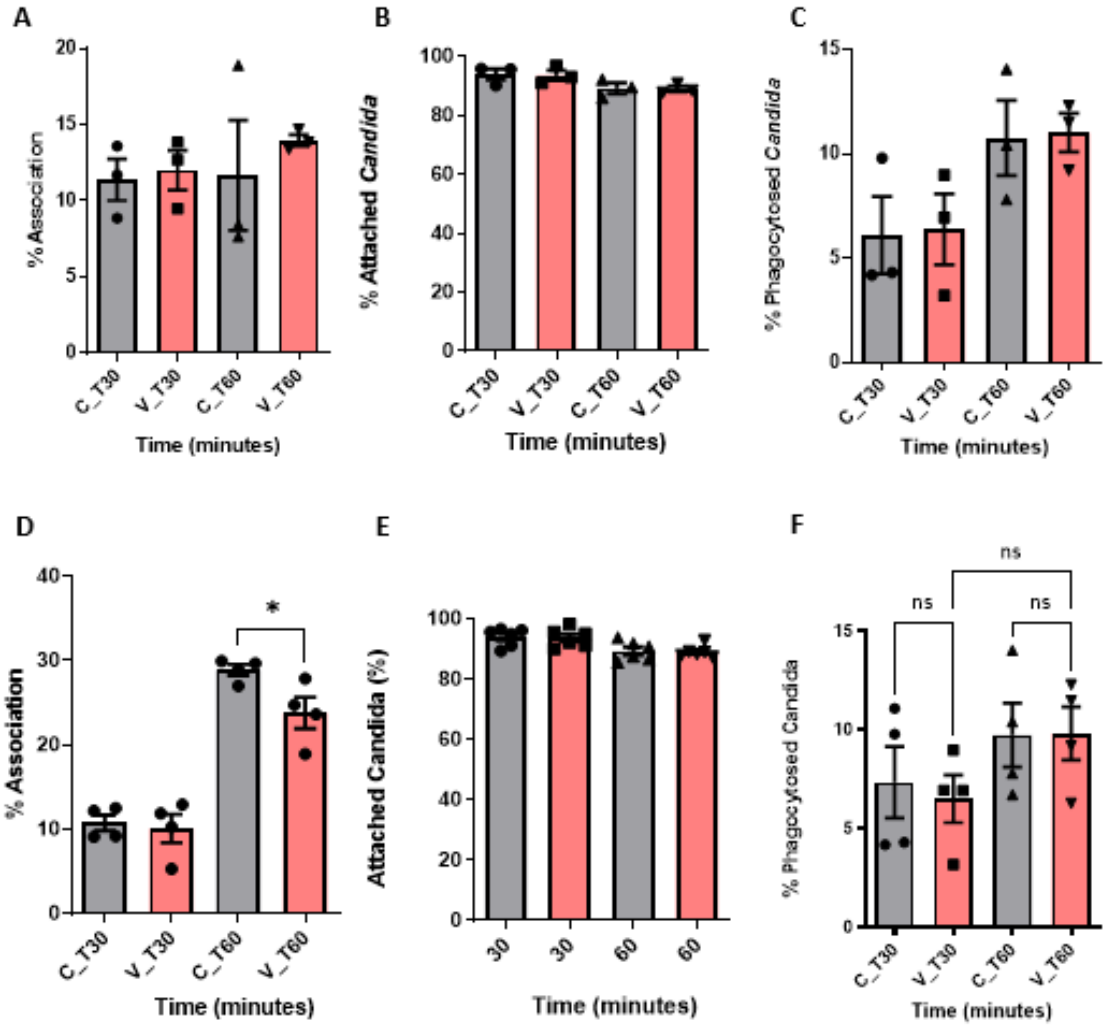

Figure 3.4. Vancomycin does not affect macrophage recognition and phagocytosis of *C. albicans*. (A) Macrophages were challenged with unopsonised *C. albicans* yeast and interaction (association) was assessed at 30 minutes and 1 hour. Surface attached (B) and phagocytosed (C) *C. albicans* were also assessed at the same times. (D) Association was also assessed when macrophages were challenged with serum opsonised *C. albicans*. Surface attached (E) and phagocytosed opsonised *C. albicans* (F) was also quantified. Data are means ± SEM of 3 or more biological replicates. Student's t-test was used to analyse data (ns not significant; * $P < 0.05$).

3.2.7 Vancomycin treatment did not affect phagocytosis of live-*Salmonella*

Since phagocytosis of *C. albicans* yeast was unaffected, I assessed if phagocytosis of live bacteria would be compromised because these are recognised by different receptors and could potentially

indicate if vancomycin influenced specific PRRs. To this end, BMDMs were challenged with mCherry-fluorescing *Salmonella* and association was assessed by flow cytometry. There was no difference in macrophage association with *Salmonella* between vancomycin treated and untreated macrophages [Fig. 3.5A]. Although it was not possible to discriminate between extracellular and internalised *Salmonella* in this assay, the results suggest that recognition (association) of live organisms is unaffected by vancomycin pre-treatment.

3.2.8 Vancomycin does affect the phagocytosis of *E. coli* K-12 bioparticles

To determine if phagocytosis might be affected in other microorganisms, BMDMs were challenged with fluorescent *E. coli* K-12 bioparticles and phagocytosis assessed by quantifying fluorescence of only intracellular *E. coli* (refer to methods). Vancomycin pre-treated macrophages showed significant reduction in *E. coli* bioparticle uptake compared to control macrophages [Fig. 3.5B], suggesting that in this case vancomycin does impair macrophage phagocytosis. Together, these results suggest that vancomycin may be affecting receptors specific for *E. coli*/bacterial uptake. However, this effect might be due to these particles being non-live.

Despite vancomycin having no significant effects on the phagocytosis of live microorganisms, it was hypothesised that autophagy might be affected as shown previously in a study (Ha et al., 2015). To this end, protein levels of p62 and LC3II were measured in cell lysates of vancomycin treated or untreated macrophages with or without *C. albicans* stimulation. There was no significant increase of both proteins in vancomycin treated macrophages compared to untreated controls (Fig 3.5C and D). However, with *C. albicans* stimulation, LC3 was increased albeit insignificantly in vancomycin pre-treated macrophages compared to controls (Fig 3.5D). The levels of p62 protein were insignificantly

increased in vancomycin pre-treated macrophages but there was no further increase with *C. albicans* stimulation [Fig. 3.5C]**.** These findings suggest that during *C. albicans* stimulation, vancomycin pre-treated macrophages potentially increase autophagosomes without blocking autophagic flux.

3.2.9 Pre-treatment of BMDMs with vancomycin does not affect phagosome maturation

Although our data show no difference with phagocytosis, there was reduction in fungal killing. We therefore examined processes happening post-phagocytosis that may contribute towards reduced killing. For that, we measured the maturation of the phagosome environment using the lysotracker-Red dye, which is a cell permeable dye that fluoresces bright red when in an acidic compartment, and is routinely used to quantify phagosome maturation (Fu et al., 2018). Because live *C. albicans* is known to suppress phagosomal acidification through actively excreting ammonia generated from amino acid catabolism into the phagosomal space (Vylkova and Lorenz, 2017), BMDMs were challenged with heat-killed *C. albicans* to tease out any differences in phagosome acidification between vancomycin treated and untreated macrophages and fluorescence was quantified from live cell images (Fig. 3.5E). There was no difference seen between vancomycin treated and untreated macrophages. This indicates that phagosome acidification is unaffected by vancomycin pre-treatment but other maturation markers such as recruitment of LAMP1 to the phagolysosome would confirm if maturation is unaffected too.

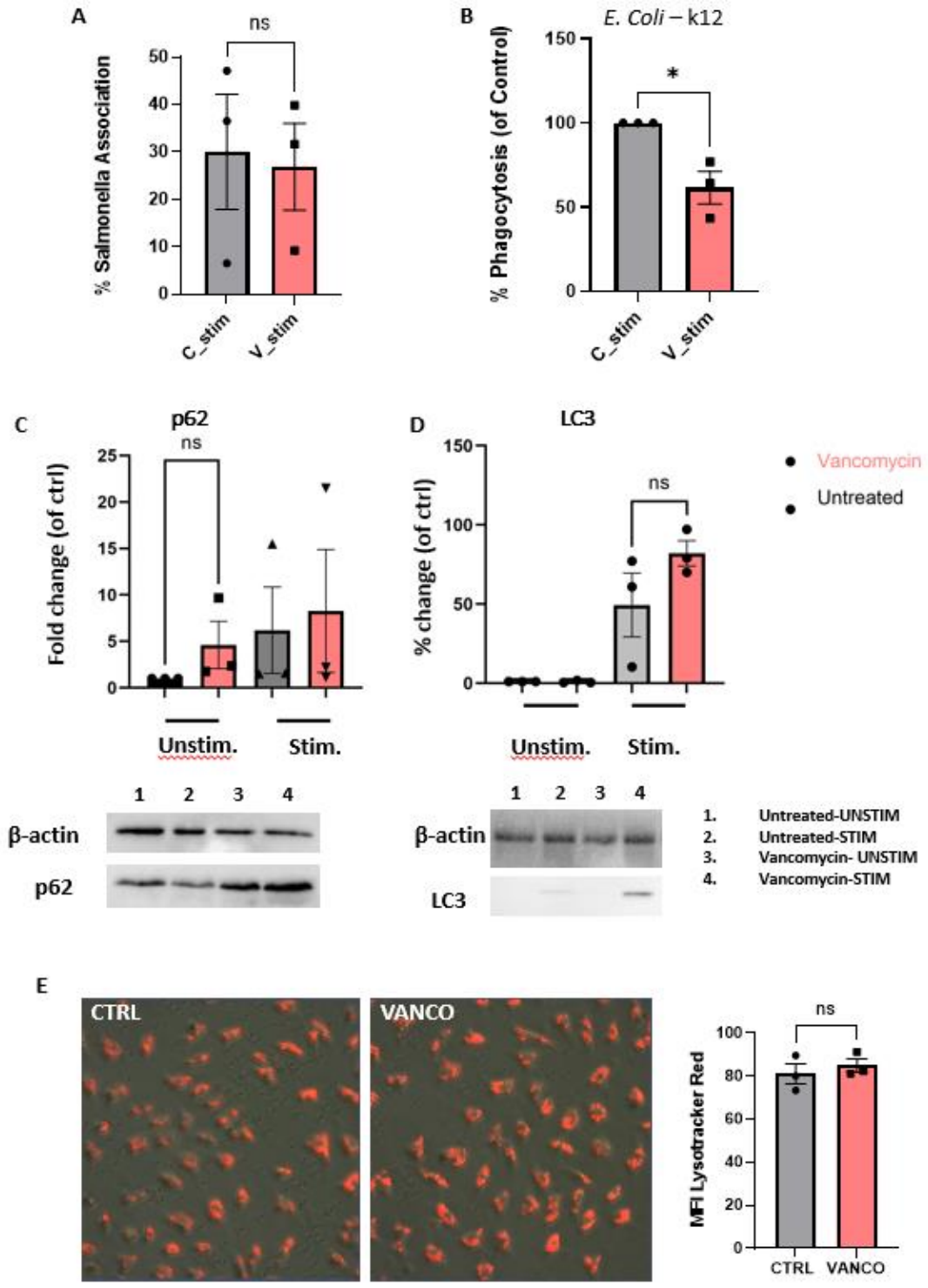

Figure 3.5. Vancomycin affects phagocytosis of *E. coli* particles but not live-*Salmonella*. (A) Macrophages were challenged with live *Salmonella* and association with macrophages assessed using flow cytometry. (B) Phagocytosis of *E. coli* k-12 particles was also assessed. Autophagy related proteins (C) p62 and (D) LC3 were assessed in cell lysates. (E) Vancomycin did not affect phagosome maturation assessed using the Lysotracker red dye.

Data are means ± SEM of 3 biological replicates. Student's t-test was used to analyse data (ns not significant; * $P < 0.05$).

3.2.10 Our RNAseq dataset reveals important transcriptional changes induced by vancomycin pre-treatment of macrophages during *C. albicans* infection

Since there was no difference in phagocytosis and phagosome maturation, we next broadly examined how vancomycin affected macrophage transcriptional responses using RNAseq. Sequencing was performed on four distinct groups [Fig. 3.6A]; untreated macrophages, untreated macrophages stimulated with *C. albicans*, vancomycin pre-treated macrophages, and vancomycin pre-treated macrophages stimulated with *C. albicans* for 2 hours only. Constructing a PCA plot of transcripts revealed that groups separated based on infection, which indicates that vancomycin treatment alone does no induce significant transcriptional changes compared to untreated controls [Fig 3.6B]. *C. albicans* infection caused transcriptional changes in both vancomycin treated and untreated macrophages compared to unstimulated controls. Next, I looked at the transcriptional changes occurring in vancomycin treated macrophages during infection by comparing vancomycin treated macrophages that were unstimulated against macrophages stimulated with *C. albicans*. There were 128 genes differentially expressed during infection. When stimulated and unstimulated controls were compared, there were 120 upregulated genes [Fig. 3.6C]. There were 76 genes differentially expressed in both the vancomycin treated and untreated groups and Kyoto Encyclopedia of Genes and Genomes (KEGG) analysis of these genes unsurprisingly identified pathways involved in macrophage activation such as TNF, NF-Kappa B, IL-17, and NOD-like receptor signalling pathways to be upregulated [Fig 3.6D]. The control group had 44 uniquely (Table 3.1) expressed genes while vancomycin treated group had 52 differentially expressed genes (Table 2.8). Taken a closer look at the uniquely expressed genes, glycolysis related genes *Pfkfb3* and *Eno1* were differentially

upregulated in control macrophages [Fig 3.6C and Table 3.1]. This group also had differentially expressed genes involved in control of pro-inflammatory function of macrophages (*Rora*), lysosome biogenesis (*Tfeb*), and biosynthesis of plasmalogens (*Tmem189*).

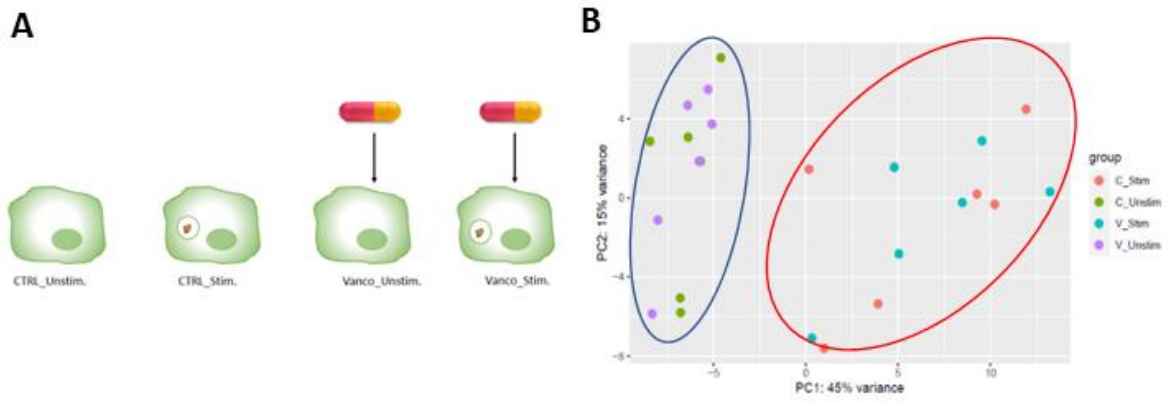
A
CTRL_Unstim.
CTRL_Stim.
Vanco_Unstim.
Vanco_Stim.
B
PC2: 15% variance
PC1: 45% variance
group
C_Stim
C_Unstim
V_Stim
V_Unstim

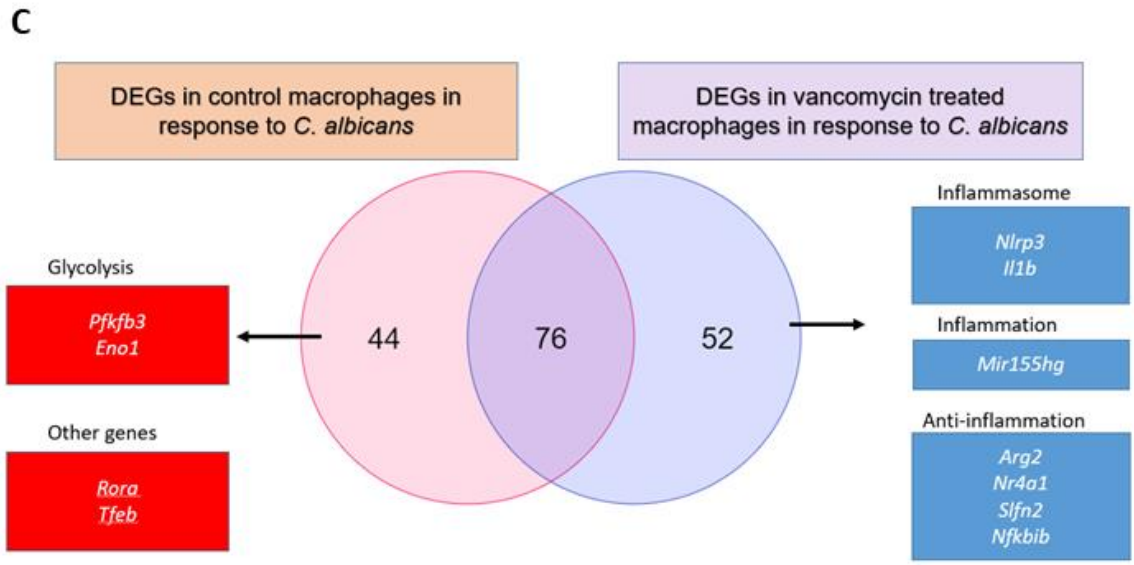
C
DEGs in control macrophages in response to C. albicans
DEGs in vancomycin treated macrophages in response to C. albicans
Glycolysis
Pfkfb3
Eno1
Other genes
Rora
Tfeb
44
76
52
Inflammasome
Nlrp3
Il1b
Inflammation
Mir155hg
Anti-inflammation
Arg2
Nr4a1
Slfn2
Nfkbib

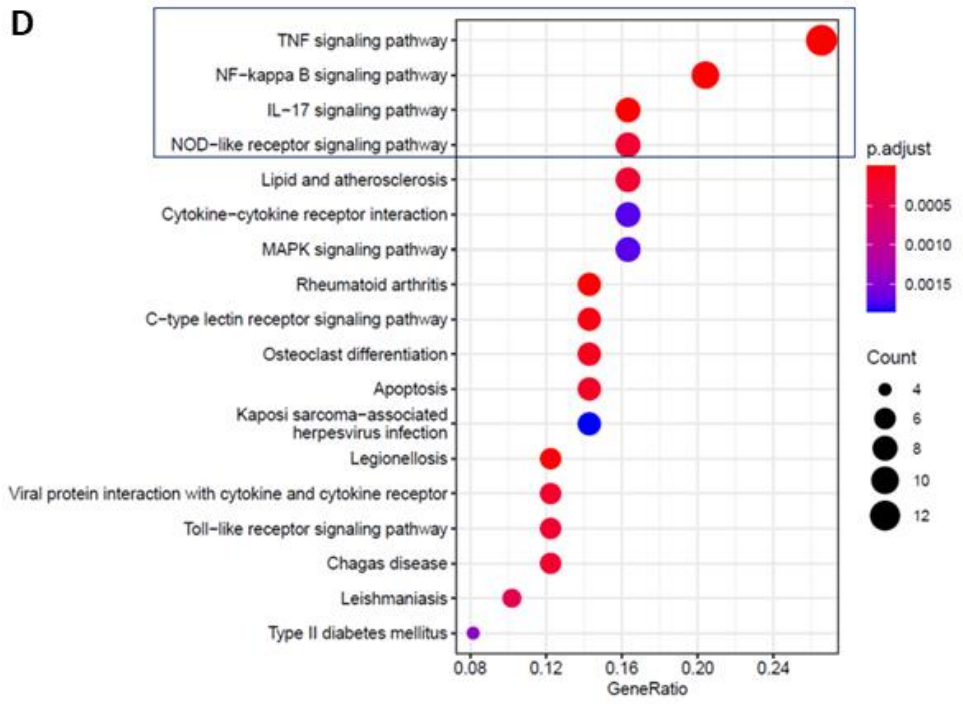
D
TNF signaling pathway
NF-kappa B signaling pathway
IL-17 signaling pathway
NOD-like receptor signaling pathway
Lipid and atherosclerosis
Cytokine-cytokine receptor interaction
MAPK signaling pathway
Rheumatoid arthritis
C-type lectin receptor signaling pathway
Osteoclast differentiation
Apoptosis
Kaposi sarcoma-associated herpesvirus infection
Legionellosis
Viral protein interaction with cytokine and cytokine receptor
Toll-like receptor signaling pathway
Chagas disease
Leishmaniasis
Type II diabetes mellitus
0.08
0.12
0.16
0.20
0.24
GeneRatio
p.adjust
0.0005
0.0010
0.0015
Count
4
6
8
10
12

Figure 3.6. Vancomycin treatment causes upregulation of inflammasome related genes during *C. albicans* infection. (A) Macrophages conditions sequenced. (B) PCA plot of transcripts (C) Differentially regulated genes during *C. albicans* infection. (D) KEGG analysis of the commonly regulated genes in untreated macrophages and vancomycin treated macrophages during *C. albicans* infection. Comparison was done from 6 biological replicates.

On the other hand, the vancomycin group had several upregulated genes that participate in anti-inflammatory mechanisms in macrophages [Fig 3.6C]. For instance, *Nfkbib* prevents *Nfkb* translocation to the nucleus by trapping it in the cytoplasm (Chen et al., 2003). *Nr4a1*, which induces an anti-inflammatory state in macrophages was also upregulated (Koenis et al., 2018). These macrophages also upregulated *Slf2*, known to maintain a quiescent state in T cells and monocytes (Berger et al., 2010). *Arg2* was also uniquely upregulated in the vancomycin treated group. *Arg2* has an anti-inflammatory role and acts within the mitochondria to suppress the secretion of IL-1β [Fig 3.6C and 3.7A]. Furthermore, there was decreased expression of the long non-coding RNA, F630028O10Rik, which has been shown to promote inflammasome and activation of pyroptosis in microglial cells (Xu et al., 2020). These are indicative of the macrophage's attempts to suppress the inflammation in vancomycin treated macrophages during infection. Additionally, there were other indications of mitochondrial and oxidative stress. For instance, there was a reduction in *Klf16* expression, which has been linked to increased mitochondrial stress and ROS burden (Sun, 2021). The *Macir* gene, that enhances inflammatory resolution in macrophages was downregulated in vancomycin treated macrophages during infection (Table 3.2). Together these results indicate the highly pro-inflammatory state of these macrophages, which the cells are actively trying to reverse by the increased expression of genes known to control inflammation.

Table 3.1. Genes differentially expressed only in the control group.

Uniquely expressed genes in the control group	
Upregulated	Downregulated
Adamts1	*A630072M18Rik*
Btg2	*Atg101*
Cd28	*Bag3*
1700017B05Rik	*Camk2g*
Cd69	*Dcaf17*
Cxcr4	*Ddx20*
Eno1	*Id1*
Etv3	*Mafb*
F10	*Myc*
Gch1	*Pdxdc1*
Gm20604	*Rusf1*
Jmjd6	*Sesn1*
Kdm6b	*Zfp217*
Klf9	*Zfpl1*
Mapkapk2	
Ndrg1	
Nfe2l2	
Olr1	
Pfkfb3	
Pmp22	
Rassf1	
Rell1	
Rora	
Ssbp3	
Tbc1d2b	
Tfeb	
Tmem189	
Tnip1	
Zc3h12c	
Zfp292	

Table 3.2. Genes differentially expressed only in the vancomycin treated group.

Uniquely expressed genes in the vancomycin group	
Upregulated	Downregulated
Rhov	*Exoc8*
Gem	*Klf16*
Slfn2	*Sema4c*
Tent5c	*Dclre1b*
Samd8	*Ccdc157*
Plk2	*2310011J03Rik*
Sh2b2	*Enc1*
Gnl3	*A130010J15Rik*
Hnrnpll	*F630028O10Rik*
Sde2	*Macir*
Rel	*Thbd*
Nlrp3	*Nuak1*
Exoc3l4	
Slc11a2	
Cdc42ep2	
Arg2	
Slc7a11	
Gadd45g	
Gpr137b-ps	
Birc3	
Dnmt3aos	
Nr4a1	
Ier5	
Flrt3	
Il1b	
Gm43430	
Amz1	
Ubc	
Tank	
Slc2a1	
Irak2	
Samsn1	
Mdm2	

Mir155hg

Egln3

Nfkbib

Cpeb4

Plagl2

Sod2

Fnip1

Interestingly, the vancomycin group also uniquely upregulated genes related to the activation of the inflammasome. Both *Nlrp3* and *Il-1β* were uniquely upregulated in these macrophages suggesting early activation of this pathway in these macrophages compared to untreated macrophages [Fig 3.6C and 3.7A]. To further validate these observations and determine the reproducibility across a wider time frame, the temporal dynamics of *Nlrp3* expression was assessed by qRT-PCR. There was a higher expression of *Nlrp3* in vancomycin pre-treated macrophages at baseline. Both treated and untreated macrophages increased *Nlrp3* expression 2 hours post *C. albicans* stimulation [Fig. 3.7B] but while this returned to baseline levels at 6 hours post infection in untreated macrophages, there was even more robust expression in vancomycin pre-treated macrophages [Fig. 3.7B]. Furthermore, our RNA seq data revealed that vancomycin treated macrophages during infection had increased expression of the microRNA, *Mir*155 [Fig.3.6C and 3.7A], which is associated with chronic inflammatory syndromes such as rheumatoid arthritis (Alivernini et al., 2017). To ascertain the temporal dynamics of this gene, qRT-PCR was performed and there was robust upregulation of this gene in vancomycin treated macrophages at 2 hours post-infection and was sustained at 6 hours post-infection (Fig. 3.7C). In comparison, this gene was continuously downregulated in untreated macrophages suggesting that while these macrophages can resolve the inflammation, vancomycin treated macrophages remain in a hyper-inflammatory state. Taken together, these findings indicate that vancomycin pre-treated macrophages adopt an inflammatory phenotype and may prime the

inflammasome shown by the increased expression of *Nlrp3* and *Il1β* with the former increasing with time.

3.2.11 IL-1β increased in culture supernatant of vancomycin pre-treated infected macrophages

Although the increased expression of inflammasome related genes suggest activation of the inflammasome, the ultimate product of inflammasome activation is the cleavage of pro- IL-1β and pro-IL-18 and the secretion of their mature forms (IL-1β and IL-18) from the cells. To determine if expression led to activation, IL-1β levels were quantified in culture supernatants by ELISA. Vancomycin pre-treatment caused elevated levels of IL-1β in infected macrophages compared to untreated controls (Fig. 3.7D). These findings support the observation of a more robust activation of the inflammasome in vancomycin treated macrophages.

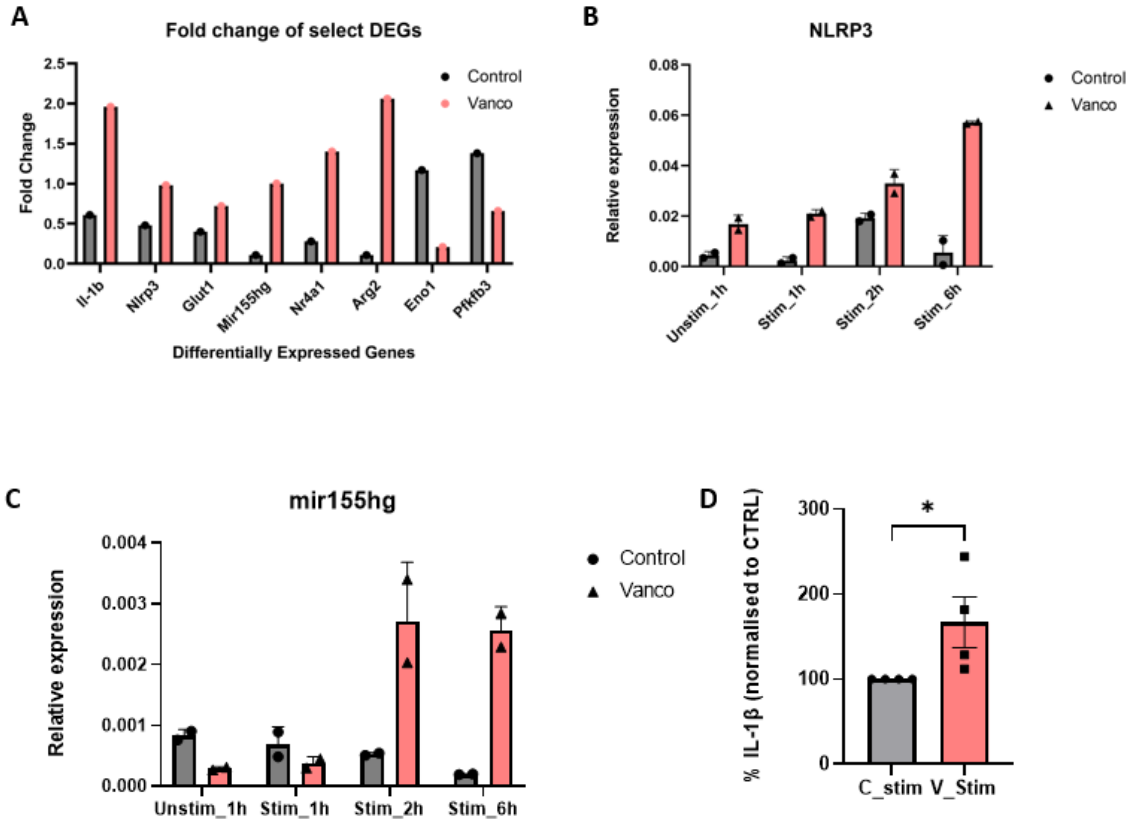

Figure 3.7. **Vancomycin treatment causes more inflammatory gene expression**. (A) Graphical representation of the fold changes of selected genes in controls and vancomycin treated macrophages during infection from RNA-Seq data. The bar chart represents the average of 6 biological replicates. Temporal dynamics of *Nlrp3* (B) and *Mir155* (C) expression in vancomycin treated macrophages during infection quantified by qRT-PCR. qRT-PCR data represents 2 biological replicates with at least 10 technical replicates. (D) IL-1β levels measured by ELISA each data are means ± SEM of 4 biological replicates. Student's t-test was used to analyse data (* $P < 0.05$).

3.2.12 IL-1β and NLRP3 protein levels were not significantly elevated in vancomycin pre-treated macrophages

To further support our earlier findings, protein levels of NLRP3 were measured from cell lysates by western blotting. While the levels of NLRP3 were not significantly elevated, they were consistently

higher in vancomycin treated macrophages infected with *C. albicans* compared to untreated controls [Fig. 3.8A]. Since inflammasome activation causes pyroptotic cell death causing pro-IL-1β (immature) levels to be raised in culture supernatants (He et al., 2015), protein levels of pro-IL-1β were measured in culture supernatants but only a small and insignificant increase was detected in vancomycin treated macrophages infected with *C. albicans* in each experiment [Fig. 3.8B].

3.2.13 Increased levels of Caspase 1 protein were not detected in vancomycin treated cells cell lysates

Caspase 1 is important for the cleavage of pro-IL-1β and pro-IL-18 during inflammasome activation but also plays an important role in cleaving the N-terminal of Gasdermin D, which forms pores in the inner membrane of macrophages during pyroptosis (He et al., 2015). Therefore, caspase 1 levels were measured in cell lysates of vancomycin treated and untreated macrophages with or without infection with *C. albicans* but no change in protein levels were detected in our experiments [Fig. 3.8C].

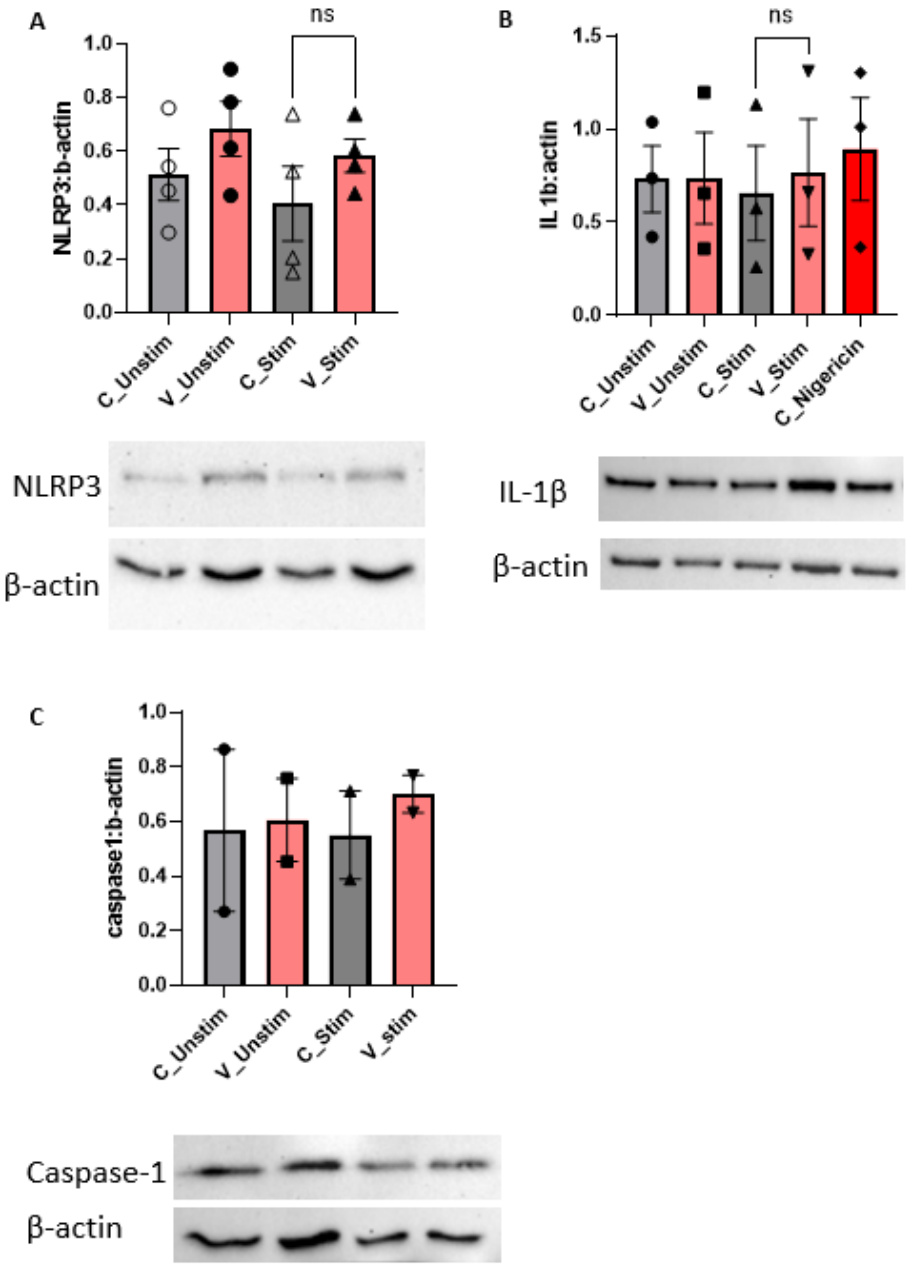

Figure 3.8. **Inflammasome related proteins were not significantly elevated.** (A) Protein levels of NLRP3 in relation to β-actin were measured in cell lysates and compared between conditions. (B) IL-1β levels were measured in culture supernatants and quantified in relation to β-actin. Nigericin was used as a positive control. (C) caspase-1 levels were measured in cell lysates. Data are means ± SEM and each data point represents a biological replicate. Student's t-test was used to analyse data (* $P < 0.05$). Underneath each graph is a representative blot.

3.2.14 Increased macrophage death in infected vancomycin macrophages

Inflammasome activation triggers the pyroptotic pathway leading to macrophage death. To determine the levels of macrophage death between the two populations, we primed macrophages with LPS (50 ng/mL) for 2 hours then infected them with *C. albicans* yeast for 4 hours and then measured lactose dehydrogenase (LDH) levels in culture supernatants. LDH is an intracellular enzyme which is released by cells when they lyse. Unsurprisingly, vancomycin treated macrophages had increased levels of LDH suggesting more macrophage death in this group (Fig. 3.9A). Furthermore, we observed more macrophage rounding off in our time-lapse microscopy images in the vancomycin pre-treated macrophages that were infected with *C. albicans* (Fig. 3.9B and C). Together, these results suggest a higher macrophage turnover when vancomycin pre-treated macrophages are challenged with *C. albicans.*

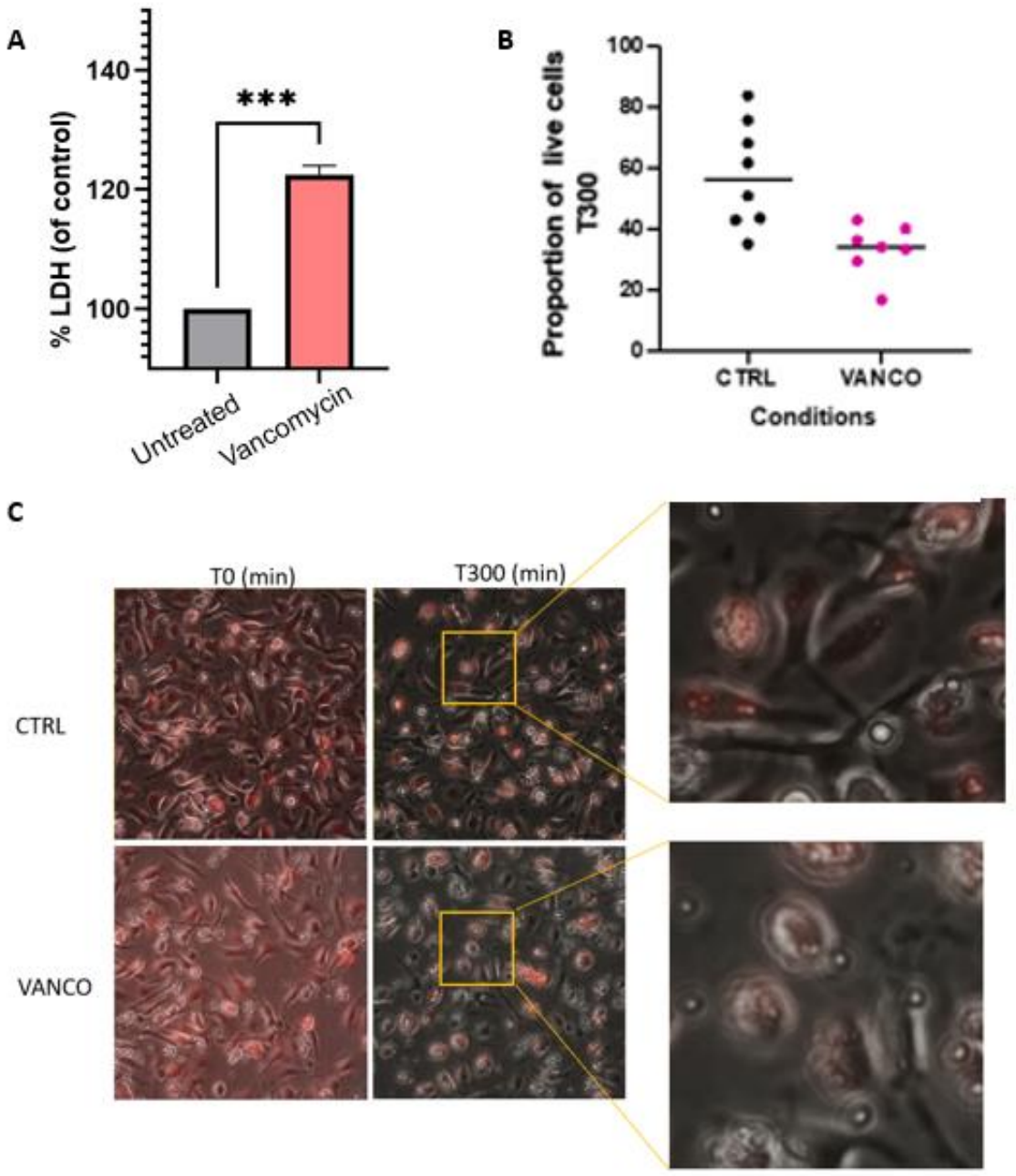

Figure 3.9. **Vancomycin treatment caused increased macrophage death during infection with *C. albicans*.** (A) LDH levels were measured in culture supernatants. (B) Proportion (%) of live macrophage was calculated from microscopic images 5 hours post infection. (C) Representative image of macrophages 5 hours post-infection in the two groups. Data are means ± SEM. Student's t-test was used to analyse data (*** $P < 0.0001$).

3.3 DISCUSSION

Here, I show that vancomycin pre-treatment of macrophages affects their killing efficiency of *C. albicans* without affecting their interaction or phagocytosis of *C. albicans* yeast. Also, presented here is that vancomycin pre-treatment of macrophages induces an early and robust activation of inflammasome related genes and proteins during *C. albicans* infection that did not resolve with time. This corresponded with increased macrophage death during *C. albicans* infection around 6 hours post infection.

Vancomycin pre-treatment of macrophages caused impaired killing of *C. albicans* yeast and interestingly, this impairment was observed in both macrophages treated with vancomycin during differentiation and macrophages exposed to high dose vancomycin for a shorter period post differentiation. This has not been reported before in the context of *C. albicans* but could have significant health implications as it could contribute to the increased candidiasis observed in patients on prolonged antibiotic use. Drummond et al., (Drummond et al., 2022) observed increased growth of *C. albicans* in the gut when vancomycin treated mice were challenged intravenously with *C. albicans*. Although disruption of the microbiota and a leaky gut were strongly linked to their phenotype, the role of macrophages was not investigated and could therefore not be completely ruled out.

Pathogens are killed within phagosomes, but this is preceded by phagocytosis. Conflicting reports exist as to the role of antibiotics on phagocytosis, and this may well be antibiotic or cell type dependent (Miller and Singer, 2022). In this chapter, it was shown that vancomycin pre-treatment of macrophages had no effect on macrophage recognition (association) or phagocytosis of *C. albicans* yeast. This corroborates most studies which show normal or even increased phagocytosis rates with

vancomycin treatment (Tawfik, 1991, Bode et al., 2015). Similarly, it was shown that vancomycin treatment caused increased phagocytosis of *C. albicans* by peritoneal macrophages (Barriga et al., 1996). However, in the latter study, vancomycin was administered at the same time as the *Candida* while we pre-exposed macrophages to vancomycin. This suggests that the effects of vancomycin on macrophages occurs after prolonged exposure or after exposure to high dose vancomycin rather than immediately, potentially explaining the increased susceptibility to candidiasis in patients on prolonged antibiotic use. Furthermore, Muenster *et al*., (Muenster et al., 2021) showed that vancomycin treatment increased phagocytosis of pHrodo *E. coli* particles by intraperitoneal macrophages *in-vivo*, however this increase was diminished in LPS-stimulated mice. Here, vancomycin pre-treated macrophages showed defective phagocytosis of *E. coli* bioparticles but not to live *Salmonella* or *Candida*. This is an interesting observation and suggests that the receptors by which macrophages engulf these live microorganisms may be different from the *E. coli* bioparticles although this was not tested in this study. However, vancomycin has also been shown to block autophagy and increase accumulation of LC3 and p62 proteins in macrophages (Ha et al., 2015). The autophagy pathway is however, partly utilised by LC3-associated phagocytosis (LAP) to clear extracellular particles such as dead cells and pathogens (Heckmann et al., 2017). Accordingly, a slight but insignificant increased protein level of LC3 and p62 were observed in the present study, suggesting protein accumulation and potentially confirming the effects of vancomycin on autophagy by previous studies (Ha et al., 2015) but also indicating that this pathway has no relevance for *C. albicans*.

Although enhanced growth of *C. albicans* by vancomycin treatment would mask macrophage killing efficiency, here, vancomycin had no impact on *C. albicans* growth. Also, vancomycin did not affect proliferation of macrophages as similar numbers were recovered from vancomycin treated and

untreated samples. In contrast, azithromycin treatment caused reduced proliferation in MCF-12A and fibroblast cell lines (Jiang et al., 2019), but very high concentrations were used in that study. Together these results suggest that vancomycin imposes a mechanistic defect rather than affecting macrophage/*C. albicans* numbers.

Microorganisms including *C. albicans* are killed within the phagosomal compartment of macrophages. Phagosome maturation involves a highly acidic compartment needed for efficient killing and elimination (Bojang et al., 2021), however, *C. albicans* is known to suppress phagosomal acidification (Vylkova and Lorenz, 2017), so to maximise acidification, macrophages were infected with heat-killed *C. albicans*, and there was no observed defects in phagosome acidification in vancomycin treated macrophages. Although other maturation markers such as Rab5, Rab7, Rab14 and LAMP1 (Okai et al., 2015) would have to be assessed to completely rule out a maturation defect, we have shown here that phagosome acidification is not the driver of the impaired *C. albicans* killing observed in our experiments.

Interestingly, there was increased expression of general inflammation and inflammasome related genes in our RNA-seq and qRT-PCR data early during infection (2 hours). Activation of the inflammasome was confirmed by increased IL-1β levels in culture supernatants in *C. albicans* infected macrophages pre-treated with vancomycin. *C. albicans* is known to activate the inflammasome and the pyroptotic pathways and several *C. albicans* PAMPs including β-glucan and candidalysin are implicated in priming or triggering Nlrp3 dependent inflammasome activation (Kasper et al., 2018). Although *C. albicans* triggers pyroptosis via inflammasome activation to escape from macrophages (Wellington et al., 2014), intriguingly, the Nlrp3 inflammasome plays a critical role in defence against *C. albicans* especially against mucosal infections. Consequently, increased

fungal burdens and death were seen in mice lacking either IL-1β, the inflammasome adapter protein Asc or Nlrp3 when challenged with *C. albicans* (Hise et al., 2009, Gross et al., 2009, Wellington et al., 2014). These findings reveal the importance of the inflammasome pathway in defence against *C. albicans* but also show the importance of maintaining a delicate balance to prevent increased macrophage turnover and *C. albicans* dissemination. Our data suggests the latter whereby vancomycin seems to exacerbate this induction causing more macrophage death and potentially giving advantage to *C. albicans*.

Furthermore, mir155 was differentially increased in vancomycin pre-treated macrophages during infection lending support to the inflammatory state of these macrophages. This gene, mir155, inhibits the anti-inflammatory action of SHIP1/SOCS-1/BCL axis leading to uncontrolled release of inflammatory cytokines, IL-1β and IL-6 (Alivernini et al., 2017). It also exerts its inflammatory properties by inhibiting the action of LXRα-1, which promotes Arg2 function and activation of the repair pathway [Fig. 3.10]. Together these data indicate a very inflammatory state of macrophages and could lead to more macrophage death by lysis.

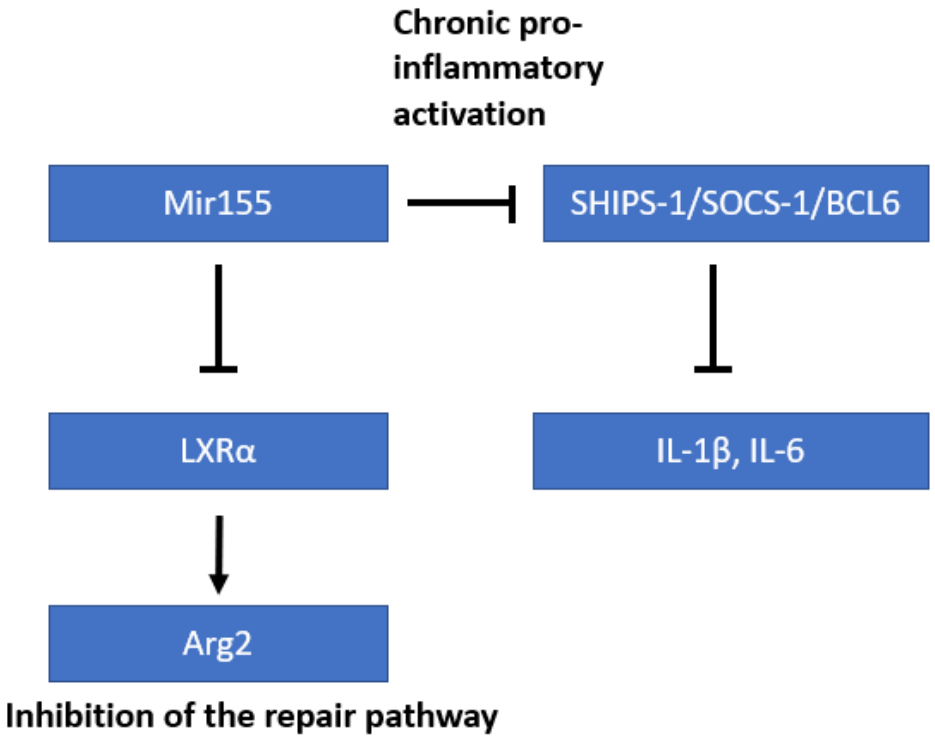

Figure 3.10. **Cartoon of the mechanism of action of mir155.** Mir155 promotes inflammation by inhibiting the anti-inflammatory action of the SHIPS-1/SOCS-1/BCL6 axis. Mir155 also inhibits LXRα, which promotes Arg2 function and the activation of the repair pathway. (Based on date from Alivernini et al., 2017)

Pyroptosis is a lytic form of cell death and causes increased release of LDH by dying cells. In this study, LDH was increased in supernatants of vancomycin pre-treated macrophages that were infected with *C. albicans* confirming that there is increased pyroptosis induced in these macrophages. In another study, Qu et al (Qu et al., 2019) showed that vancomycin caused increased LDH release in LLC-PK1 without infection, however, in their study, they used a higher dose of vancomycin to treat these cells and they only observed a phenotypic effect 12 hours post treatment. In this study, LDH release was not increased with physiological levels of vancomycin but only during *C. albicans* infection of treated cells. Interestingly, there was also decreased expression of the long non-coding

RNA, F630028O10Rik, which has been shown to promote pyroptosis in microglial cells (Xu et al., 2020). This is further indication of the macrophages' efforts to suppress death by pyroptosis. The increased macrophage death seen in the current study likely occurs before macrophages can exert their full anti-fungal potential on *C. albicans.*

In the next chapter, I explored how vancomycin exerts its effects on macrophages and the potential triggers of the inflammasome during *C. albicans* infection.

4 VANCOMYCIN DISRUPTS MACROPHAGE MITOCHONDRIAL MORPHOLOGY AND METABOLIC FUNCTION.

4.1 INTRODUCTION

Mitochondria are dynamic organelles that are highly conserved within mammalian cells. According to the endo-symbiotic theory of evolution, they evolved from α-proteobacteria as they strived to escape increasing environmental stresses and thus formed an endosymbiotic relationship with eukaryotic precursor cells (Suárez-Rivero et al., 2021, Gray et al., 1999). They serve as the powerhouse of cells by producing more than 90% of the cell's energy through oxidative phosphorylation (OXPHOS) and ATP production at homeostasis (Newmeyer and Ferguson-Miller, 2003). Oxygen is needed to drive this process and even more oxygen is needed during stress until a maximum oxygen consumption is reached (Kalghatgi et al., 2013). The more the mitochondria can increase oxygen consumption, the better it is at dealing with stress. This is referred to as the mitochondrial spare capacity, which can be used as a marker for mitochondria stress resistance (Yamamoto et al., 2016). Furthermore, mitochondria contribute to essential metabolic functions such as calcium homeostasis (Duchen, 1999), inflammation (Missiroli et al., 2020), and cell death (Green and Kroemer, 2004).

Mitochondria possess their own DNA known as the mitochondrial genome, which encodes several proteins including two rRNAs, twenty-two tRNAs and thirteen polypeptides that are mainly involved in OXPHOS, highlighting the importance of this process to mitochondria (Chatzispyrou et al., 2015, Anderson et al., 1981). Additionally, mitochondria possess ribosomes of bacterial origin that are

different from the host ribosomes in the cytoplasm (Wang et al., 2015). Nonetheless, most of the proteins within mitochondria are nuclear derived and are imported into mitochondria to form complexes with mitochondria encoded proteins (Suárez-Rivero et al., 2021). These complexes are critical for OXPHOS and ATP production (Lane and Martin, 2010). ATP production is driven by complex V of the electron transport chain (ETC). The mitochondrial complexes I, III and IV serve as proton pumps that help generate the mitochondrial membrane potential. This creates a negatively charged inner membrane that helps to create a transmembrane potential of hydrogen ions through complex V (ATP synthase) necessary for ATP production (Zorova et al., 2018). Thus, the energy capacity of the inner membrane is determined by how high the membrane potential is and this potentially dictates the level of ATP production (Zorova et al., 2018). Furthermore, the mitochondrial membrane potential helps in the transportation of important charged compounds (i.e. Ca^{2+}, Fe^{2+}) and nuclear proteins necessary for mitochondrial viability and is also important in mechanisms by which damaged mitochondria are eliminated (Zorova et al., 2018). Consequently, a loss of membrane potential is indicative of mitochondrial dysfunction and can lead to degradation.

The morphology of the mitochondria can often indicate their health. Healthy mitochondria are mostly fused with several branches, but in conditions such as during oxidative stress, the mitochondria develop a more fragmented phenotype (Seo et al., 2010). This is driven by a shift to increased fission and these mitochondria can also present with a swollen phenotype (Seo et al., 2010). However, a few mitochondria are still fragmented at steady state due to continuous fission and fusion events, which are essential for mitochondrial bioenergetics (Seo et al., 2010). While fused mitochondria are linked to biogenesis, fragmentation is more related to degradation. Also, mitochondrial fusion is essential for masking detrimental DNA mutations (that might be introduced during biogenesis) perhaps by diluting their impact with wild-type DNA. In fact, mice deficient of the fusion proteins (mnf1 and

mnf2) have impaired mitochondrial function which is accompanied with increased point mutations and deletions leading to phenotypic changes in these mice (Chen et al., 2010).

Taken together, it is unsurprising that mitochondrial dysfunction whether inherited or induced has been linked to several diseases such as neurodegenerative disorders and cell death during conditions like ischaemia (Duchen, 1999).

Antibiotic-induced mitochondrial dysfunction has gained much interest due to their bacterial origin and their well conserved bacteria-like ribosomes (Kalghatgi et al., 2013, Salimi et al., 2016). Many classes of antibiotics exist based on their origin, structure and/or mode of action with some being bactericidal and others bacteriostatic (Hutchings et al., 2019). Each class target different components (i.e. bacterial DNA, RNA, and cell wall synthesis) to exert their effects, but additionally some antibiotics can affect the ETC to induce oxidative damage and death of bacteria, but this same mechanism can affect host cell mitochondria, causing activation of programmed cell death pathways during prolonged use (Xiao et al., 2019, Kalghatgi et al., 2013). For example, some bactericidal antibiotics have been shown to cause oxidative damage and mitochondrial dysfunction in mammalian cells while gentamycin and azithromycin were shown to cause collapse of mitochondrial membrane potential in mammalian cells (Kalghatgi et al., 2013, Salimi et al., 2016, Xiao et al., 2019). Tetracycline also affects mitochondria by inhibiting mitochondrial protein translation, which causes an imbalance between mitochondrial protein and nuclear protein (mitonuclear protein imbalance) (Moullan et al., 2015, Wang et al., 2015). Consequently, worms and flies treated with doxycycline had developmental delays and physiological impairment (Chatzispyrou et al., 2015, Moullan et al., 2015). Furthermore, vancomycin has been shown to affect protein and glycoprotein synthesis in liver and brain mitochondria (Bosmann and Winston, 1972), and was shown to induce nephrotoxicity in an *in-vitro* assay using porcine proximal tubular cell line through increased mitochondrial reactive

oxygen species (ROS) (Arimura et al., 2012). Mitochondria are the most important source of ROS, generating about 90% of cellular ROS as by-products of oxygen metabolism (Pizzino et al., 2017). However, ROS is continuously converted by antioxidants to H_2O_2, which is further converted to H_2O and O_2 by enzymes such as catalase (Turrens, 2003). Oxidative stress occurs when there is an imbalance between ROS production and removal either due to reduced removal by antioxidants or overproduction of ROS (Turrens, 2003, Pizzino et al., 2017). Furthermore, vancomycin causes impaired tricarboxylic acid (TCA) cycle, reduced membrane potential and increased apoptosis via cardiolipin peroxidation (Arimura et al., 2012, Qu et al., 2019, Sakamoto et al., 2017). There is growing evidence of the effect of antibiotics on lipid metabolism (Lei et al., 2023). While some studies have indicated an antibiotic mediated dysfunction of lipid metabolism, others have shown that antibiotics can improve metabolic dysfunction induced by high-fat diet in mice (Luo et al., 2023, Zhang et al., 2021). Disruption of lipid metabolism has been implicated in lipid accumulation and obesity (Meng et al., 2021). Azithromycin was shown to affect lipid metabolism by inducing increased levels of short-chain fatty acids (SCFA), which induces lipogenesis when absorbed through the portal circulation and primary bile acids (Li et al., 2017). SCFA and bile acids are metabolised by gut microbiota and azithromycin potentially disrupts these beneficial bacteria causing accumulation of these molecules (Gérard, 2014, Weingarden et al., 2013). Furthermore, bactericidal antibiotics were shown to cause lipid damage in mammalian cells and vancomycin and neomycin were also shown to promote lipid accumulation by inhibiting the expression of proliferator-activated receptor-gamma (PPARγ) (Luo et al., 2023, Kalghatgi et al., 2013). However, the direct effects of these antibiotics on immune cells and how that may increase susceptibility to candidiasis has not been studied.

The aim of this chapter was to assess the impact of vancomycin on mitochondrial function. Firstly, we assessed the effects of vancomycin on ROS production and mitochondrial morphology. The chapter then investigates how vancomycin might affect mitochondrial membrane potential and overall function using the seahorse assay. The effects of vancomycin on the TCA cycle metabolites were investigated and the binding dynamics of vancomycin on mitochondria were also assessed. Finally, the effects of vancomycin treatment on general lipid metabolites were assessed during *C. albicans* stimulation or not.

4.2 RESULTS

4.2.1 Vancomycin causes increased oxidative stress in bone-marrow derived macrophages (BMDMs)

Prolonged use of vancomycin causes increased mitochondrial ROS production and apoptosis in renal tubular cells (Arimura et al., 2012). To assess whether similar effects occurred in macrophages, the level of ROS was quantified in macrophages pre-treated with vancomycin, at baseline and during infection. First the sensitivity of the assay was assessed by treating macrophages with different doses of menadione, which is a known inducer of ROS and acts as a positive control. It was found that menadione-treated cells had a dose dependent increase in ROS levels [Fig 4.1A]. Similarly, vancomycin pre-treatment caused increased levels of ROS compared to control macrophages, both at baseline and during infection, although this was only statistically significant during infection [Fig 4.1B-C].

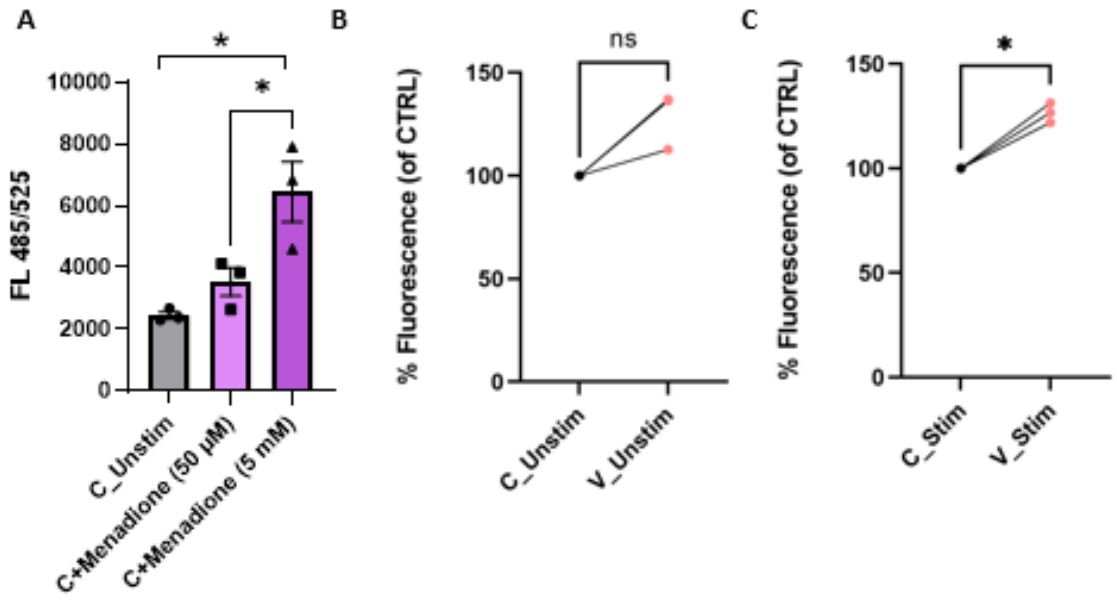

Figure 4.1. **Vancomycin causes increased ROS production**. (A) Fully differentiated and untreated macrophages were incubated with menadione at the indicated concentrations and ROS measured after 3 hours using H2DCFDA. (B) ROS levels were measured in macrophages differentiated in 20 µg/ml vancomycin and compared to untreated controls. (C) ROS levels were measured in vancomycin treated and untreated macrophages stimulated with heat-killed *C. albicans* for 3 hours. One-way ANOVA was used to analyse data in A with Tukey's multiple comparison test. Student's paired t-test was used to analyse the rest of the data with each data point representing a biological replicate (ns not significant; * $P < 0.05$). C_Unstim – control unstimulated, V_Unstim – vancomycin unstimulated, C_Stim – control stimulated, V_Stim – control stimulated.

Interestingly, in our RNA-Seq dataset introduced in chapter 3, there was upregulation of *Sod2* and *Arg2*, which are antioxidants and anti-inflammatory genes respectively known to act specifically within the mitochondria (Dowling et al., 2021). This may suggest that vancomycin causes a high inflammatory state in macrophages which they then try to resolve by upregulating anti-inflammatory genes such as *Arg2* and *Sod2* which are indicative of both an inflammatory state and increased oxidative stress within the mitochondria (Dowling et al., 2021, Cox et al., 2018). Furthermore, the fact that the expression of *Enc1* is increased in vancomycin pre-treated macrophages infected with *C. albicans* lends support to the higher oxidative stress seen in these macrophages. *Enc1* downregulates the expression of *Nrf2,* a transcription factor that plays an important role in activating cellular

antioxidant pathways and suppression of inflammatory pathways (Li et al., 2008). *Klf16* knock-out has also been linked to mitochondrial stress and oxidative stress (Sun, 2021) in mice and indeed this gene was downregulated in the vancomycin treated macrophages infected with *C. albicans* (Table 3.2). Taken together, these data confirm that vancomycin induces increased ROS production in macrophages causing oxidative stress which is exacerbated during *C. albicans* infection.

4.2.2 Vancomycin causes mitochondrial hyper-fragmentation in BMDMs

ROS production can disrupt the balance between mitochondrial fusion and fission thus resulting to increased fragmentation of the mitochondria (Seo et al., 2010). To assess the potential impact of oxidative stress on mitochondria within vancomycin pre-treated macrophages, mitochondria were stained with MitoTracker Red, and their morphology examined using confocal microscopy. Vancomycin treated macrophages had hyper-fragmented mitochondria with less branching and looked swollen compared to the mitochondria in control macrophages, which were elongated with branching [Fig. 4.2A]. The perimeters, circularity, and aspect ratios of the mitochondria were quantified from microscopy images. These data confirmed that vancomycin treated macrophages had mitochondria with smaller perimeters [Fig 4.2B] and aspect ratios (typical of fragmented morphology) [Fig. 4.2C] compared to control macrophages, which are more fused and elongated and thus have bigger perimeters and aspect ratios [Fig 4.2B and C]. The circularity is a measure of how circular the mitochondria were with 1 representing a perfect circle and lower values represent more elongated shapes. Here, the vancomycin pre-treated macrophages had higher circularity than control macrophages [Fig 4.2D]. Taking advantage of the mitochondrial staining, the mitochondrial content was also quantified, and showed a reduction in vancomycin pre-treated macrophages [Fig 4.2E].

Collectively, these data confirm that vancomycin treatment promoted mitochondria fragmentation leading to reduced mitochondrial mass in the macrophage.

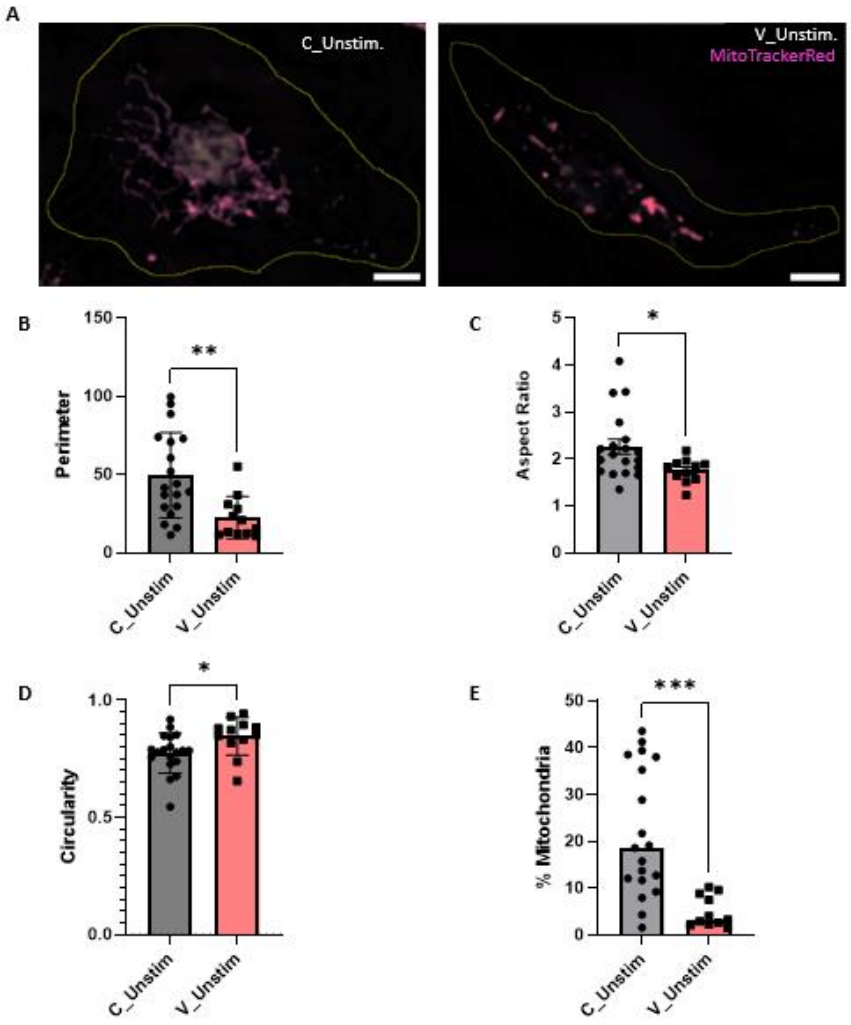

Figure 4.2. **Vancomycin causes mitochondrial hyper-fragmentation and reduced mass** (A) Mitochondrial were stained using MitoTracker Red and imaged on the LSM880 confocal microscope. Fiji was then used to assess mitochondrial morphology by measuring (B) perimeters, (C) aspect ratio, (D) circularity and (E) mitochondrial mass. Data are means ± SEM of 3 biological replicates (each data point is the mean of cells within the same field of view). Student's t-test was used to analyse the data (ns not significant; * $P < 0.05$; ** $P < 0.005$; *** $P < 0.0005$). C_Unstim – control unstimulated, V_Unstim – vancomycin unstimulated, C_Stim – control stimulated, V_Stim – control stimulated. Scale bar represents 50 μM.

4.2.3 Vancomycin causes depolarisation of the mitochondrial membrane

Next, I assessed if the increased ROS and changes in mitochondrial morphology within vancomycin-treated macrophages affected mitochondrial membrane potential. An intact mitochondrial membrane

potential is essential for optimal function. Studies have shown that cellular stress causes mitochondrial depolarisation, increased ROS production and decreased ATP production (Green and Kroemer, 2004, Kalghatgi et al., 2013). Because vancomycin pre-treatment caused increased levels of ROS, mitochondrial membrane potential was assessed using the JC-1 dye, which stains mitochondria based on their membrane potential and thus polarised membrane potential causes greater aggregation of the dye and fluoresces red, while it fluoresces green in depolarised mitochondria (Jiang et al., 2019). Vancomycin treated macrophages were stained with the JC-1 dye for 30 minutes and imaged using an inverted epifluorescence microscope. The ratio between the red and green fluorescence were measured using image J [Fiji]. BAM15, a known membrane depolariser was used as a positive control (Figure 4.3A). Vancomycin pre-treated macrophages had higher levels of green fluorescence than control macrophages, which indicated less aggregation of the stain caused by reduced mitochondrial membrane potential [Fig 4.3A and B]. In line with that, vancomycin-treated macrophages looked like the BAM15-treated macrophages (Fig 4.3). Together these results show that mitochondria membrane potential is compromised in vancomycin pre-treated macrophages.

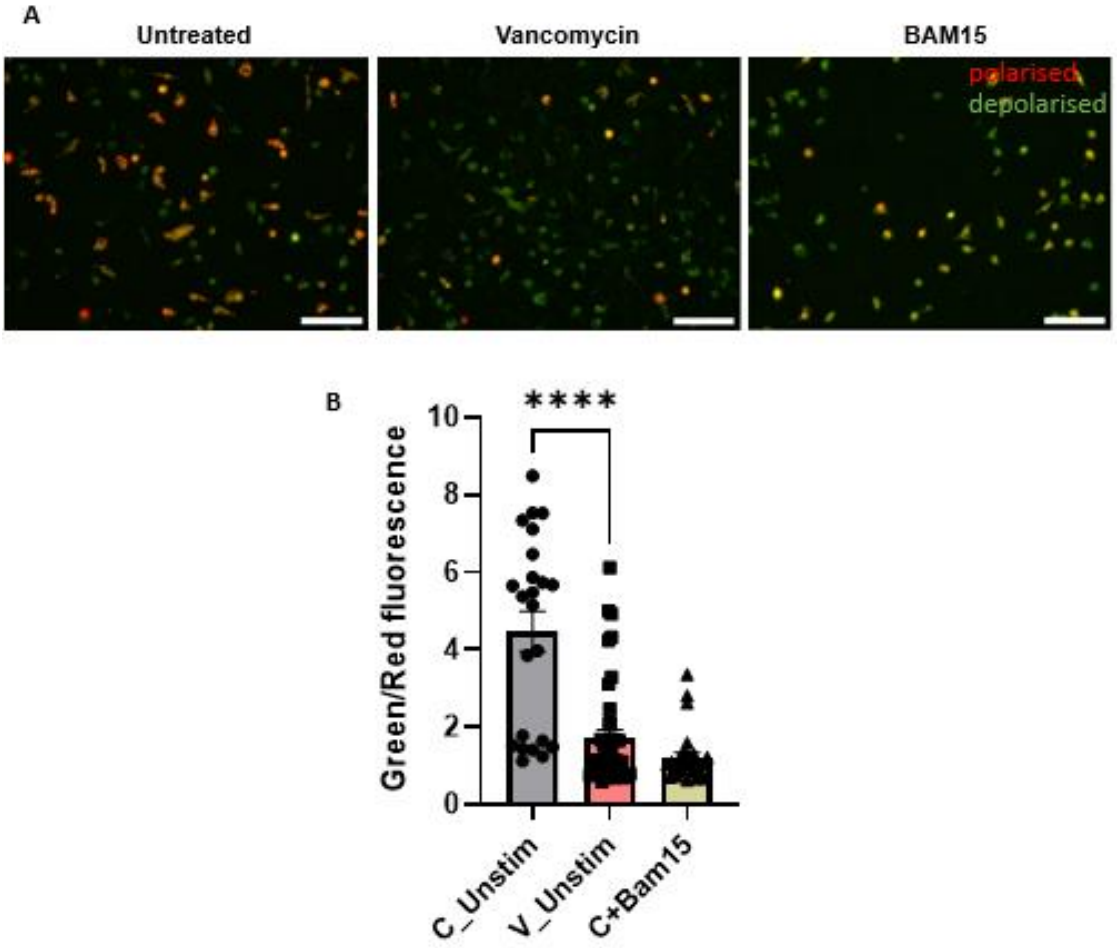

Figure 4.3. **Vancomycin treatment caused reduced mitochondrial membrane potential.** Macrophages were treated with the JC-1 dye for 30 mins. Mitochondria with intact membrane potential has higher accumulation of the dye and fluoresces red while green fluorescence indicates depolarised membrane potential. (a) shows representative fluorescent images of untreated (control) macrophages, vancomycin pre-treated macrophages and BAM15 treated macrophages and (b) the ratio of red to green were quantified for each group. Data are means ± SEM collected from 3 biological replicates (each data point on the graph is the mean of cells within the same field of view). Student's t-test was used to analyse the data (**** $P < 0.0001$). C_Unstim – control unstimulated, V_Unstim – vancomycin unstimulated, C+BAM15 – control macrophages treated with BAM15. Scale bar represents 100 μm.

4.2.4 Mitochondrial function is compromised by vancomycin treatment

The results so far indicated that vancomycin affected mitochondrial function. To directly test that, the respiratory capacity of the mitochondria in vancomycin pre-treated macrophages was measured using

a Seahorse flux analyser to measure oxygen consumption rate (OCR), a surrogate measure of mitochondria function. Vancomycin pre-treated macrophages were also stimulated with heat-killed *C. albicans* to evaluate oxygen consumption in the context of infection/fungal stimulation. There was no difference in baseline oxygen consumption in both treated and untreated groups [Fig 4.4A and B] Next, ATP related oxygen consumption was assessed, which is indicative of mitochondrial ATP production. Vancomycin treatment alone caused reduced mitochondrial ATP compared to untreated controls [Fig 4.4C]. However, despite seeing a slight but insignificant reduction in both groups after *C. albicans* stimulation, the difference between treated and untreated controls was lost [Fig 4.4C]. This indicates that vancomycin pre-treatment caused reduced mitochondrial ATP production but may indicate increased glycolysis. Next, the ability of the mitochondria to respond to stress was quantified by measuring their spare respiratory capacity. The spare capacity is the difference between the maximal oxygen consumption [Fig 4.4D] and the basal consumption rates [Fig 4.4B], and it indicates how well the mitochondria can respond to stress. Here, vancomycin pre-treated macrophages that were stimulated with *C. albicans* had a significantly impaired response to the uncoupler, carbonyl cyanide p-(trifluoromethoxy) phenylhydrazone (FCCP), which resulted in reduced spare capacity [Fig 4.4E]. Taken together, these data show that vancomycin affects macrophage bioenergetics and reduces their capacity to respond to *C. albicans* stimulation.

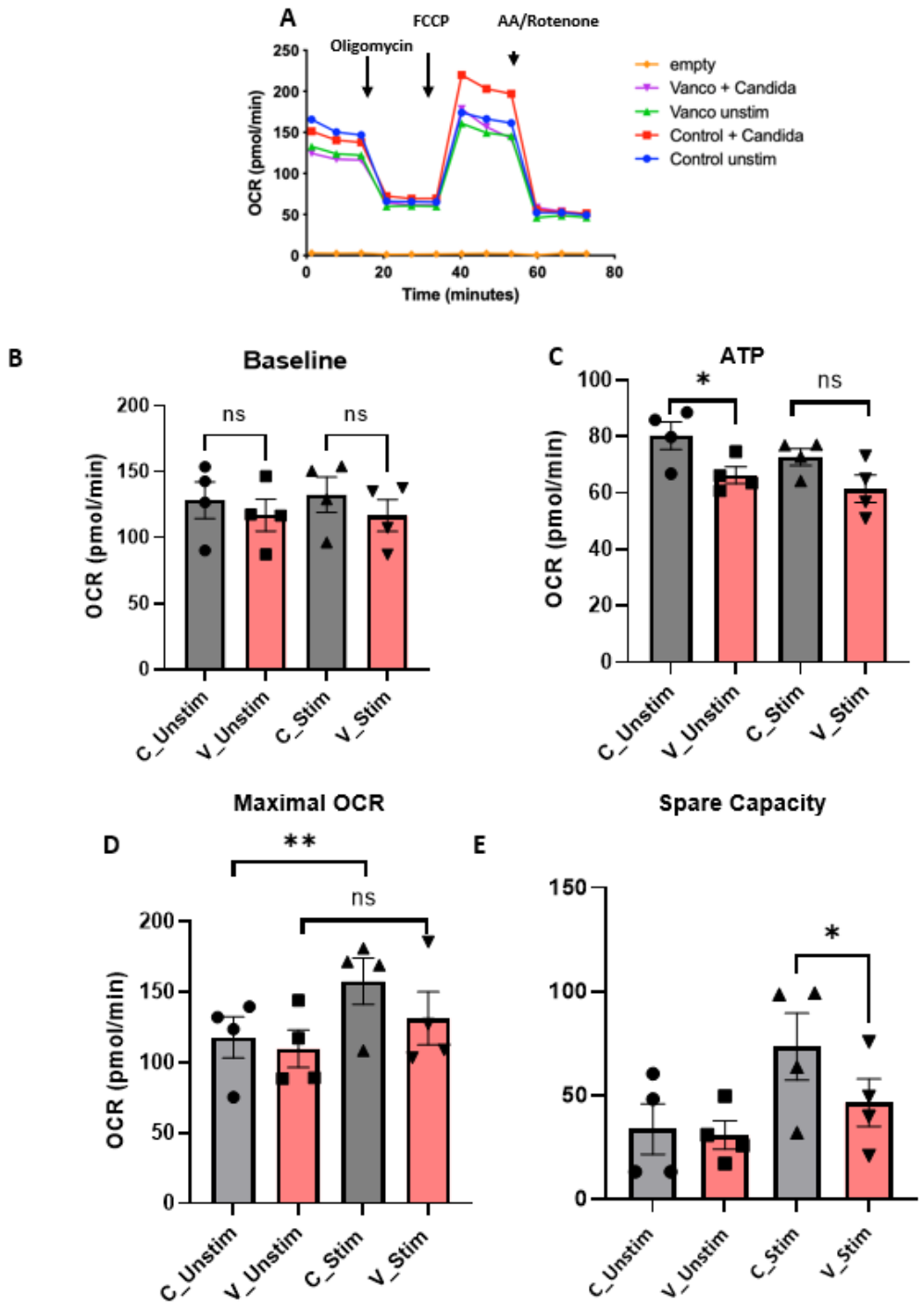
A
FCCP
AA/Rotenone
Oligomycin
OCR (pmol/min)
Time (minutes)
empty
Vanco + Candida
Vanco unstim
Control + Candida
Control unstim
B
Baseline
C
ATP
D
Maximal OCR
E
Spare Capacity
ns
*
**
C_Unstim
V_Unstim
C_Stim
V_Stim

Figure 4.4. Vancomycin treatment causes mitochondrial dysfunction. Seahorse assay was performed to assess the functioning of the mitochondria from vancomycin pre-treated and control macrophages stimulated or not with heat-killed *C. albicans*. (A) a representative trace of the oxygen consumption rate of the mitochondria throughout the assay. The values are plotted to show the (B) baseline oxygen consumption for each group, (C) ATP related oxygen consumption, (D) maximal oxygen consumption when the uncoupler, fccp was added and (E) the spare capacity. Data are means ± SEM of 4 biological replicates. Student's paired t-test with was used to analyse the data (ns not significant; * $P < 0.05$; ** $P < 0.005$).

4.2.5 TCA cycle metabolites are not affected by vancomycin treatment

The TCA cycle is a key component of mitochondrial bioenergetics through generation of $FADH^{2+}$ and $NADH^{2+}$ required by the electron transfer chain for ATP production (Martínez-Reyes and Chandel, 2020). Accumulation of metabolites within this pathway have been shown to induce activation of inflammatory pathways (Scagliola et al., 2020). Since it was found there were defects in mitochondrial spare capacity in vancomycin-treated macrophages, we assessed whether the TCA cycle was affected in these cells to gain a better understanding of how the antibiotic was affecting mitochondrial function. For that, we performed an unbiased metabolite screen (LC-MS) on macrophages either untreated or vancomycin-treated with or without stimulation for 2 hours with heat-killed *C. albicans*. Within this dataset, we examined the levels of the major TCA metabolites between the conditions. None of the major TCA metabolites were statistically significant between the different conditions [Fig 4.5]. However, there was a trend of reduced citrate/isocitrate and 2-oxaglutarate levels in vancomycin pre-treated macrophages [Fig 4.5A and B]. Similarly, we observed trends of reduced cis-aconitate [4.5C] and itaconate [4.5D] in vancomycin treated and *C. albicans* stimulated macrophages as compared to unstimulated control macrophages. Together these results show that TCA is not significantly affected by vancomycin pre-treatment and may not be the mechanism by which macrophage function is compromised during *C. albicans* stimulation.

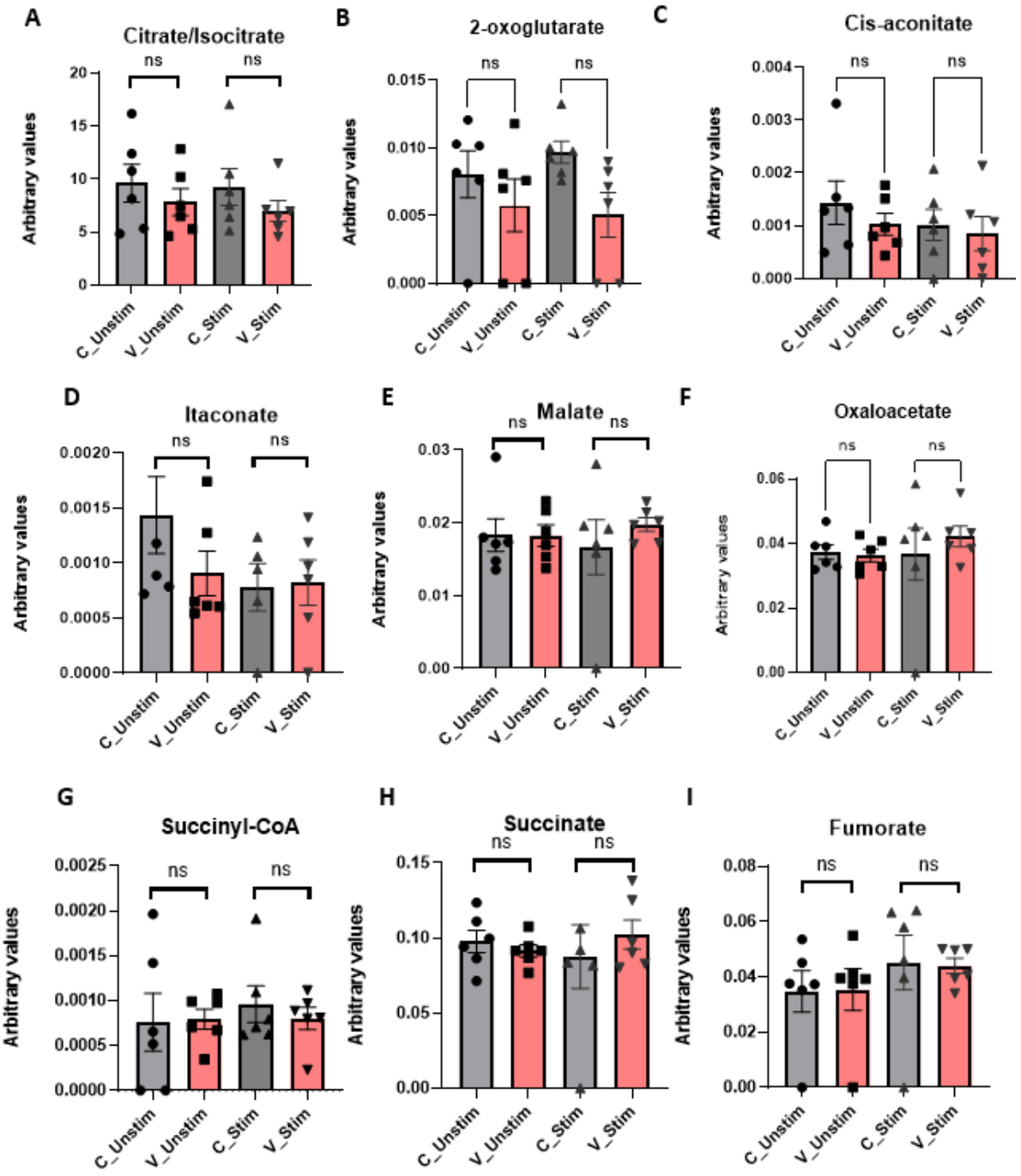

Figure 4.5. Vancomycin treatment does not affect TCA metabolites. A metabolite screen (LC-MS) was performed, and levels of TCA cycle metabolite quantified. Data are means ± SEM of 6 biological replicates. Student's t-test was used to analyse data (ns not significant).

4.2.6 Vancomycin binds to the macrophage plasma membrane and co-localises to the mitochondria.

As we had found that vancomycin was affecting mitochondrial morphology and function, we wanted to understand the binding dynamics of vancomycin within macrophages to develop an understanding of how these effects were mediated. Since vancomycin is an antibiotic that targets the cell wall of Gram-positive bacteria, it is unknown how it exerts its effect on macrophage mitochondria. To try and elucidate that, macrophages were co-incubated for 5 hours with a fluorescently tagged vancomycin and the binding examined by confocal microscopy. There was indeed binding of vancomycin to lipidated structures in the cell, including on the macrophage plasma membrane. Interestingly, vancomycin also co-localised with a mitochondrial stain, suggesting binding within the mitochondria and intracellular structures [Fig 4.6A]. Mitochondria are rich for lipids such as phosphatidylglycerol (PG) and cardiolipin, and vancomycin has been previously shown to bind to these lipids (Tam, 2017). Interestingly, vancomycin also stained nuclear structures. Vancomycin staining of the nucleus mirrored chromatin staining that has been previously described (Malik et al., 2014), which suggests that vancomycin may also bind chromatin [Fig. 4.6A].

Drummond et al (Drummond et al., 2022) showed that vancomycin had no direct effects on the function of CD4+ T cells (as measured by cytokine production and proliferation). Therefore, we set out to assess if the binding pattern to CD4+ T cells was different to macrophages, which would potentially explain whether physical binding or some other mechanism is responsible for the effects of vancomycin on macrophage mitochondrial morphology and function. Although little or no binding was observed on T cell outer membrane, vancomycin appeared to stain CD4+ T cell mitochondria [Fig 4.6B and C] suggesting that binding to mitochondria alone may not account for the full effects of vancomycin on macrophages.

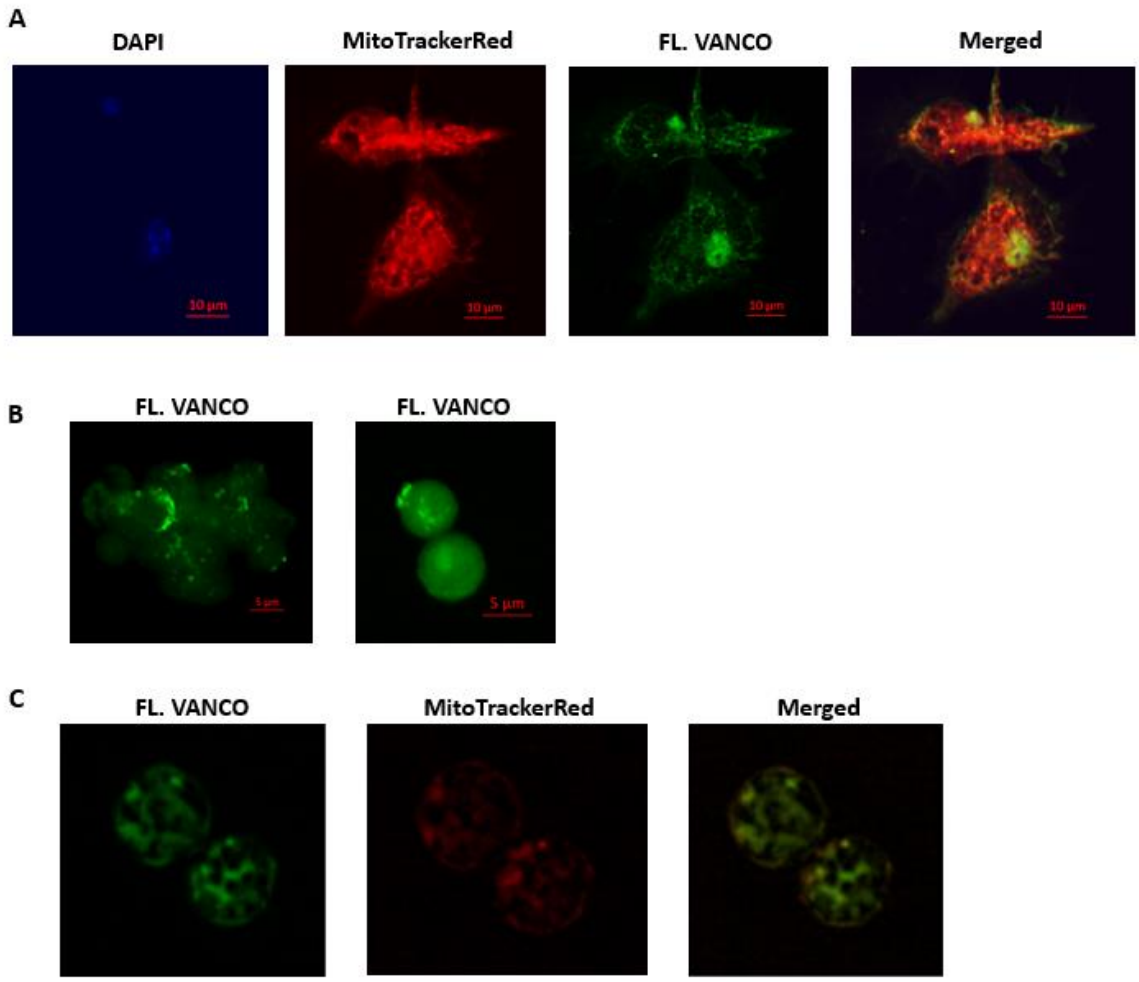

Figure 4.6. Vancomycin binds lipid membranes. (A) Macrophages were stained with FL-vancomycin for 5 hours. Then mitochondria were stained with MitoTrackerRed for 30 minutes. Cells were then fixed in 4% PFA and stained with DAPI. (B) CD4+ T cells were also incubated with FL-Vancomycin for 5 hours, cells were fixed and imaged using the LSM 880 confocal microscope. (C) CD4+ T cells were also stained with both FL-Vancomycin and MitoTrackerRed dye to stain mitochondria.

4.2.7 Vancomycin causes disruption of lipid metabolites

Since vancomycin appeared to be binding lipidated structures in macrophages, we used our metabolite screen, which included lipid data to see how different lipid species were affected by vancomycin at baseline and during *C. albicans* stimulation. In the global context, several lipids were changed between groups (see Appendix 1). Vancomycin alone caused a decrease in several lysophospholipids (Appendix 1) which are precursors for membrane biogenesis and contribute to cell

signalling (Tan et al., 2020). Vancomycin pre-treatment also caused increased levels of PE and PS species containing polyunsaturated fatty acids (PUFA), which are known for their antioxidant properties (Saccà et al., 2018). This may be increased to help ease the oxidative stress within these macrophages. Furthermore, phosphatidylcholines (PC) species PC (40:6) was decreased by vancomycin treatment [Fig. 4.7A]. Although PC levels increased after *C. albicans* infection, they did not recover to the levels of untreated controls [Fig. 4.7A]. On the other hand, there was a trend of increased baseline levels of PE (36:2) in vancomycin pre-treated macrophages, and although there was no increase with infection, untreated controls increased PE levels significantly during *C. albicans* stimulation [Fig. 4.7B]. The levels of PE containing plasmalogens, PE(P-18:1/18:1) were also reduced in vancomycin pre-treated macrophages compared to untreated controls [Fig. 4.7D]. However, there was no difference during *C. albicans* stimulation. These data show that treatment of macrophages with vancomycin causes changes in lipid composition at baseline and during anti-*C. albicans* responses.

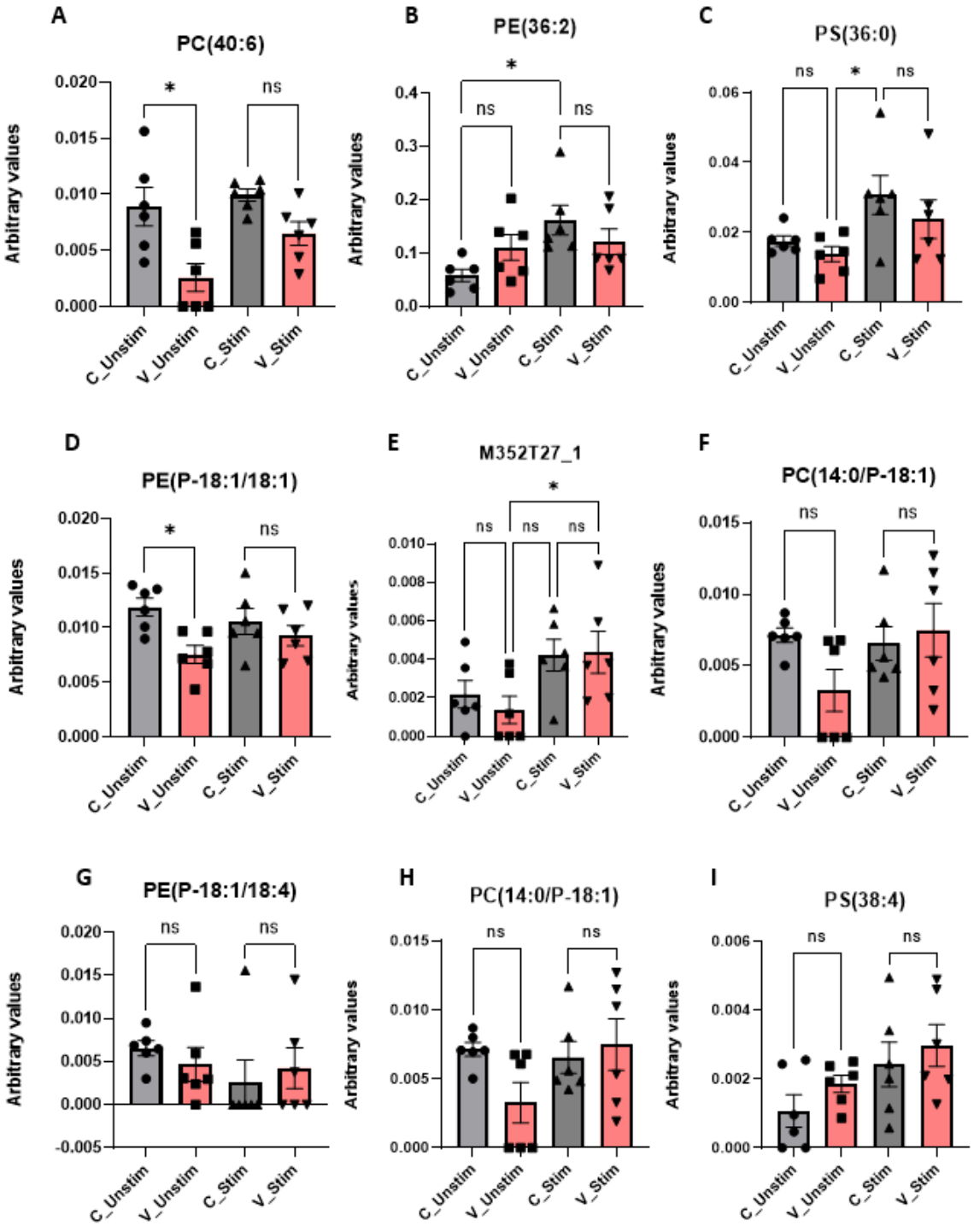

Figure 4.7. Vancomycin treatment causes disruption of lipid metabolites in macrophages. An unbiased metabolic screen (LC-MS) was performed on vancomycin treated macrophages with or without *C. albicans* stimulation. (A) phosphatidylcholine (40:6). (B) phosphatidylethanolamine (36:2). (C) phosphatidylserine (36:0). (D) phosphatidylethanolamine (P-18:1/18:1). (E) Undetermined yet. (F) phosphatidylcholine (14:0/P-18:1). (G) phosphatidylethanolamine (P-18:1/18:4). (H) phosphatidylglycerol (34:0) and (I) phosphatidylserine (38:4). Data are mean ± 6 biological replicates. Friedman Test was used to analyse this data with Dunn's multiple comparison test (ns not significant; * $P < 0.05$)

4.3 DISCUSSION

The data presented in this chapter shows that vancomycin pre-treatment of macrophages causes mitochondrial dysfunction through oxidative stress, leading to reduced membrane potential and an overall impairment of stress resistance. This has serious implications in the health of these cells and their ability to carry out their immune responsibilities.

Antibiotic therapy is an important component of modern medicine, but studies have shown antibiotics to have immuno-suppressive effects on immune cells, which would potentially increase susceptibility to subsequent infections (Nau and Tauber, 2008, Lin et al., 2000). Although the exact mechanisms by which immune cells are affected is not completely understood, various antibiotics from different classes have been shown to exert detrimental effects on mammalian cells through the targeting of their mitochondria (Kalghatgi et al., 2013, Jiang et al., 2019, Chatzispyrou et al., 2015). In this study, vancomycin pre-treatment caused increased oxidative stress in macrophages which was exacerbated by *C. albicans* infection. Similarly, vancomycin was shown to induce nephrotoxicity by increased oxidative stress and triggering apoptosis in renal tubular cells (Arimura et al., 2012). Several antibiotics have also been shown to induce oxidative stress in mammalian cells. For instance, Jiang et al (Jiang et al., 2019) observed a similar induction of ROS when human mammary epithelial cell line, MCF-12A and fibroblasts were treated with azithromycin. Furthermore, mitochondria from cardiomyocytes were also affected by macrolides including erythromycin and azithromycin, whereby they induced oxidative stress, reduced membrane potential, caused mitochondrial swelling, and release of cytochrome c but these antibiotics did not have a similar effect on mitochondria isolated from liver cells (Salimi et al., 2016). These results corroborate our findings but also indicate that different cells may respond differently to antibiotic-induced stress, which may be dependent on class and mechanism of action.

Increased ROS is a known trigger of death pathways such as apoptosis and pyroptosis (Kalghatgi et al., 2013, Zitvogel et al., 2012). Activation of the inflammasome is required for the latter. Inflammasome activators such as uric acid crystals have been shown to induce the dissociation of thioredoxin interacting protein (TXNIP) from thioredoxin in a ROS sensitive manner, and TXNIP then binds to NLRP3 to activate the inflammasome pathway (Zhou et al., 2010). ROS also plays a role in sustained innate immune responses (Missiroli et al., 2020). These downstream consequences of ROS could have implications for the health of macrophages since early and sustained activation of the inflammasome can lead to pyroptosis, which is known to be triggered by *C. albicans* in macrophages as part of their escape mechanism (Krysan et al., 2014). Therefore, the increase of ROS induced by vancomycin would potentially exacerbate this effect and lead to early inflammasome activation, as observed in Chapter 3 and may also underlie the reduced fungal killing as it may cause premature macrophage death before exerting their full anti-fungal potential on internalised *C. albicans*.

To counteract oxidative stress, cells produce antioxidants such as the superoxide dismutase (SOD) enzymes (Cox et al., 2018). SOD enzymes help to convert superoxide radicals to hydrogen peroxide (H_2O_2), which is subsequently broken down into water and oxygen by mitochondrial enzymes such as catalase (Cox et al., 2018, Turrens, 2003). In an earlier study, azithromycin was shown to induce increased expression of the mitochondria specific *Sod2* in treated cells (Jiang et al., 2019) but this increase was observed from day 2 post treatment. In this study, it was observed that *C. albicans* caused a rapid transcriptional increase of *Sod2* in vancomycin treated macrophages occurring at 2 hours post stimulation. These increases are indicative of mitochondrial oxidative stress induced by these antibiotics and the subsequent earlier activation of defence mechanisms by macrophages in this

study suggests a more profound ROS mediated damage induced by vancomycin treatment during *C. albicans* infection.

Increased oxidative stress causes mitochondria to adopt a more fragmented morphology (Seo et al., 2010). Here, we showed that vancomycin caused hyper fragmentation of the mitochondria and reduced overall mitochondrial mass. This was unsurprising as previous studies have linked the hyper-fragmented phenotype with increased mitochondrial degradation by mitophagy (Missiroli et al., 2020, Twig et al., 2008). Also, hyper-fragmentation could lead to loss of metabolic function and membrane potential (Seo et al., 2010), which potentially explains their impaired response to *C. albicans*-induced stress.

In line with the hyper-fragmented phenotype, vancomycin treated macrophages caused reduced mitochondrial membrane potential compared to untreated controls. Bactericidal antibiotics had a similar effect on mammary gland epithelial cells (Kalghatgi et al., 2013) thus suggesting that different antibiotics may have similar effects on different mammalian cells. Dissipation of the membrane potential has serious consequences on the bioenergetics of the mitochondria as it inhibits ATP production due to the dysregulated in-flow of hydrogen ions through complex V (Zorova et al., 2018). Consequently, there was decreased ATP production in vancomycin pre-treated macrophages, but this difference was lost after *C. albicans* stimulation. There was a lack of significant changes to the TCA cycle metabolites, which could have also led to decreased ATP production due to its role in the generation of $FADH^{2+}$ and $NADH^{2+}$. However, we observed a trend of lower levels of citrate, which is an important precursor for lipid biosynthesis. These could have an impact on the mitochondrial architecture since this metabolite plays an essential role in the biosynthesis of important lipids within membranes (Williams and O'Neill, 2018). Taken together, these results point to a more subtle

reduction in ATP levels but could still have biological relevance due to the high energy demands imposed on cells during stressful situations, such as *C. albicans* infection.

The overall respiratory capacity of the mitochondria was also assessed using the Seahorse assay. Although basal respiration was insignificantly reduced, the spare respiratory capacity was significantly reduced in the context of *C. albicans* stimulation. What this reduction indicates is the inability of mitochondria from vancomycin pre-treated macrophages to adequately increase their respiratory capacity during *C. albicans* stress thus further lending support to the reduced killing efficiency of these macrophages observed in Chapter 3. Bactericidal antibiotics also caused reduced spare respiratory capacity in renal tubular cells (Kalghatgi et al., 2013), but these antibiotics also caused reduced OCR at baseline which was not observed in this study. Taken together, these findings suggest that vancomycin treatment has a subtle but biologically relevant impact on mitochondrial function.

When macrophages were treated with a fluorescent vancomycin, we were able to track vancomycin binding in these cells. These experiments led to the discovery that there was extensive binding to macrophage plasma membrane and to the mitochondria. Vancomycin was previously shown to have high affinity to phospholipids (Tam, 2017). The endoplasmic reticulum (ER) and mitochondria are major sources of phospholipids, and the mitochondrial membrane is rich for lipids including phosphatidylethanolamine (PE) and cardiolipin (Osman et al., 2011, Vance, 2015) with the latter unique to mitochondrial and bacterial membranes (Calzada et al., 2016). In fact, using liposomes as membrane mimics showed that vancomycin binds to 1-palmitoyl-2-oleoyl-sn-glycero-3-phospho-(1'-rac-glycerol) (sodium salt) (POPG), 1-hexadecanoyl-2-(9Z-octadecenoyl)-sn-glycero-3-phosphoethanolamine (POPE) and cardiolipin, even though it has greater preference to binding POPG

than POPE and cardiolipin (Tam, 2017). The increased affinity is thought to be promoted by hydrogen bonding with the two hydroxyls on the head group of POPG, which are less accessible in the other two lipids (Tam, 2017). Consequently, this pattern of vancomycin binding was found to disrupt the levels of numerous lipid metabolites. Vancomycin treatment alone caused a reduction in lysophospholipids, which are precursors for other lipids and are essential for membrane biogenesis thus their reduction could have both functional and structural consequences to these cells (Tan et al., 2020). Furthermore, PC (40:6) was found to be reduced in vancomycin treated macrophages while PE (36:2) was trending on towards increase. This could have biological implications as very low or high ratios between PE and PC affects mitochondrial bioenergetics (van der Veen et al., 2017). Additionally, vancomycin treatment caused reduced plasmalogen levels in macrophages and this could have important implications as plasmalogens have been shown to play several important roles such as in improving membrane dynamics during respiration, signal transduction, acting as endogenous antioxidants, regulating fission and fusion, and are involved in supporting poly unsaturated fatty acids (Messias et al., 2018). In renal tubular cells, vancomycin was also shown to cause cardiolipin peroxidation, which is an important lipid in the inner mitochondrial membrane (Sakamoto et al., 2017). Reduced levels of cardiolipin can trigger phosphatidylglycerol (PG) accumulation in the mitochondria, which compensates cellular functions of cardiolipin. However, vancomycin has high affinity for PG, potentially causing membrane permeability through this binding (Watanakunakorn, 1984, Tam, 2017). This can lead to a loss of membrane potential as seen in proximal tubular cells (Jiang et al., 2000, Osman et al., 2011). Together, these data provide evidence of vancomycin binding to lipid moieties within bacterial cell membranes, and potentially explains the initiation of cell membrane permeabilization by this glycopeptide and its potential role in mitochondrial dysfunction.

Interestingly, we found that vancomycin also co-localises to mitochondria in CD4+ T-cells despite being shown to have no direct effects on cytokine production, differentiation, or proliferation of Th17 cells (Drummond et al., 2022). This potentially disputes the fact that direct binding to mitochondria is necessary for the phenotypic changes seen in macrophages. However, this could not be completely ruled out as vancomycin may be affecting other T-cell functions not tested in this study as antibiotics have been shown to differentially effect different mammalian cells (Salimi et al., 2016).

In summary, vancomycin causes mitochondrial dysfunction and an inability to adequately respond to *C. albicans* stimulation. This is perhaps driven by oxidative stress within the mitochondria marked by elevated levels of ROS. However, this occurs without significantly affecting the TCA cycle. Vancomycin also binds to macrophage lipid membranes and co-localises to the mitochondria, thus causes disruption of lipid metabolites. These results may partly explain the defective killing of *C. albicans* seen in vancomycin pre-treated macrophages and has significant clinical implications as candidiasis is prevalent in patients with prolonged antibiotic use.

5 VANCOMYCIN PRE-TREATMENT OF MACROPHAGES DOES NOT AFFECT PHAGOSOME INDUCED CELL WALL REMODELLING IN *C. ALBICANS*

5.1 INTRODUCTION – CELL WALL CHANGES INDUCED BY DIFFERENT ENVIRONMENTAL CUES

C. albicans cell wall is its first point of contact with its environment and with immune cells and most of the cell wall components are PAMPs that can trigger an immune response (Cottier et al., 2019). Consequently, *C. albicans* regulates the composition of these components at various instances by exposing or masking these PAMPs as a form of immune evasion mechanism but can also be just to adapt to the various environments it encounters within the host. For instance, growth in lactate causes increased masking of *C. albicans* β1,3-glucan (Ballou et al., 2016). Lactate is abundant in the vaginal environment and *C. albicans* has evolved lactate sensing mechanisms to conceal this major PAMP and thus evade clearance by immune cells during vaginal colonisation and infection (Ballou et al., 2016). Conversely, *C. albicans* remodels its cell wall to expose β1,3-glucan during growth in acidic conditions (Sherrington et al., 2017). Acidic pH causes increased exposure of β1,3-glucan at the early stages which is then re-masked with time (Cottier et al., 2019). While the mechanism by which *C. albicans* modulates chitin remasking remains elusive, the density dependent quorum sensing molecule, farnesol mediates β1,3-glucan remasking (Cottier et al., 2019). Increased β1,3-glucan causes more recognition by immune cells and greater phagocytosis and cytokine production by macrophages *in-vitro* (Sherrington et al., 2017). *C. albicans* encounters acidic pH when they are confined within phagosomes as the phagosomes undergo maturation and phagocytosed macrophages

have been shown to have increased exposure of cell wall chitin with less changes to β1,3-glucan exposure (Wagener et al., 2017). *C. albicans* are adept at escaping the phagosomal environment and although increased β1,3-glucan exposure triggers robust immune responses, chitin polarizes macrophages to the alternatively activated phenotype with less nitric oxide production hence increasing their chances of survival (Wagener et al., 2017). However, the impact of antibiotics on the phagosomal environment and how these would impact cell wall changes in *C. albicans* is not understood. The aim of this chapter is to first establish the cell wall changes that occur within macrophage phagosomes and during interaction with neutrophils and to then elucidate the impact of vancomycin pre-treatment of macrophages on *C. albicans* cell wall remodelling.

5.2 RESULTS

5.2.1 Cell wall changes occur within macrophage phagosomes not treated with vancomycin

It was previously shown that cell wall remodelling occurs within macrophage phagosomes (Wagener et al., 2017). To assess if these changes were time dependent, macrophages were co-incubated with *C. albicans* yeast cells for the indicated times and then the exposure of chitin and β1,3-glucan were quantified by microscopy and flow cytometry. Internalised and non-phagocytosed *C. albicans* were discriminated using the gating strategy outlined in [Fig. 5.1]. There was increased chitin exposure in *C. albicans* cells that had been phagocytosed as early as 1 hour post co-incubation [Fig. 5.2A]. Interestingly, there was no staining of chitin in extracellular *C. albicans*suggesting that the increased chitin exposure is induced by the phagosomal environment. This is also shown at greater magnification in Figure 5.3, whereby most *C. albicans* that have been phagocytosed show some degree of chitin staining. Interestingly, very high exposure levels were observed in *C. albicans* that were fully internalised within phagosomes (blue arrow) [Fig., 5.3]. These observations were supported by flow cytometry data whereby increased MFIs were recorded for chitin at 1 hour and continued to increase with time till 3 hours post co-incubation with macrophages [Fig. 5.2B].

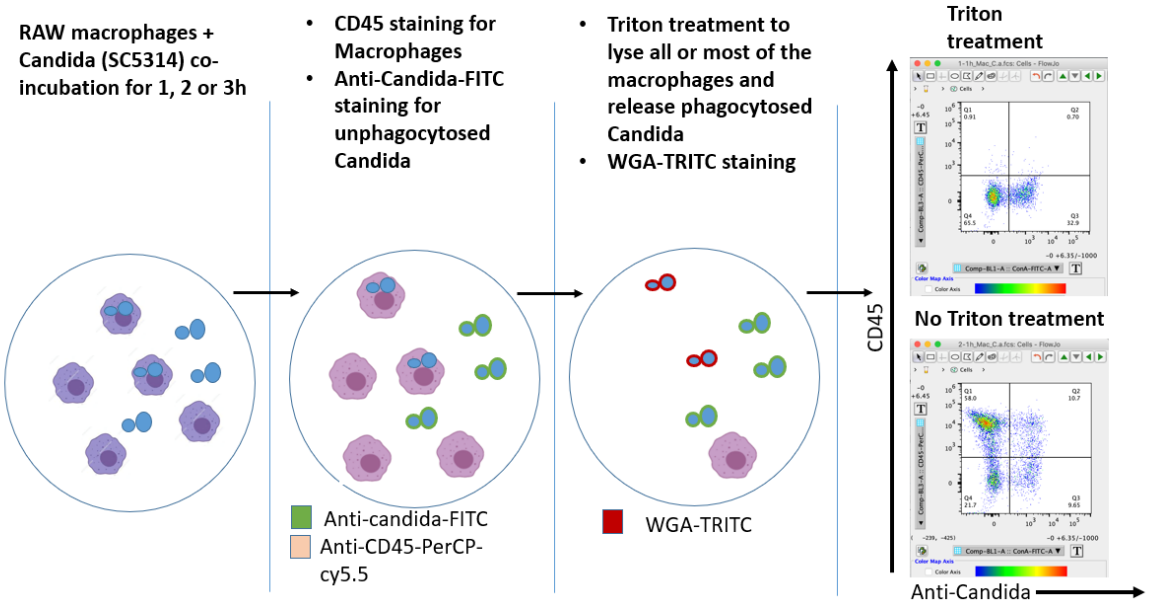

Figure 5.1. **Assessing chitin exposure in *C. albicans* cells**. Macrophages were infected with wild-type *C. albicans* and incubated for 1, 2 and 3 hours. Non-phagocytosed cells were stained with anti-*Candida*-FITC before lysing macrophages to assess internalised *C. albicans*. Cell wall exposed chitin was stained for using WGA-TRITC and cells analysed by flow cytometry.

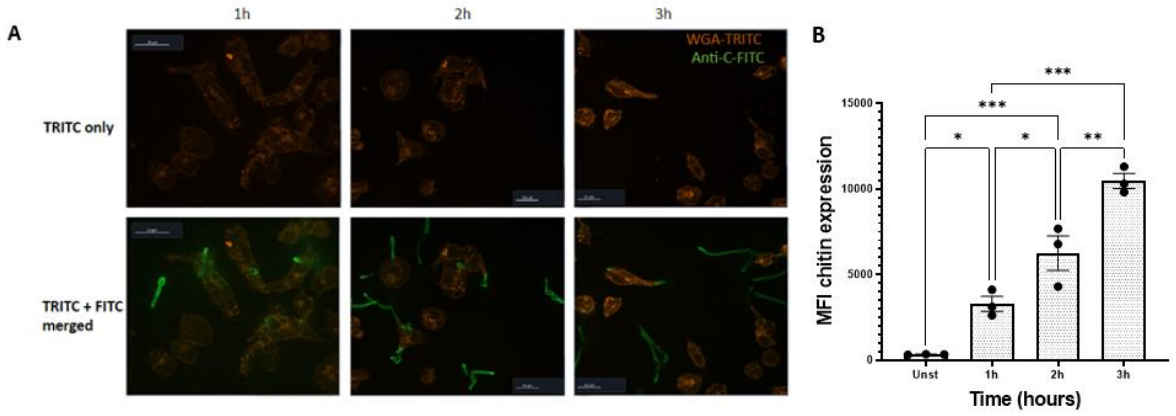

Figure 5.2. ***C. albicans*** **increases chitin exposure within RAW 264.7 macrophages.** RAW 264.7 macrophages were co-incubated with wild-type *C. albicans* (SC5314) for the indicated times. Extracellular *C. albicans* were stained with anti-*Candida*-FITC before macrophages were permeabilized and intracellular *C. albicans* stained with WGA-TRITC (**A**) Fluorescent microscopy revealed increasing levels of chitin staining from 1 h to 3 h post phagocytosis. (**B**) We also measured the fluorescent intensities of intracellular *C. albicans* by flow cytometry. There was an increase at 2 h post-infection from 1 h. At 3 hours post-infection, there was a bigger increase in chitin exposure compared to 1 h and 2 h post infection. Data are means ± SEM of 3 biological replicates. One-way ANOVA was used to analyse data with Tukey's multiple comparison test (ns not significant; * $P < 0.05$; ** $P < 0.005$; *** $P < 0.0005$).

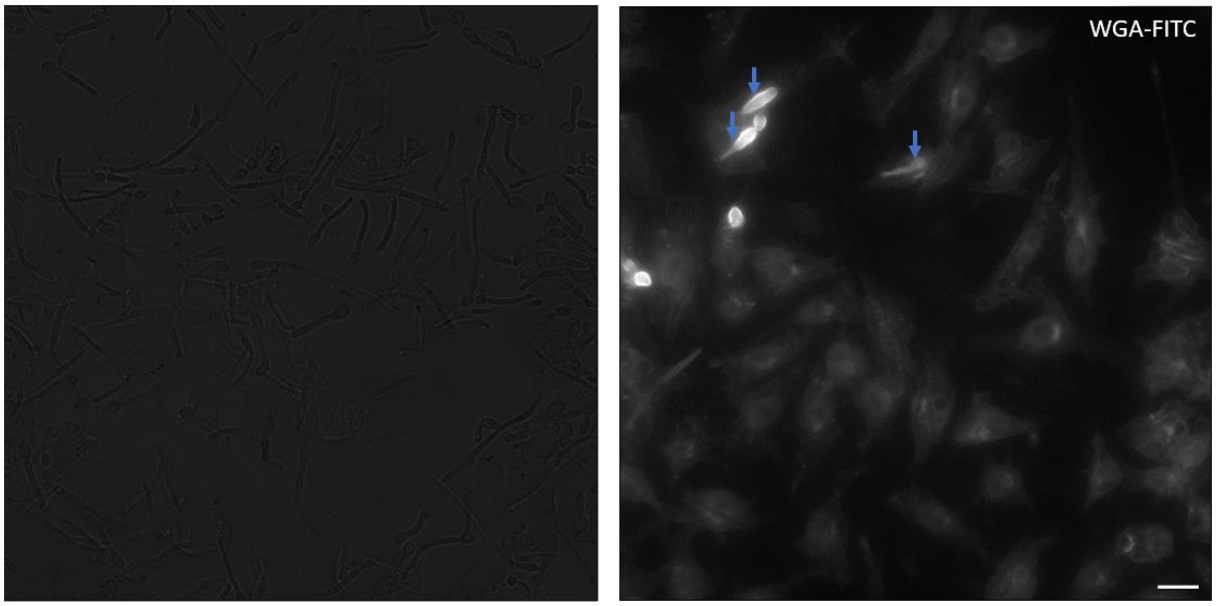

Figure 5.3. **Cell wall chitin exposure is increased within phagosomes.** Staining of cell wall exposed chitin is increased in internalised *C. albicans*. The image on the left shows a brightfield image and the image on the right shows WGA-FITC staining shown I grey-scale. Blue arrows showing fully internalised *C. albicans* with high chitin exposure levels. Scale bar 50 μm.

Increases in chitin exposure, quite often correlate with increases in glucan exposure. Therefore, as chitin exposure was significantly increased in phagocytosed *C. albicans* cells, the levels of β1,3-glucan exposure was also quantified. There was increased exposure of β-glucan between 1- and 2-hours post exposure, which was more pronounced at 3 hours post exposure as measured by microscopy [Fig. 5.4A and B]. Indeed, our flow cytometry data did reflect these observations as slight increase of MFI levels were observed at 1 and 2 hours with a further increased at the 3-hour time-points [Fig. 5.4C]. Together these depict a time-dependent increase in exposure of these two PAMPs within macrophage phagosomes.

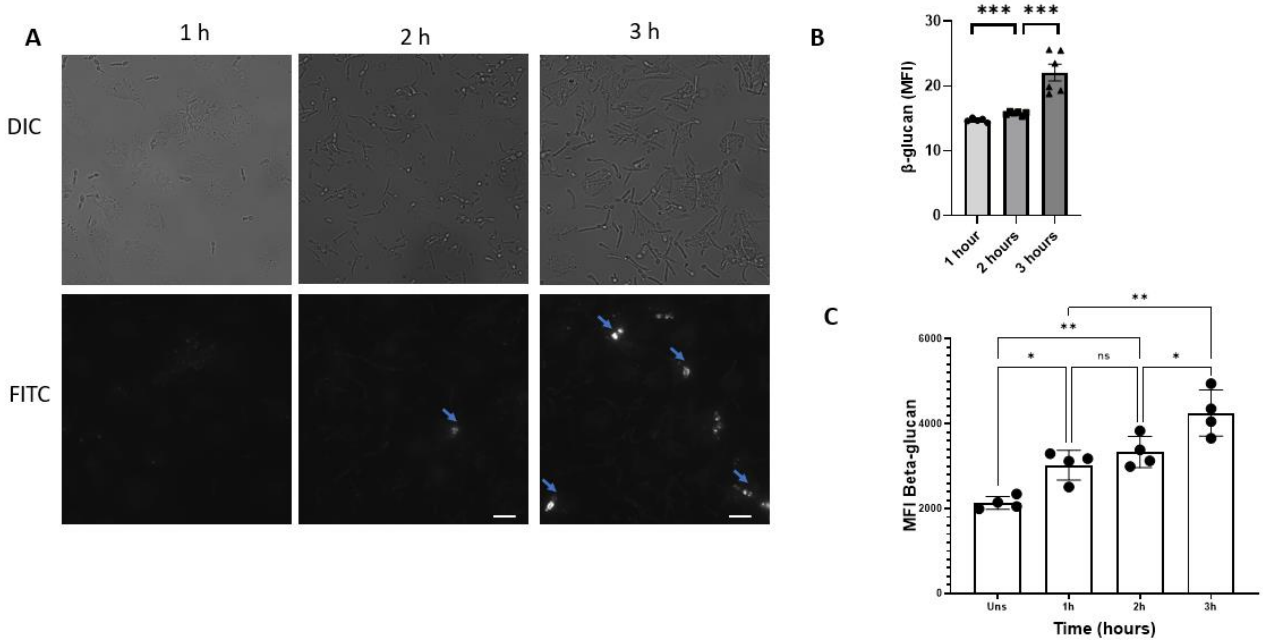

Figure 5.4. ***Candida albicans β*-glucan exposure at different time-points post incubation with RAW264.7 macrophages**. *C. albicans* at mid-exponential growth phase was incubated with PMA activated and serum starved RAW macrophages ($1x10^5$) at an MOI of 5. The assays were stopped at 1 h (left panels), 2 h (middle panels) and 3 h (right panels) post-infection and stained with Dectin-1-Alexa Fluor 488. (A) The upper panels are the DIC images, and the lower panels are the fluorescent images. At 1 h post infection, little *β*-glucan exposure can be seen at bud scars. Two hours post infection, increased glucan exposure was seen in a very few cells (blue arrow) and even more cells with greater exposure was seen 3 h post infection (blue arrows). (B) Fluorescent intensities were measured from microscopic images at different time-points from 3 independent experiments (each data point is the mean of cells within the same field of view). (C) The median fluorescent intensities at the different time points were measured by flow cytometry- data points are the average of independent replicates. Scale bar 50 μm.

To determine whether cell wall remodelling genes are significantly enriched in *C. albicans* upon phagocytosis, we utilised a previously published RNA seq dataset from Munoz et al., (Muñoz et al., 2019). In this dataset, macrophages were infected with *C. albicans* for different timepoints, cells were then divided into subpopulations (macrophages infected with live *C. albicans*, macrophages infected with dead *C. albicans*, macrophages exposed to *C. albicans* but uninfected, and *C. albicans* exposed to macrophages but un-phagocytosed) and single cell RNA-Seq performed on these cells to assess transcriptional changes. Here, I compared and quantified differentially expressed genes between live

C. albicans that were exposed to macrophages but not phagocytosed and those engulfed by macrophages at different time points. Engulfed *C. albicans* cells differentially upregulated genes related to both chitin and β-glucan as early as 1 hour of phagocytosis including KRE6 and Chs8 (see Table 2.9). Taken together, these data suggest that *C. albicans* undergoes cell wall remodelling within macrophages and this could affect subsequent encounters with immune cells when they escape from the initial macrophage.

Table 5.1. Phagosome induced differentially expression of cell wall genes.

Gene	**DEGs (Chitin)**	**DEGs (Glucan)**	**Brief description**	**Time (h)**	**Fold Change**	**P-value**
KRE6		Yes	Essential beta-1,6-glucan synthase subunit	1	5.2	0.01
BIG1		Yes	required for beta-1,6-glucan synthesis	4	26.5	<0.001
UTR2	Yes		induced during cell wall regeneration	1	3.4	0.03
Chs2	Yes		CaChs2p encodes the major chitin synthase activity in vitro; are upregulated shortly after induction of hyphal formation	2	10.2	0.03
Chs8	Yes		CaChs8p and CaChs2p account for almost all the measurable in vitro chitin synthase activity in membrane preparations but are non-essential for growth	1	3.4	0.001

Cht4	Yes	Chitinase; homozygous null mutation causes no obvious defects; transcription decreases upon yeast-to-hyphal switch	1	7.0	0.02
Pga31	Yes	Chitin biosynthesis	4	58.3	0.03

5.2.2 Neutrophils

Neutrophils are key players in *C. albicans* clearance and having confirmed that *C. albicans* undergoes significant cell wall remodelling upon internalisation into macrophage phagosomes, we then assessed whether internalisation of *C. albicans* by human neutrophils results in similar cell wall remodelling. For this experiment, human neutrophils were isolated from peripheral blood and co-incubated with *C. albicans* yeast. Although there was no discrimination in internalised and extracellular *C. albicans*, there was an apparent increase in the levels of chitin [Fig. 5.5]. Therefore, *C. albicans* undergoes significant cell wall remodelling upon internalisation into both macrophage and neutrophil phagosomes.

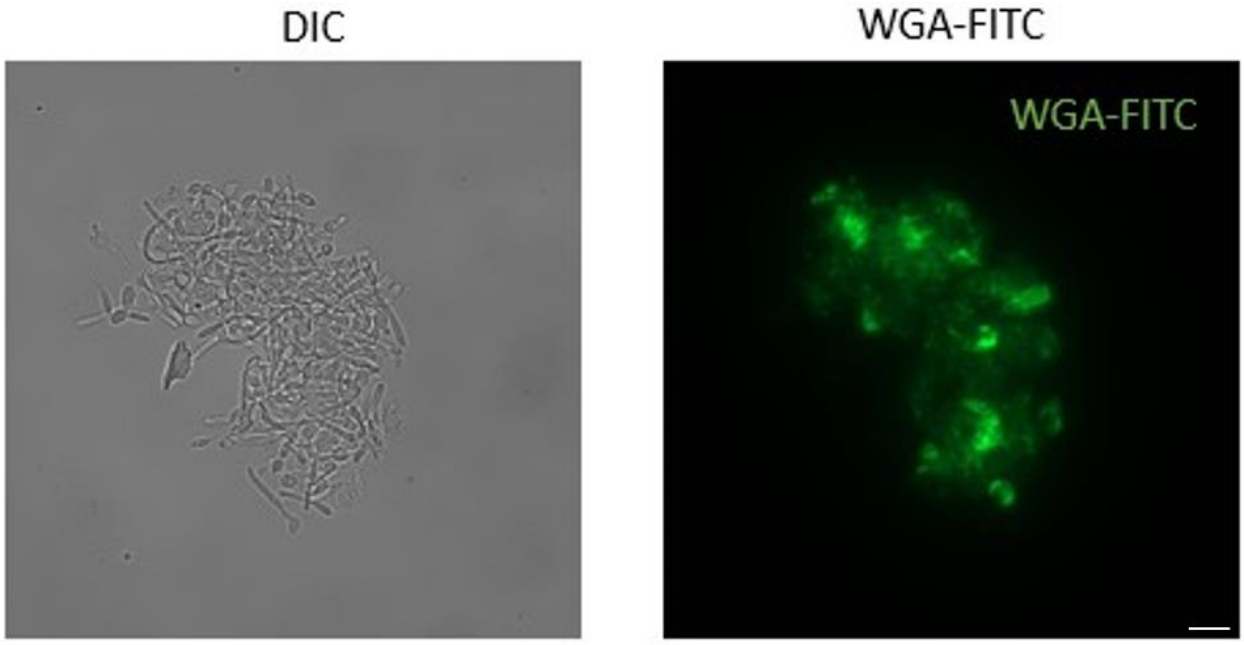

Figure 5.5. **Human neutrophils cause increased chitin exposure in *C. albicans*.** Neutrophils were incubated with *C. albicans* yeast for 3 hours. Neutrophils were then lysed and *C. albicans* stained for chitin exposure with WGA-FITC. The panel on the left represents the DIC image while the lower panel shows substantial chitin staining on the cell wall. Scale bar 50 μm.

5.2.3 TLR9 recruitment to *C. albicans* containing phagosomes – microscopy

Macrophages possess intracellular pattern recognition receptors and TLR9 has been identified to detect fungal DNA and is recruited to phagosomes containing specific fungal pathogens including *C. albicans*, *Cryptococcus neoformans* and *Saccharomyces cerevisiae* (Netea et al., 2008, Kasperkovitz et al., 2011)]. Importantly, TLR9 has also been shown to detect *C. albicans* chitin and acts in concert with NOD2 and mannose receptor to initiate an anti-inflammatory response, which is thought to be important in the resolution of disease after the elimination of *C. albicans* (Wagener et al., 2014). However, *C. albicans* may also increase chitin exposure to manipulate inflammatory immune responses and facilitate their escape (Wagener et al., 2014). To understand the temporal dynamics of this recruitment, macrophages were transfected with fluorescently tagged TLR9 and the recruitment of TLR9 to *C. albicans* containing phagosomes monitored by microscopy. When these macrophages

were incubated without *C. albicans* stimulation, there was little accumulation of TLR9 in macrophages. However, incubation with *C. albicans* caused time dependent accumulation to *C. albicans* containing phagosomes [Fig 5.6A, B and C]. There was little or no recruitment of TLR9 to the phagosome at 1 hour, but this increased 2 hours post co-incubation [Fig. 5.7]. However, this increase was transient as reduced recruitment of TLR9 was observed 3 hours post co-incubation [Fig. 5.6A, B and C]. Together these preliminary data suggest interesting recruitment dynamics of TLR9 to *C. albicans* containing phagosomes, which needs to be verified with more biological replicates.

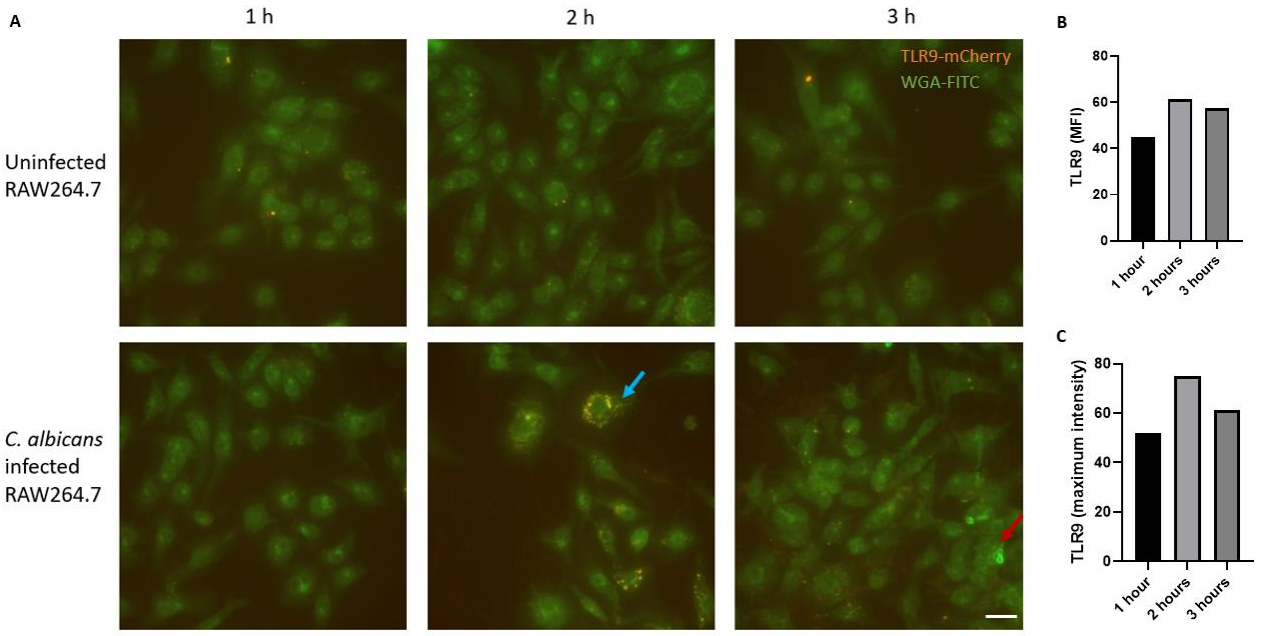

Figure 5.6. **TLR9 recruitment dynamics in *C. albicans* infected RAW264.7 macrophages.** Macrophages transfected with TLR9 fused to mCherry were infected with *C. albicans* for 1, 2 and 3 hours and TLR9 recruitment assessed by comparing the level of fluorescence between *C. albicans* infected and uninfected macrophages. (A) The top panels represent uninfected macrophages, and the bottom panels are the infected macrophages (n=1). (B) The MFI of TLR9 fluorescent in macrophages with engulfed *C. albicans* was measured. (C) The maximum intensity of TLR9 spots was also quantified in at least 50 macrophages. Blue arrow – TLR9 colocalizing to *C. albicans* containing phagosome. Red arrow – Chitin staining in phagocytosed *C. albicans*. The scale bar represents 50 μm.

5.2.4 Vancomycin has no effect on fungal cell wall changes

In Chapter 3, it was observed that vancomycin had no direct effects on fungal growth or hyphal formation. However, these parameters do not identify any possible impact on the cell wall. Therefore, the direct effect of vancomycin on the cell wall structure was investigated. Chitin is highly exposed in acidic media (Sherrington et al 2017) and was therefore used as a proxy for cell wall remodelling. Vancomycin was added at different concentrations and incubated for different times [Fig. 5.7]. When *C. albicans* was incubated with 20, 50 or 100 µg/mL of vancomycin, there was no significant effect on the level of chitin exposed on the cell wall. The levels also did not change with a longer incubation time as similar levels were observed at both 1 hour and 2 hours post incubation, which were comparable to untreated controls. Furthermore, the proportion of cells exposing chitin on their cell wall was comparable to untreated controls suggesting that vancomycin treatment even at doses as high as 100 µg/mL does not cause cell wall remodelling in *C. albicans* [Fig. 5.7].

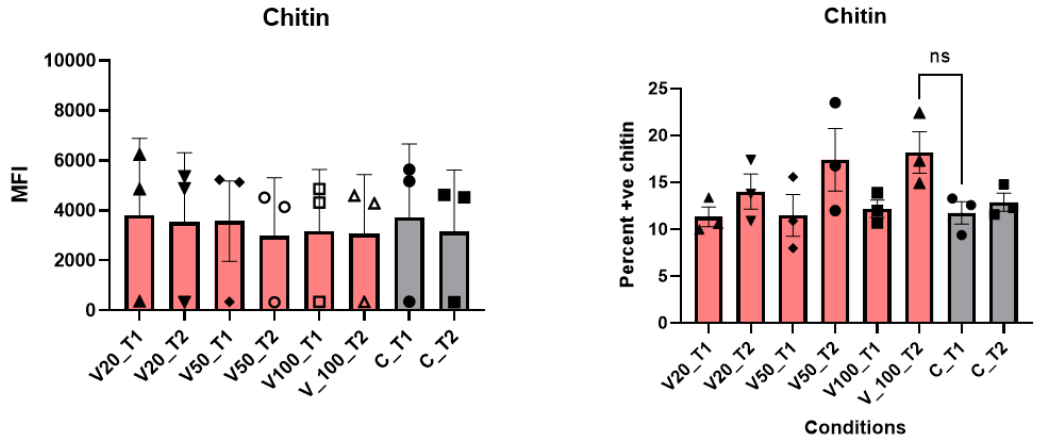

Figure 5.7. **Vancomycin does not cause increased chitin exposure**. *C. albicans* cells were incubated in 20, 50 or 100 µg/mL of vancomycin or control media (RPMI) for 1 and 2 hours of incubation and chitin exposure quantified using flow cytometry. Each data point represents a biological replicate.

5.2.5 Vancomycin treated macrophage did not differentially increase cell wall remodelling

Since we have shown that vancomycin pre-treated macrophages are hyper-inflammatory during *C. albicans* infection, we wanted to assess if this affected *C. albicans* cell wall remodelling. Vancomycin pre-treated macrophages were infected with *C. albicans* yeast for the indicated times, extracellular *C. albicans* were stained with anti-*Candida*-FITC before macrophages were lysed to access intracellular *C. albicans*. These cells were stained for chitin exposure and analysed using flow cytometry. Vancomycin pre-treated macrophages did not differentially induce cell wall remodelling as similar chitin levels were seen in control macrophages [Fig. 5.8]. This is probably unsurprising as acidic pH is one of the triggers of cell wall remodelling, but we observed no acidification of the phagosome in both vancomycin treated and untreated controls during infection with live *C. albicans* and similar acidification levels were observed during infection with heat-killed *C. albicans* (Chapter 3).

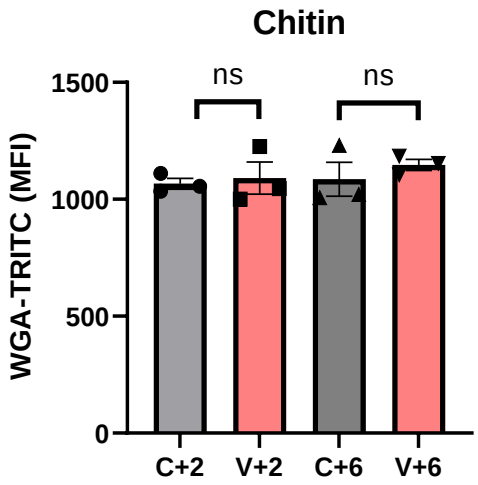

Figure 5.8. **Vancomycin pre-treated macrophages do not affect chitin exposure levels in phagocytosed *C. albicans***. Vancomycin pre-treated and control macrophages were infected with *C. albicans* yeast for 2 hours. Extracellular candida was discriminated with anti-*Candida*-FITC staining before lysing macrophages to stain for exposed chitin. Each data point represents a biological replicate. C+2 and V+2 - infected at an MOI of 2. C+6 and V+6 - infected at an MOI of 6.

5.3 DISCUSSION

In this chapter, we show that *C. albicans* undergoes cell wall remodelling within innate cell phagosomes, which is time dependent. There was early exposure of chitin, but a more delayed β-glucan exposure was observed. TLR9 recruitment was also time dependent, whereby we see robust recruitment at around 2 hours post infection, which subsides around the 3-hour time-point. Vancomycin treatment was shown in the previous chapters to trigger early activation of the inflammasome, but our results indicate no effects on *C. albicans* cell wall changes.

Chitin and β-glucan are buried in the cell wall but can be differentially exposed depending on environmental cues. Here, we show that chitin exposure within macrophage phagosomes is time dependent with more chitin exposed with time up to 3 hours post infection. This finding corroborates findings in Wagener et al ., (Wagener et al., 2017) whereby chitin exposure was increased within phagosomes. Intriguingly, *C. albicans* chitin is a known cell wall PAMP and its uptake is mediated by mannose receptor, and this induces secretion of the anti-inflammatory cytokine, IL-10 in a mechanism involving NOD2 and TLR9 (Wagener et al., 2014). This is an interesting finding as the sensing of chitin can be used by immune cells to indicate fungal damage and thus dampen pro-inflammatory responses. However, *C. albicans* may also be elevating chitin exposure to hijack this pathway to manipulate the immune system from a destructive pro-inflammatory response to an anti-inflammatory response in other to escape elimination by innate immune cells. Adaptation to acidic pH also causes enhanced exposure of both chitin and *C. albicans*, which causes greater neutrophil recruitment and production of pro-inflammatory cytokines (Sherrington et al., 2017). Cottier *et al* (Cottier et al., 2019) also showed a time-dependent increase in chitin during growth in acidic pH. Interestingly, during normal phagosome maturation, the phagosomal compartment becomes increasingly acidic, however, *C. albicans* is known to cause alkalinisation of the phagosome in at

least two distinct ways including amino acid catabolism dependent alkalinisation to enhance hyphal growth (Vylkova et al., 2011, Vylkova and Lorenz, 2014) and hyphae induced proton leakage due to membrane distension as hyphae grow (Westman et al., 2018). Therefore, acidic pH might be playing a limited role in phagosome induced cell wall remodelling and other phagosomal cues, which were not examined in the present study may also be contributing to the enhanced chitin exposure.

Neutrophils play a key role in the clearance of *C. albicans*. These cells differ slightly to macrophages in the mechanisms by which they combat *C. albicans* such as the use of NETs and they undergo much quicker phagosome maturation, which fuses with neutrophil granules containing antimicrobial peptides and proteolytic enzymes (Lee et al., 2003, Nauclér et al., 2002, Nordenfelt and Tapper, 2011). Here, we observed similar chitin exposure in human neutrophil exposed *C. albicans*. Although we did not discriminate between phagocytosed and non-phagocytosed *C. albicans* in this assay, the fact that macrophage exposed but un-phagocytosed *C. albicans* have no evidence of increased chitin exposure in macrophages, we speculate that these *C. albicans* showing increased chitin exposure had been phagocytosed by neutrophils, but we are not ruling out the effect of NETs on inducing chitin exposure.

Additionally, our analysis of the single cell RNA-Seq to investigate transcriptional changes in cell wall remodelling related genes revealed interesting findings. There was an increase in chitin related genes such as Utr2, Chs8 and Cht4 as early as 1-hour post-phagocytosis. The cell wall protein, Utr2 has been shown to be important for *C. albicans* cell wall integrity and maintenance and plays a role in filamentation and virulence (Alberti-Segui et al., 2004). Chs8 and Chs2 are class I chitin synthases that were both upregulated with Chs2 increased 10-fold at 2 hours. These chitin synthases play a vital role in maintaining cell wall integrity (Preechasuth et al., 2015). Upregulation of these genes have

also been reported in caspofungin and Calcofluor White plus Ca^{2+} induced stresses (Munro et al., 2007, Walker et al., 2013) thus supporting our observation that these genes are upregulated in response to phagosomal stresses. These cells might be acting to protect *C. albicans* by reinforcing the cell wall with more chitin. Finally, we also identified early upregulation of Cht4 gene and although this gene has been described as a chitinase encoding gene, its specific function is yet to be determined (Jiang and Yan, 2023). Chitinases play a key role in cell wall remodelling during morphogenesis by breaking down glycosidic bonds in the chitin (Gow and Lenardon, 2023, Tanaka et al., 2001). However, because the null mutant of Cht4 has no detectable defects, it is highly likely that it is a redundant gene. Together, these data suggests that increased chitin exposure in *C. albicans* is a stress resistant mechanism that is not only induced by macrophage phagosomes but also occur during their interaction with human neutrophils.

Furthermore, β-glucan is exposed at bud-scars of yeast, but we observed increased exposure in macrophage associated *C. albicans* with time and the most exposure was observed 3 hours post infection. Adaptation to acidic pH also causes increase of β-glucan with time and in Cottier *et al* (Cottier et al., 2019), they observed a time dependent increase of β-glucan which plateaued between 2- and 3-hours post infection. Furthermore, they showed that *C. albicans* undergoes remasking of both chitin and β-glucan with time and this remasking becomes apparent around 5 hours post incubation (Cottier et al., 2019). Although this is an interesting finding, remasking of these PAMPs was not assessed in this study as extensive hyphal formation precludes assessing phagosome induced cell wall changes at later times so our latest incubation time was 3 hours post infection.

Our analysis of single cell RNA-Seq also revealed increased expression of glucan related genes Big1 and Kre6 in phagocytosed *C. albicans*. Although their role during cell wall remodelling within

phagosomes is not known, these genes are involved in the synthesis of β-1,6-glucan and they play an indispensable role in the viability of *Saccharomyces* mutants (gas1Δ) with defective β-1,3-glucan processing (Tomishige et al., 2003). In another study, hemizygous mutation of Kre6 caused more than 80% reduction in β-1,6-glucan and these mutants were more sensitive to Calcofluor White stress and have partial defects in cell separation showing the importance of this gene in both growth and response to stress (Mio et al., 1997).

In chapter 3 and 4, our data shows that vancomycin did not affect the growth of *C. albicans* or directly bind to it and in this chapter, growth in vancomycin media had no impact on chitin exposure on the cell wall. Similarly, vancomycin pre-treated macrophages did not differentially cause changes in chitin exposure. This is despite these macrophages being hyper-inflammatory with increased oxidative stress and inflammasome activation. In future studies, it will be interesting to investigate if TLR9 recruitment is affected by vancomycin treatment. Since, chitin causes an anti-inflammatory response through TLR9 signalling, vancomycin might affect this recruitment, which could further explain the inflammatory status of these macrophages.

In summary, the effects of vancomycin in anti-fungal immunity are macrophage specific. Vancomycin does not affect the growth of *C. albicans* or induce cell wall changes either directly or when within macrophages.

6 DISCUSSION

The discovery of antibiotics and its subsequent introduction into clinical practice remains as one of the greatest medical breakthroughs in the 20th century. Antibiotics have drastically reduced deaths related to infectious diseases in the pre-antibiotic era and has contributed to increased human life-expectancy (Hutchings et al., 2019, Suárez-Rivero et al., 2021). For instance, bacterial meningitis was associated with 90% death in children before antibiotics (UK, 2018). Antibiotics have also contributed to advancing modern medicine by making it possible to conduct life-saving medical practices such as bone marrow and solid organ transplantations. Consequently, antibiotics form a key component in modern medicine. However, along with their benefits comes their detrimental side effects, which includes hepatic and renal dysfunction, antibiotics resistance and an increased growth of opportunistic pathogens such as *C. albicans* (Suárez-Rivero et al., 2021, Fan et al., 2015). Invasive *C. albicans* infections are associated with very high mortality rates and very high hospital costs, which range from approximately $10,000 to $38,000 (Wan Ismail et al., 2020). Therefore, advancing our knowledge on how antibiotics increase the risk of invasive candidiasis is important and could save many lives.

Although studies have described the contribution of the microbiota in antibiotic induced susceptibility to invasive candidiasis, the potential direct effects of antibiotics on immune cells that may predispose individuals to these infections is not completely understood. Drummond et al., (Drummond et al., 2022) showed that vancomycin treated mice have enhanced mortality following intravenous challenge with *C. albicans* compared to untreated controls, but the role of macrophages in this phenotype is not known despite their known importance in maintaining fungal levels in the gut.

In this study we show that vancomycin caused reduced *C. albicans* killing without affecting recognition or phagocytosis. These macrophages had increased oxidative stress, decreased mitochondrial function, and fragmented morphology (Fig. 6.1). Furthermore, vancomycin pre-treated macrophages infected with *C. albicans* were more inflammatory, had increased activation of the inflammasome, which is hypothesised to be driven by increased oxidative stress (ROS) and eventually death by pyroptosis.

Graphical Abstract

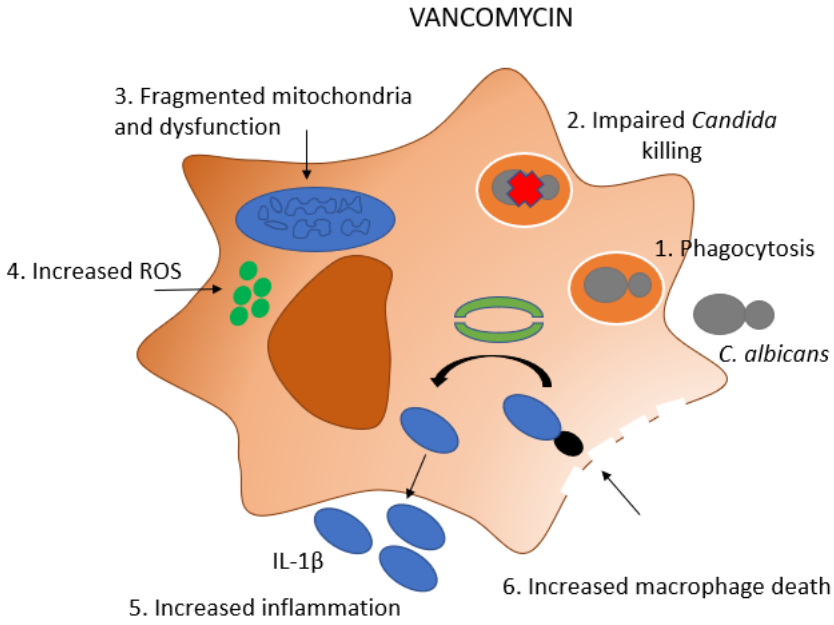

Figure 6.1. Proposed model for the effect of vancomycin on macrophage anti-*C albicans* function. (1) Pretreating macrophages with vancomycin did not affect their recognition or phagocytosis of *C. albicans*. (2) Vancomycin pre-treatment caused reduced killing efficiency. (3) The treatment also mitochondrial fragmentation and dysfunction. (4) There was increased oxidative stress in treated macrophages. (5) There was increased inflammsome activation in treated macrophages during infection with *C. albicans* which potentially led to (6) death by pyroptosis.

6.1 VANCOMYCIN DOES NOT DIRECTLY AFFECT C. ALBICANS

C. albicans inhabits several body niches and at such needs to constantly adapt to its environment. Part of its adaptive strategies is to remodel its cell wall (Sherrington et al., 2017). We did not observe any significant remodelling of the cell wall, and this is important because cell wall changes influence its interaction with innate immune cells. This could have led to increased or decreased phagocytosis by macrophages, which would have had an impact on the rate of killing seen. However, our data suggest vancomycin treated macrophages were equally able to recognise and phagocytose *C. albicans* further supporting the lack of cell wall changes.

Furthermore, hyphal formation is tightly linked to virulence (Lo et al., 1997, Saville et al., 2003). Hyphal formation is important to *C. albicans* because hyphae express more adhesion protein (i.e. ALS3 and HWP1) on the cell wall (Naglik et al., 2011), which facilitates adhesion to epithelial and endothelial cells and hyphal growth contributes to the invasion of epithelial cells (Naglik et al., 2011). Additionally, hyphal formation is associated with production of candidalysin, which is a major virulence factor of *C. albicans* and aids its escape from immune cells when produced in large amounts (Moyes et al., 2016). *C. albicans* hyphae size also makes it particularly challenging for macrophage phagocytosis (Maxson et al., 2018, Lewis et al., 2012). Again, our data reveal no direct effect on hyphal formation suggesting that vancomycin treatment did not change the virulence potential of these *C. albicans* cells. The lack of vancomycin's effect on *C. albicans* is intriguing because *C. albicans* possesses mitochondria and we show the effects of vancomycin on macrophages largely occurred via the mitochondria. However, this could be because of the *C. albicans* cell wall, which is multi-layered with an outer mannan layer largely covering the inner layer of chitin and β-glucan (Gow and Lenardon, 2023). Vancomycin targets peptidoglycan of Gram-positive bacteria and has a strong affinity for lipids, which are all lacking in the *C. albicans* cell wall. Consequently, we observed no

binding of the fluorescent vancomycin on *C. albicans* despite extensive staining of macrophages (Fig. 3.1B) suggesting that vancomycin has no binding targets on the *C. albicans* cell wall. This is an important finding since *C. albicans* colonises up to 70% of individuals and any intervention that enhances their virulence potential would have raised serious public health concerns.

6.2 VANCOMYCIN'S EFFECT ON MACROPHAGES

6.2.1 Hyper-inflammatory state of macrophages

Vancomycin treated macrophages are hyper-inflammatory during *C. albicans* infections and we have several supporting data for this including transcriptional changes and cytokine profile. For instance, there was increased expression of *Mir155,* which blocks two different anti-inflammatory pathways to promote inflammation (Alivernini et al., 2017). There was also increased activation of the inflammasome pathway in these macrophages (Chapter 3). *C. albicans* is known to hijack this pathway to facilitate its escape by activating pyroptosis and there was increased macrophage death in vancomycin pre-treated macrophages compared to control macrophages (Erwig and Gow, 2016). In the absence of increased hyphal growth in the vancomycin treated group, these data indicate that early and robust activation of the inflammasome is causing the premature death of macrophage, which would significantly reduce their capacity to kill *C. albicans* as seen in this study. Macrophages are important in maintaining fungal burden and maintaining gut barrier integrity (Chikina et al., 2020) and their inability to adequately respond to *C. albicans* could contribute to the increased fungal burden within the gut of vancomycin treated mice (Drummond et al., 2022). *C. albicans* has also been described to induce macrophage death by out-competing macrophages for glucose as both *C. albicans* and macrophages switch to glycolysis during infection (Tucey et al., 2018). However, this is unlikely

to be the case in our study as this occurs at around 9 hours post infection, which is beyond our incubation times.

6.2.2 Mitochondrial fragmentation, increased ROS, and metabolic changes

Our data revealed that vancomycin induced hyper-fragmented mitochondria with increased oxidative stress, which led to loss of metabolic function, and this concurs with its effects on renal tubular cells (Seo et al., 2010, Kalghatgi et al., 2013). ROS is known to prime/activate the inflammasome (Heid et al., 2013) and its plausible that vancomycin induced ROS seen in this study primes the inflammasome and subsequently cause early activation of the inflammasome pathway during infection. In support of this hypothesis, vancomycin treatment alone did not cause inflammasome activation suggesting that ROS alone is not driving the phenotypes seen in these macrophages but may be working in concert with other fungal elements such as β-glucan, a known trigger of the inflammasome pathway (Erwig and Gow, 2016). Interestingly, vancomycin does not cause any more increase in β-glucan exposure either directly or through macrophage phagosomes. This could suggest the significance of the priming step in the inflammasome pathway or may suggest that other activators of the inflammasome pathway not tested in this study may be playing a role.

These hyper-inflammatory macrophages are also shown to be metabolically less capable of responding to the added stress of *C. albicans* as indicated by their spare respiratory capacity. This is further supported by the loss of mitochondrial membrane potential, which is essential for both efficient ATP production and maintaining mitochondrial viability and thus explains the reduced ATP seen during vancomycin treatment alone (Zorova et al., 2018). The reduced killing of *C. albicans* is therefore of little surprise since vancomycin treated macrophages fail to adequately respond to *C.*

albicans stress. This result would suggest that other antibiotics that can affect macrophage mitochondria in a similar way would also affect macrophage anti-fungal effects. For instance, one study reported cefotaxime's role in inhibition of intracellular killing and phagocytosis of *Listeria monocytogenes* by rabbit peritoneal macrophages, but imipenem, a beta-lactam antibiotic has no effect on phagocytosis or killing of *C. albicans* by peritoneal macrophages (Miller and Singer, 2022). Furthermore, teicoplanin and vancomycin (both glycopeptides) were shown to affect neutrophil phagocytosis and killing of *C. albicans* at high concentrations (Miller and Singer, 2022). These suggest that different antibiotics would affect immune cells differently. Although we did not assess the direct effects of other antibiotics on macrophage anti-fungal responses in this study, Drummond et al (Drummond et al., 2022) showed that only vancomycin had a major effect on susceptibility to intravenous challenge of *C. albicans*. Vancomycin has high binding affinity to lipids including PG and cardiolipin, which are abundant in macrophage and mitochondrial membranes (Tam, 2017), and this potentially explains why they caused increased susceptibility in relation to other tested antibiotics. However, vancomycin could also be exerting its effects via disruption of the gut microbiota, which was observed in that study. The gut microbiota plays a key role in several processes from regulating excessive pathogenic growth due to competition with other microbes to the maturation and function of microglia (Erny et al., 2015). Importantly, it contributes to the differentiation of Th17 cells, which are important for mucosal antifungal immunity (Ivanov et al., 2009). Therefore, disruption of the gut microbiota is potentially a major factor in these phenotypes.

Nonetheless, further research is needed using antibiotics with similar mode of action to assess if the phenotypes observed in this study are unique to vancomycin. We anticipate that other antibiotics may also have effects on macrophage function but may do so differently to what is observed in this study. This illustrates the need to study the unwanted effects of antibiotics just as we monitor antibiotic

resistance as this knowledge can be incorporated into medical practices to prevent exposing patients to unwanted consequences.

6.3 CLINICAL IMPLICATIONS

The importance of macrophages in maintaining fungal burden within the gut means that affecting their function would pose serious medical concerns. Clinically, vancomycin use is usually prolonged due to the nature of infections it is used to treat such as patients infected with *Enterococcus faecium, Clostridium difficile, and Staphylococcus aureus* including methicillin resistant *Staphylococcus aureus* (MRSA) infections with or without endocarditis (Bode et al., 2015, Ingram et al., 2008, van Opstal et al., 2016). However, vancomycin affects renal cells in very similar ways as seen in our study (Arimura et al., 2012). With these effects, it is somewhat unsurprising that candidaemia was more prevalent in patients receiving vancomycin for the treatment of *Clostridium difficile* infection thus confirming its role in susceptibility to invasive candidiasis (Russo et al., 2015). It is interesting however that treating renal tubular cells with vitamin E reverses the detrimental effects of vancomycin (Arimura et al., 2012) and therefore in situations where prolonged vancomycin use is unavoidable such as people with complicated MRSA infections or in patients with penicillin resistance, the use of combination therapy with vitamin E can be explored. Alternatively, the flavonol glycoside rutin, which has also been shown to protect renal tubular cells (Qu et al., 2019) from the detrimental effects of vancomycin can also be co-administered with vancomycin.

Furthermore, our data suggests a direct effect of vancomycin on mitochondria which is partly due to increased oxidative stress. ROS plays a role in inflammatory pathways and perhaps the use of vancomycin with ROS scavenging drugs might also offer protection for these patients. Combination

therapy with drugs that inhibit the inflammasome pathway would also need to be explored as an option to reduce macrophage death. Nonetheless, the role of ROS would first have to be established in future experiments.

6.4 FUTURE PERSPECTIVE

Our data suggests a direct link between prolonged antibiotic use and disrupted macrophage anti-fungal responses. Mitochondrial dysfunction and increased inflammation play a key role in this pathway; however, the complete mechanism has not been fully determined. For instance, the role of ROS in inflammasome activation is well documented but if ROS is the only driver or works in conjunction with other factors in activating this pathway would have to be established in future experiments. To assess this, ROS would be induced in macrophages with ROS inducing agents and then macrophages will be challenged with *C. albicans* to try and replicate these phenotypes.

The research would benefit by replicating some of these findings in an *in-vivo* setting. The effects of vancomycin on the gut microbiota have already been shown to contribute to increased susceptibility to invasive candidiasis (Drummond et al., 2022). To elucidate the direct effects of vancomycin on immune cells *in-vivo*, it will be vital to perform these experiments in germ-free mice. This can be performed using a similar protocol to Drummond *et al*., (Drummond et al., 2022). Mice will be treated with vancomycin through their drinking water for 28 days and then challenged intravenously with *C. albicans*. Gut macrophages will then be isolated and inflammatory markers and markers of oxidative and mitochondrial stresses would be assessed. Alternatively, mice can be macrophage depleted and treated with or without vancomycin and compare the effects against wild-type mice. This will

potentially explain the direct or indirect effects of vancomycin on macrophages and other immune cells.

This study has made significant steps towards understanding how antibiotics might be affecting macrophage anti-fungal responses. Although these findings need to be validated in relevant *in-vivo* models, it provides us with an understanding of what to look for in these models.

7 REFERENCES

ALBERTI-SEGUI, C., et al. (2004) Identification of potential cell-surface proteins in Candida albicans and investigation of the role of a putative cell-surface glycosidase in adhesion and virulence. *Yeast,* **21** (4), 285-302.

ALGARRA, I., et al. (2002) Suppression of splenic macrophage *Candida albicans* phagocytosis following in vivo depletion of natural killer cells in immunocompetent BALB/c mice and T-cell-deficient nude mice. *FEMS Immunology & Medical Microbiology,* **33** (3), 159-163.

ALIVERNINI, S., et al. (2017) MicroRNA-155-at the Critical Interface of Innate and Adaptive Immunity in Arthritis. *Front Immunol,* **8**, 1932.

AMBE, N. F., et al. (2020) The prevalence, risk factors and antifungal sensitivity pattern of oral candidiasis in HIV/AIDS patients in Kumba District Hospital, South West Region, Cameroon. *Pan Afr Med J,* **36**, 23.

ANDERSON, S., et al. (1981) Sequence and organization of the human mitochondrial genome. *Nature,* **290** (5806), 457-465.

ARIMURA, Y., et al. (2012) Mitochondrial superoxide production contributes to vancomycin-induced renal tubular cell apoptosis. *Free Radic Biol Med,* **52** (9), 1865-73.

AUSTERMEIER, S., et al. (2020) I want to break free - macrophage strategies to recognize and kill *Candida albicans*, and fungal counter-strategies to escape. *Curr Opin Microbiol,* **58**, 15-23.

AYBAY, C. and IMIR, T. (1996) Tumor necrosis factor (TNF) induction from monocyte/macrophages by *Candida* species. *Immunobiology,* **196** (4), 363-74.

AZEVEDO, E. P., et al. (2015) A Metabolic Shift toward Pentose Phosphate Pathway Is Necessary for Amyloid Fibril- and Phorbol 12-Myristate 13-Acetate-induced Neutrophil Extracellular Trap (NET) Formation. *Journal of Biological Chemistry,* **290** (36), 22174-22183.

BAERT, K., et al. (2015) Cell type-specific differences in β-glucan recognition and signalling in porcine innate immune cells. *Dev Comp Immunol,* **48** (1), 192-203.

BALLOU, E. R., et al. (2016) Lactate signalling regulates fungal β-glucan masking and immune evasion. *Nat Microbiol,* **2**, 16238.

BÄR, E., et al. (2014) IL-17 regulates systemic fungal immunity by controlling the functional competence of NK cells. *Immunity,* **40** (1), 117-27.

BARRIGA, C., et al. (1996) Comparative study of the effect of teicoplanin and vancomycin upon the phagocytic process of peritoneal macrophages. *Rev Esp Fisiol,* **52** (4), 215-22.

BERGER, M., et al. (2010) An Slfn2 mutation causes lymphoid and myeloid immunodeficiency due to loss of immune cell quiescence. *Nature Immunology,* **11** (4), 335-343.

BODE, C., et al. (2015) Linezolid, vancomycin and daptomycin modulate cytokine production, Toll-like receptors and phagocytosis in a human in vitro model of sepsis. *The Journal of Antibiotics,* **68** (8), 485-490.

BOJANG, E., et al. (2021) Immune Sensing of *Candida albicans*. *J Fungi (Basel),* **7** (2).

BOSMANN, H. B. and WINSTON, R. A. (1972) Antibiotics and macromolecular synthesis in microsomes and mitochondria: I. Antibiotics acting in the same manner in mitochondria and microsomes. *Chemico-Biological Interactions,* **4** (2), 113-128.

BRANZK, N., et al. (2014) Neutrophils sense microbe size and selectively release neutrophil extracellular traps in response to large pathogens. *Nat Immunol,* **15** (11), 1017-25.

BREAK, T. J., et al. (2021) Aberrant type 1 immunity drives susceptibility to mucosal fungal infections. *Science,* **371** (6526), eaay5731.
BRINKMANN, V. and ZYCHLINSKY, A. (2012) Neutrophil extracellular traps: is immunity the second function of chromatin? *J Cell Biol,* **198** (5), 773-83.
BROWN, G. D. and GORDON, S. (2001) A new receptor for β-glucans. *Nature,* **413** (6851), 36-37.
BRUNO, V. M., et al. (2015) Transcriptomic analysis of vulvovaginal candidiasis identifies a role for the NLRP3 inflammasome. *mBio,* **6** (2).
CALZADA, E., et al. (2016) Phosphatidylethanolamine Metabolism in Health and Disease. *Int Rev Cell Mol Biol,* **321**, 29-88.
CAMPELLONE, K. G. and WELCH, M. D. (2010) A nucleator arms race: cellular control of actin assembly. *Nat Rev Mol Cell Biol,* **11** (4), 237-51.
CANTON, J., et al. (2014) Contrasting phagosome pH regulation and maturation in human M1 and M2 macrophages. *Mol Biol Cell,* **25** (21), 3330-41.
CAPODICASA, E., et al. (1991) In-vitro effects of teicoplanin, teicoplanin derivative MDL 62211 and vancomycin on human polymorphonuclear cell function. *J Antimicrob Chemother,* **27** (5), 619-26.
CHATZISPYROU, I. A., et al. (2015) Tetracycline antibiotics impair mitochondrial function and its experimental use confounds research. *Cancer Res,* **75** (21), 4446-9.
CHAUHAN, N., et al. (2006) Signalling and oxidant adaptation in *Candida albicans* and Aspergillus fumigatus. *Nat Rev Microbiol,* **4** (6), 435-44.
CHEN, H., et al. (2010) Mitochondrial fusion is required for mtDNA stability in skeletal muscle and tolerance of mtDNA mutations. *Cell,* **141** (2), 280-9.
CHEN, Y., et al. (2003) KappaB-Ras binds to the unique insert within the ankyrin repeat domain of IkappaBbeta and regulates cytoplasmic retention of IkappaBbeta x NF-kappaB complexes. *J Biol Chem,* **278** (25), 23101-6.
CHENG, R. Y., et al. (2017) Vancomycin and ceftriaxone can damage intestinal microbiota and affect the development of the intestinal tract and immune system to different degrees in neonatal mice. *Pathogens and Disease,* **75** (8), ftx104.
CHIKINA, A. S., et al. (2020) Macrophages Maintain Epithelium Integrity by Limiting Fungal Product Absorption. *Cell,* **183** (2), 411-428.e16.
CHIN, V. K., et al. (2014) Early expression of local cytokines during systemic *Candida albicans* infection in a murine intravenous challenge model. *Biomed Rep,* **2** (6), 869-874.
CHOW, E. W. L., et al. (2021) From Jekyll to Hyde: The Yeast-Hyphal Transition of *Candida albicans*. *Pathogens,* **10** (7).
COTTIER, F., et al. (2019) Remasking of *Candida albicans* β-Glucan in Response to Environmental pH Is Regulated by Quorum Sensing. *mBio,* **10** (5).
COX, C. S., et al. (2018) Mitohormesis in Mice via Sustained Basal Activation of Mitochondrial and Antioxidant Signaling. *Cell Metab,* **28** (5), 776-786.e5.
D'OSTIANI, C. F., et al. (2000) Dendritic cells discriminate between yeasts and hyphae of the fungus *Candida albicans*. Implications for initiation of T helper cell immunity in vitro and in vivo. *The Journal of experimental medicine,* **191** (10), 1661-1674.
DALLE, F., et al. (2010) Cellular interactions of *Candida albicans* with human oral epithelial cells and enterocytes. *Cell Microbiol,* **12** (2), 248-71.
DAVID, L., et al. (2021) Artificial Intelligence and Antibiotic Discovery.) *Antibiotics.*
DE BONT, C. M., et al. (2018) Stimulus-dependent chromatin dynamics, citrullination, calcium signalling and ROS production during NET formation. *Biochim Biophys Acta Mol Cell Res,* **1865** (11 Pt A), 1621-1629.

DENNING, D. W., et al. (2018) Global burden of recurrent vulvovaginal candidiasis: a systematic review. *Lancet Infect Dis,* **18** (11), e339-e347.
DESAI, J. V. and LIONAKIS, M. S. (2018) The role of neutrophils in host defense against invasive fungal infections. *Curr Clin Microbiol Rep,* **5** (3), 181-189.
DESHMUKH, H. S., et al. (2014) The microbiota regulates neutrophil homeostasis and host resistance to Escherichia coli K1 sepsis in neonatal mice. *Nature Medicine,* **20** (5), 524-530.
DIGNANI, M. C., et al. (2005) Immunomodulation with interferon-gamma and colony-stimulating factors for refractory fungal infections in patients with leukemia. *Cancer,* **104** (1), 199-204.
DOWLING, J. K., et al. (2021) Mitochondrial arginase-2 is essential for IL-10 metabolic reprogramming of inflammatory macrophages. *Nature Communications,* **12** (1), 1460.
DREWNIAK, A., et al. (2013) Invasive fungal infection and impaired neutrophil killing in human CARD9 deficiency. *Blood,* **121** (13), 2385-92.
DRUMMOND, R. A., et al. (2015) CARD9-Dependent Neutrophil Recruitment Protects against Fungal Invasion of the Central Nervous System. *PLoS Pathog,* **11** (12), e1005293.
DRUMMOND, R. A., et al. (2022) Long-term antibiotic exposure promotes mortality after systemic fungal infection by driving lymphocyte dysfunction and systemic escape of commensal bacteria. *Cell Host Microbe,* **30** (7), 1020-1033.e6.
DRUMMOND, R. A., et al. (2018) Human CARD9: A Critical Molecule of Fungal Immune Surveillance. *Frontiers in Immunology,* **9**.
DRUMMOND, R. A., et al. (2019) CARD9(+) microglia promote antifungal immunity via IL-1β- and CXCL1-mediated neutrophil recruitment. *Nat Immunol,* **20** (5), 559-570.
DUCHEN, M. R. (1999) Contributions of mitochondria to animal physiology: from homeostatic sensor to calcium signalling and cell death. *J Physiol,* **516 (Pt 1)** (Pt 1), 1-17.
DÜESBERG, U., et al. (2020) Risk factors for respiratory Aspergillus fumigatus in German Cystic Fibrosis patients and impact on lung function. *Sci Rep,* **10** (1), 18999.
ELEWSKI, B. E. and TOSTI, A. (2015) Risk Factors and Comorbidities for Onychomycosis: Implications for Treatment with Topical Therapy. *J Clin Aesthet Dermatol,* **8** (11), 38-42.
ENDO, D., et al. (2017) Genetic Phagocyte NADPH Oxidase Deficiency Enhances Nonviable *Candida albicans*–Induced Inflammation in Mouse Lungs. *Inflammation,* **40** (1), 123-135.
ENE, I. V., et al. (2013) Growth of *Candida albicans* cells on the physiologically relevant carbon source lactate affects their recognition and phagocytosis by immune cells. *Infect Immun,* **81** (1), 238-48.
ERNY, D., et al. (2015) Host microbiota constantly control maturation and function of microglia in the CNS. *Nat Neurosci,* **18** (7), 965-77.
ERWIG, L. P. and GOW, N. A. R. (2016) Interactions of fungal pathogens with phagocytes. *Nature Reviews Microbiology,* **14** (3), 163-176.
FAN, D., et al. (2015) Activation of HIF-1α and LL-37 by commensal bacteria inhibits *Candida albicans* colonization. *Nat Med,* **21** (7), 808-14.
FARAH, C. S., et al. (2002) Primary role for CD4(+) T lymphocytes in recovery from oropharyngeal candidiasis. *Infect Immun,* **70** (2), 724-31.
FINK, S. L. and COOKSON, B. T. (2007) Pyroptosis and host cell death responses during Salmonella infection. *Cellular Microbiology,* **9** (11), 2562-2570.
FINKEL, J. S. and MITCHELL, A. P. (2011) Genetic control of *Candida albicans* biofilm development. *Nat Rev Microbiol,* **9** (2), 109-18.
FOXMAN, B., et al. (2013) Prevalence of recurrent vulvovaginal candidiasis in 5 European countries and the United States: results from an internet panel survey. *J Low Genit Tract Dis,* **17** (3), 340-5.

FRADIN, C., et al. (2005) Granulocytes govern the transcriptional response, morphology and proliferation of *Candida albicans* in human blood. *Molecular Microbiology,* **56** (2), 397-415.
FRANK, C. F. and HOSTETTER, M. K. (2007) Cleavage of E-cadherin: a mechanism for disruption of the intestinal epithelial barrier by *Candida albicans*. *Transl Res,* **149** (4), 211-22.
FU, M. S., et al. (2018) Cryptococcus neoformans urease affects the outcome of intracellular pathogenesis by modulating phagolysosomal pH. *PLoS Pathog,* **14** (6), e1007144.
GANESAN, S., et al. (2014) Caspase-8 modulates dectin-1 and complement receptor 3-driven IL-1β production in response to β-glucans and the fungal pathogen, *Candida albicans*. *J Immunol,* **193** (5), 2519-2530.
GARCÍA-SÁNCHEZ, S., et al. (2004) *Candida albicans* biofilms: a developmental state associated with specific and stable gene expression patterns. *Eukaryot Cell,* **3** (2), 536-45.
GAVINO, C., et al. (2014) CARD9 Deficiency and Spontaneous Central Nervous System Candidiasis: Complete Clinical Remission With GM-CSF Therapy. *Clinical Infectious Diseases,* **59** (1), 81-84.
GAVIRIA, J. M., et al. (1999) Modulation of Neutrophil-Mediated Activity Against the Pseudohyphal Form of *Candida albicans* by Granulocyte Colony-Stimulating Factor (G-CSF) Administered In Vivo. *The Journal of Infectious Diseases,* **179** (5), 1301-1304.
GAZENDAM, R. P., et al. (2014) Two independent killing mechanisms of *Candida albicans* by human neutrophils: evidence from innate immunity defects. *Blood,* **124** (4), 590-7.
GÉRARD, P. (2014) Metabolism of Cholesterol and Bile Acids by the Gut Microbiota.) *Pathogens.*
GHANNOUM, M., et al. (2015) The Role of Echinocandins in *Candida* Biofilm–Related Vascular Catheter Infections: In Vitro and In Vivo Model Systems. *Clinical Infectious Diseases,* **61** (suppl_6), S618-S621.
GILLUM, A. M., et al. (1984) Isolation of the Candida albicans gene for orotidine-5'-phosphate decarboxylase by complementation of S. cerevisiae ura3 and E. coli pyrF mutations. *Mol Gen Genet,* **198** (2), 179-82.
GIRALDO, P. C., et al. (2007) Mannose-binding lectin gene polymorphism, vulvovaginal candidiasis, and bacterial vaginosis. *Obstet Gynecol,* **109** (5), 1123-8.
GLOCKER, E. O., et al. (2009) A homozygous CARD9 mutation in a family with susceptibility to fungal infections. *N Engl J Med,* **361** (18), 1727-35.
GOLD, E. S., et al. (1999) Dynamin 2 is required for phagocytosis in macrophages. *The Journal of experimental medicine,* **190** (12), 1849-1856.
GONÇALVES, B., et al. (2016) Vulvovaginal candidiasis: Epidemiology, microbiology and risk factors. *Crit Rev Microbiol,* **42** (6), 905-27.
GOW, N. A. and HUBE, B. (2012) Importance of the *Candida albicans* cell wall during commensalism and infection. *Curr Opin Microbiol,* **15** (4), 406-12.
GOW, N. A. R. and LENARDON, M. D. (2023) Architecture of the dynamic fungal cell wall. *Nature Reviews Microbiology,* **21** (4), 248-259.
GRAY, J. I. and FARBER, D. L. (2022) Tissue-Resident Immune Cells in Humans. *Annual Review of Immunology,* **40** (1), 195-220.
GRAY, M. W., et al. (1999) Mitochondrial evolution. *Science,* **283** (5407), 1476-81.
GREEN, D. R. and KROEMER, G. (2004) The Pathophysiology of Mitochondrial Cell Death. *Science,* **305** (5684), 626-629.
GROSS, O., et al. (2009) Syk kinase signalling couples to the Nlrp3 inflammasome for anti-fungal host defence. *Nature,* **459** (7245), 433-6.
GUDLAUGSSON, O., et al. (2003) Attributable mortality of nosocomial candidemia, revisited. *Clin Infect Dis,* **37** (9), 1172-7.

HA, Y. E., et al. (2015) Vancomycin blocks autophagy and induces interleukin-1β release in macrophages. *The Journal of Antibiotics,* **68** (2), 76-80.
HALL, R. A. (2015) Dressed to impress: impact of environmental adaptation on the *Candida albicans* cell wall. *Mol Microbiol,* **97** (1), 7-17.
HALL, R. A. and GOW, N. A. R. (2013) Mannosylation in *Candida albicans*: role in cell wall function and immune recognition. *Molecular Microbiology,* **90** (6), 1147-1161.
HAMMAD, N. M., et al. (2018) Mannose-Binding Lectin Gene Polymorphism and Its Association with Susceptibility to Recurrent Vulvovaginal Candidiasis. *Biomed Res Int,* **2018**, 7648152.
HARDISON, S. E. and BROWN, G. D. (2012) C-type lectin receptors orchestrate antifungal immunity. *Nat Immunol,* **13** (9), 817-22.
HE, W. T., et al. (2015) Gasdermin D is an executor of pyroptosis and required for interleukin-1β secretion. *Cell Res,* **25** (12), 1285-98.
HECKMANN, B. L., et al. (2017) LC3-Associated Phagocytosis and Inflammation. *J Mol Biol,* **429** (23), 3561-3576.
HEID, M. E., et al. (2013) Mitochondrial reactive oxygen species induces NLRP3-dependent lysosomal damage and inflammasome activation. *J Immunol,* **191** (10), 5230-8.
HENRIET, S., et al. (2013) Invasive fungal infections in patients with chronic granulomatous disease. *Adv Exp Med Biol,* **764**, 27-55.
HIENGRACH, P., et al. (2022a) Macrophage depletion alters bacterial gut microbiota partly through fungal overgrowth in feces that worsens cecal ligation and puncture sepsis mice. *Scientific Reports,* **12** (1), 9345.
HIENGRACH, P., et al. (2022b) Macrophage depletion alters bacterial gut microbiota partly through fungal overgrowth in feces that worsens cecal ligation and puncture sepsis mice. *Sci Rep,* **12** (1), 9345.
HISE, A. G., et al. (2009) An essential role for the NLRP3 inflammasome in host defense against the human fungal pathogen *Candida albicans*. *Cell Host Microbe,* **5** (5), 487-97.
HO, J., et al. (2019) Candidalysin activates innate epithelial immune responses via epidermal growth factor receptor. *Nature Communications,* **10** (1), 2297.
HOPE, W. W., et al. (2007) Effect of neutropenia and treatment delay on the response to antifungal agents in experimental disseminated candidiasis. *Antimicrobial agents and chemotherapy,* **51** (1), 285-295.
HOYER, L. L., et al. (2008) Discovering the secrets of the *Candida albicans* agglutinin-like sequence (ALS) gene family — a sticky pursuit. *Medical Mycology,* **46** (1), 1-15.
HUBE, B., et al. (2001) The role and relevance of phospholipase D1 during growth and dimorphism of *Candida albicans*. *Microbiology,* **147** (4), 879-889.
HUTCHINGS, M. I., et al. (2019) Antibiotics: past, present and future. *Curr Opin Microbiol,* **51**, 72-80.
IFRIM, D. C., et al. (2016) The Role of Dectin-2 for Host Defense Against Disseminated Candidiasis. *J Interferon Cytokine Res,* **36** (4), 267-76.
INGRAM, P. R., et al. (2008) Risk factors for nephrotoxicity associated with continuous vancomycin infusion in outpatient parenteral antibiotic therapy. *Journal of Antimicrobial Chemotherapy,* **62** (1), 168-171.
IVANOV, I. I., et al. (2009) Induction of Intestinal Th17 Cells by Segmented Filamentous Bacteria. *Cell,* **139** (3), 485-498.
JAE-CHEN, S., et al. (2015) Mechanism underlying renal failure caused by pathogenic *Candida albicans* infection. *Biomed Rep,* **3** (2), 179-182.
JAEGER, M., et al. (2016) Association of a variable number tandem repeat in the NLRP3 gene in women with susceptibility to RVVC. *Eur J Clin Microbiol Infect Dis,* **35** (5), 797-801.

JANKOWSKI, A., et al. (2002) Determinants of the phagosomal pH in neutrophils. *J Biol Chem,* **277** (8), 6059-66.
JAWALE, C. V., et al. (2020) Restoring glucose uptake rescues neutrophil dysfunction and protects against systemic fungal infection in mouse models of kidney disease. *Science Translational Medicine,* **12** (548), eaay5691.
JIANG, F., et al. (2000) Absence of cardiolipin in the crd1 null mutant results in decreased mitochondrial membrane potential and reduced mitochondrial function. *J Biol Chem,* **275** (29), 22387-94.
JIANG, L. and YAN, H. (2023) Cloning and biochemical characterization of a recombinant chitinase encoded by the CHT4 gene from Candida albicans. *Protein Expr Purif,* **211**, 106343.
JIANG, X., et al. (2019) Mitochondrial Toxicity of Azithromycin Results in Aerobic Glycolysis and DNA Damage of Human Mammary Epithelia and Fibroblasts. *Antibiotics (Basel),* **8** (3).
KALGHATGI, S., et al. (2013) Bactericidal antibiotics induce mitochondrial dysfunction and oxidative damage in Mammalian cells. *Sci Transl Med,* **5** (192), 192ra85.
KASPER, L., et al. (2018) The fungal peptide toxin Candidalysin activates the NLRP3 inflammasome and causes cytolysis in mononuclear phagocytes. *Nature Communications,* **9** (1), 4260.
KASPERKOVITZ, P. V., et al. (2011) Toll-like receptor 9 modulates macrophage antifungal effector function during innate recognition of Candida albicans and Saccharomyces cerevisiae. *Infect Immun,* **79** (12), 4858-67.
KESSENBROCK, K., et al. (2009) Netting neutrophils in autoimmune small-vessel vasculitis. *Nature Medicine,* **15** (6), 623-625.
KIRTI, Y. K. (2019) Prevalence of Oral Candidiasis in Indian HIV Sero-Positive Patients with CD4(+) Cell Count Correlation. *Indian J Otolaryngol Head Neck Surg,* **71** (1), 124-127.
KISAND, K., et al. (2010) Chronic mucocutaneous candidiasis in APECED or thymoma patients correlates with autoimmunity to Th17-associated cytokines. *J Exp Med,* **207** (2), 299-308.
KOENIS, D. S., et al. (2018) Nuclear Receptor Nur77 Limits the Macrophage Inflammatory Response through Transcriptional Reprogramming of Mitochondrial Metabolism. *Cell Rep,* **24** (8), 2127-2140.e7.
KOH, A. Y., et al. (2008) Mucosal damage and neutropenia are required for *Candida albicans* dissemination. *PLoS Pathog,* **4** (2), e35.
KÖHLER, J. R., et al. (2017) Fungi that Infect Humans. *Microbiol Spectr,* **5** (3).
KRYSAN, D. J., et al. (2014) Catching fire: *Candida albicans*, macrophages, and pyroptosis. *PLoS Pathog,* **10** (6), e1004139.
KUMWENDA, P., et al. (2022) Estrogen promotes innate immune evasion of Candida albicans through inactivation of the alternative complement system. *Cell Rep,* **38** (1), 110183.
LANE, N. and MARTIN, W. (2010) The energetics of genome complexity. *Nature,* **467** (7318), 929-34.
LEE, W. L., et al. (2003) Phagocytosis by neutrophils. *Microbes Infect,* **5** (14), 1299-306.
LEHMAN, H. K. and SEGAL, B. H. (2020) The role of neutrophils in host defense and disease. *Journal of Allergy and Clinical Immunology,* **145** (6), 1535-1544.
LEI, Y., et al. (2023) Antibiotics disrupt lipid metabolism in zebrafish (Danio rerio) larvae and 3T3-L1 preadipocytes. *Sci Total Environ,* **858** (Pt 1), 159755.
LEIBUNDGUT-LANDMANN, S., et al. (2007) Syk- and CARD9-dependent coupling of innate immunity to the induction of T helper cells that produce interleukin 17. *Nat Immunol,* **8** (6), 630-8.
LEONARDI, I., et al. (2018) CX3CR1(+) mononuclear phagocytes control immunity to intestinal fungi. *Science,* **359** (6372), 232-236.

LEVIN, R., et al. (2016) The life cycle of phagosomes: formation, maturation, and resolution. *Immunological Reviews,* **273** (1), 156-179.
LEWIS, K. (2001) Riddle of biofilm resistance. *Antimicrob Agents Chemother,* **45** (4), 999-1007.
LEWIS, L. E., et al. (2012) Stage Specific Assessment of *Candida albicans* Phagocytosis by Macrophages Identifies Cell Wall Composition and Morphogenesis as Key Determinants. *PLOS Pathogens,* **8** (3), e1002578.
LI, R., et al. (2017) Effects of oral florfenicol and azithromycin on gut microbiota and adipogenesis in mice. *PLoS ONE,* **12** (7).
LI, S. S., et al. (2018) Identification of the fungal ligand triggering cytotoxic PRR-mediated NK cell killing of Cryptococcus and *Candida*. *Nature Communications,* **9** (1), 751.
LI, W., et al. (2008) Activation of Nrf2-antioxidant signaling attenuates NFkappaB-inflammatory response and elicits apoptosis. *Biochem Pharmacol,* **76** (11), 1485-9.
LI, X., et al. (2011) The β-glucan receptor Dectin-1 activates the integrin Mac-1 in neutrophils via Vav protein signaling to promote *Candida albicans* clearance. *Cell Host Microbe,* **10** (6), 603-15.
LILES, W. C., et al. (1997) Granulocyte Colony-Stimulating Factor Administered In Vivo Augments Neutrophil-Mediated Activity against Opportunistic Fungal Pathogens. *The Journal of Infectious Diseases,* **175** (4), 1012-1015.
LIMPER, A. H., et al. (2017) Fungal infections in HIV/AIDS. *Lancet Infect Dis,* **17** (11), e334-e343.
LIN, H. C., et al. (2000) Erythromycin inhibits beta2-integrins (CD11b/CD18) expression, interleukin-8 release and intracellular oxidative metabolism in neutrophils. *Respir Med,* **94** (7), 654-60.
LIONAKIS, M. S., et al. (2023) Immune responses to human fungal pathogens and therapeutic prospects. *Nature Reviews Immunology*.
LIONAKIS, M. S., et al. (2012) Chemokine receptor Ccr1 drives neutrophil-mediated kidney immunopathology and mortality in invasive candidiasis. *PLoS Pathog,* **8** (8), e1002865.
LIONAKIS, M. S. and LEVITZ, S. M. (2018) Host Control of Fungal Infections: Lessons from Basic Studies and Human Cohorts. *Annu Rev Immunol,* **36**, 157-191.
LIONAKIS, M. S., et al. (2011) Organ-specific innate immune responses in a mouse model of invasive candidiasis. *J Innate Immun,* **3** (2), 180-99.
LO, H. J., et al. (1997) Nonfilamentous C. albicans mutants are avirulent. *Cell,* **90** (5), 939-49.
LOPES, J. P. and LIONAKIS, M. S. (2022) Pathogenesis and virulence of *Candida albicans*. *Virulence,* **13** (1), 89-121.
LUO, S., et al. (2023) Antibiotics administration alleviates the high fat diet-induced obesity through altering the lipid metabolism in young mice. *Lipids,* **58** (1), 19-32.
MAIONE, A., et al. (2022) Undesired Effect of Vancomycin Prolonged Treatment: Enhanced Biofilm Production of the Nosocomial Pathogen *Candida auris*. *Antibiotics,* **11** (12), 1771.
MALIK, P., et al. (2014) NET23/STING promotes chromatin compaction from the nuclear envelope. *PLoS One,* **9** (11), e111851.
MARIE-ANAÏS, F., et al. (2016) Dynamin-Actin Cross Talk Contributes to Phagosome Formation and Closure. *Traffic,* **17** (5), 487-499.
MARTÍNEZ-REYES, I. and CHANDEL, N. S. (2020) Mitochondrial TCA cycle metabolites control physiology and disease. *Nature Communications,* **11** (1), 102.
MATHÉ, L. and VAN DIJCK, P. (2013) Recent insights into *Candida albicans* biofilm resistance mechanisms. *Curr Genet,* **59** (4), 251-64.
MATSUDA, T., et al. (2002) Differences in Neutrophil Death Among β-Lactam Antibiotics After In Vitro Killing of Bacteria. *Shock,* **18** (1).

MAXSON, M. E., et al. (2018) Integrin-based diffusion barrier separates membrane domains enabling the formation of microbiostatic frustrated phagosomes. *Elife,* **7**.
MCNULTY, K. M., et al. (2005) Characterization of CD8+ T cells and microenvironment in oral lesions of human immunodeficiency virus-infected persons with oropharyngeal candidiasis. *Infect Immun,* **73** (6), 3659-67.
MEDICI, N. P. and DEL POETA, M. (2015) New insights on the development of fungal vaccines: from immunity to recent challenges. *Mem Inst Oswaldo Cruz,* **110** (8), 966-73.
MENG, X., et al. (2021) Dose-response association of early-life antibiotic exposure and subsequent overweight or obesity in children: A meta-analysis of prospective studies. *Obesity Reviews,* **22** (11), e13321.
MESSIAS, M. C. F., et al. (2018) Plasmalogen lipids: functional mechanism and their involvement in gastrointestinal cancer. *Lipids in Health and Disease,* **17** (1), 41.
METZLER, KATHLEEN D., et al. (2014) A Myeloperoxidase-Containing Complex Regulates Neutrophil Elastase Release and Actin Dynamics during NETosis. *Cell Reports,* **8** (3), 883-896.
MILLER, M. and SINGER, M. (2022) Do antibiotics cause mitochondrial and immune cell dysfunction? A literature review. *Journal of Antimicrobial Chemotherapy,* **77** (5), 1218-1227.
MILLSOP, J. W. and FAZEL, N. (2016) Oral candidiasis. *Clinics in Dermatology,* **34** (4), 487-494.
MIO, T., et al. (1997) Isolation of the Candida albicans homologs of Saccharomyces cerevisiae KRE6 and SKN1: expression and physiological function. *J Bacteriol,* **179** (7), 2363-72.
MISSIROLI, S., et al. (2020) The Role of Mitochondria in Inflammation: From Cancer to Neurodegenerative Disorders. *J Clin Med,* **9** (3).
MITCHELL, K. F., et al. (2015) Community participation in biofilm matrix assembly and function. *Proc Natl Acad Sci U S A,* **112** (13), 4092-7.
MOHAMMADI, F., et al. (2020) Relationship between antifungal susceptibility profile and virulence factors in *Candida albicans* isolated from nail specimens. *Revista da Sociedade Brasileira de Medicina Tropical,* **53**.
MORÁN, F. J., et al. (1991) Activity of vancomycin and teicoplanin against human polymorphonuclear leucocytes: a comparative study. *Journal of Antimicrobial Chemotherapy,* **28** (3), 415-418.
MOULLAN, N., et al. (2015) Tetracyclines Disturb Mitochondrial Function across Eukaryotic Models: A Call for Caution in Biomedical Research. *Cell Rep,* **10** (10), 1681-1691.
MOYES, D. L., et al. (2016) Candidalysin is a fungal peptide toxin critical for mucosal infection. *Nature,* **532** (7597), 64-8.
MUENSTER, S., et al. (2021) Vancomycin and daptomycin modulate the innate immune response in a murine model of LPS-induced sepsis. *Int J Immunopathol Pharmacol,* **35**, 20587384211031373.
MUKAREMERA, L., et al. (2017) *Candida albicans* Yeast, Pseudohyphal, and Hyphal Morphogenesis Differentially Affects Immune Recognition. *Frontiers in immunology,* **8**, 629-629.
MUÑOZ, J. F., et al. (2019) Coordinated host-pathogen transcriptional dynamics revealed using sorted subpopulations and single macrophages infected with Candida albicans. *Nature Communications,* **10** (1), 1607.
MUNRO, C. A., et al. (2007) The PKC, HOG and Ca2+ signalling pathways co-ordinately regulate chitin synthesis in Candida albicans. *Mol Microbiol,* **63** (5), 1399-413.
MURAD, A. M., et al. (2001) NRG1 represses yeast-hypha morphogenesis and hypha-specific gene expression in *Candida albicans*. *Embo j,* **20** (17), 4742-52.

MURCIANO, C., et al. (2012) Evaluation of the role of *Candida albicans* agglutinin-like sequence (Als) proteins in human oral epithelial cell interactions. *PLoS One,* **7** (3), e33362.
NAGLIK, J., et al. (2004) *Candida albicans* proteinases and host/pathogen interactions. *Cellular Microbiology,* **6** (10), 915-926.
NAGLIK, J. R., et al. (2019) Candidalysin: discovery and function in *Candida albicans* infections. *Curr Opin Microbiol,* **52**, 100-109.
NAGLIK, J. R., et al. (2017) *Candida albicans*-epithelial interactions and induction of mucosal innate immunity. *Curr Opin Microbiol,* **40**, 104-112.
NAGLIK, J. R., et al. (2008) Quantitative expression of the *Candida albicans* secreted aspartyl proteinase gene family in human oral and vaginal candidiasis. *Microbiology (Reading),* **154** (Pt 11), 3266-3280.
NAGLIK, J. R., et al. (2011) *Candida albicans* interactions with epithelial cells and mucosal immunity. *Microbes Infect,* **13** (12-13), 963-76.
NAU, R. and TAUBER, C. S. (2008) Immunomodulatory Properties of Antibiotics. *Current Molecular Pharmacology,* **1** (1), 68-79.
NAUCLÉR, C., et al. (2002) Signaling to localized degranulation in neutrophils adherent to immune complexes. *Journal of Leukocyte Biology,* **71** (4), 701-710.
NEGORO, P. E., et al. (2020) Spleen Tyrosine Kinase Is a Critical Regulator of Neutrophil Responses to *Candida Species*. *mBio,* **11** (3).
NETEA, M. G., et al. (2008) An integrated model of the recognition of *Candida albicans* by the innate immune system. *Nat Rev Microbiol,* **6** (1), 67-78.
NEWMEYER, D. D. and FERGUSON-MILLER, S. (2003) Mitochondria: releasing power for life and unleashing the machineries of death. *Cell,* **112** (4), 481-90.
NIEWERTH, M. and KORTING, H. C. (2001) Phospholipases of *Candida albicans*. *Mycoses,* **44** (9-10), 361-367.
NOBILE, C. J., et al. (2006) Critical role of Bcr1-dependent adhesins in C. albicans biofilm formation in vitro and in vivo. *PLoS Pathog,* **2** (7), e63.
NOBILE, C. J., et al. (2008) Complementary adhesin function in C. albicans biofilm formation. *Curr Biol,* **18** (14), 1017-24.
NOBLE, S. M., et al. (2017) *Candida albicans* cell-type switching and functional plasticity in the mammalian host. *Nature reviews. Microbiology,* **15** (2), 96-108.
NORDENFELT, P. and TAPPER, H. (2011) Phagosome dynamics during phagocytosis by neutrophils. *J Leukoc Biol,* **90** (2), 271-84.
O'TOOLE, G., et al. (2000) Biofilm formation as microbial development. *Annu Rev Microbiol,* **54**, 49-79.
ODDS, F. C., et al. (2003) Antifungal agents: mechanisms of action. *Trends Microbiol,* **11** (6), 272-9.
OKAI, B., et al. (2015) Rab14 regulates maturation of macrophage phagosomes containing the fungal pathogen Candida albicans and outcome of the host-pathogen interaction. *Infect Immun,* **83** (4), 1523-35.
OLIVIER, F. A. B., et al. (2022) The escape of *Candida albicans* from macrophages is enabled by the fungal toxin candidalysin and two host cell death pathways. *Cell Rep,* **40** (12), 111374.
ORANGE, J. S. and BALLAS, Z. K. (2006) Natural killer cells in human health and disease. *Clin Immunol,* **118** (1), 1-10.
ORLOVA, E. M., et al. (2017) Expanding the Phenotypic and Genotypic Landscape of Autoimmune Polyendocrine Syndrome Type 1. *J Clin Endocrinol Metab,* **102** (9), 3546-3556.
OSMAN, C., et al. (2011) Making heads or tails of phospholipids in mitochondria. *Journal of Cell Biology,* **192** (1), 7-16.

PAPAYANNOPOULOS, V., et al. (2010) Neutrophil elastase and myeloperoxidase regulate the formation of neutrophil extracellular traps. *Journal of Cell Biology,* **191** (3), 677-691.
PAPAYANNOPOULOS, V., et al. (2011) Neutrophil elastase enhances sputum solubilization in cystic fibrosis patients receiving DNase therapy. *PLoS One,* **6** (12), e28526.
PAPPAS, P. G., et al. (2018) Invasive candidiasis. *Nature Reviews Disease Primers,* **4** (1), 18026.
PASQUALE, T. R. and TAN, J. S. (2005) Nonantimicrobial Effects of Antibacterial Agents. *Clinical Infectious Diseases,* **40** (1), 127-135.
PERLROTH, J., et al. (2007) Nosocomial fungal infections: epidemiology, diagnosis, and treatment. *Med Mycol,* **45** (4), 321-46.
PFALLER, M. A., et al. (2010) Variation in Candida spp. distribution and antifungal resistance rates among bloodstream infection isolates by patient age: report from the SENTRY Antimicrobial Surveillance Program (2008-2009). *Diagn Microbiol Infect Dis,* **68** (3), 278-83.
PHAN, Q. T., et al. (2007) Als3 is a *Candida albicans* invasin that binds to cadherins and induces endocytosis by host cells. *PLoS Biol,* **5** (3), e64.
PIZZINO, G., et al. (2017) Oxidative Stress: Harms and Benefits for Human Health. *Oxidative Medicine and Cellular Longevity,* **2017**, 8416763.
PONNIAH, G., et al. (2007) State of differentiation defines buccal epithelial cell affinity for cross-linking to *Candida albicans* Hwp1. *Journal of Oral Pathology & Medicine,* **36** (8), 456-467.
POORE, T. S., et al. (2021) Fungal Infection and Inflammation in Cystic Fibrosis. *Pathogens,* **10** (5).
PREECHASUTH, K., et al. (2015) Cell wall protection by the Candida albicans class I chitin synthases. *Fungal Genet Biol,* **82**, 264-76.
PREVENTION, C. F. D. C. A. (2021) *Candida* infections of the mouth, throat, and esophagus.
PUEL, A., et al. (2011) Chronic mucocutaneous candidiasis in humans with inborn errors of interleukin-17 immunity. *Science,* **332** (6025), 65-8.
QIAN, Q., et al. (1994) Elimination of mouse splenic macrophages correlates with increased susceptibility to experimental disseminated candidiasis. *The Journal of Immunology,* **152** (10), 5000-5008.
QU, S., et al. (2019) Rutin attenuates vancomycin-induced renal tubular cell apoptosis via suppression of apoptosis, mitochondrial dysfunction, and oxidative stress. *Phytother Res,* **33** (8), 2056-2063.
RAMAGE, G., et al. (2006) *Candida* biofilms on implanted biomaterials: a clinically significant problem. *FEMS Yeast Res,* **6** (7), 979-86.
RAMY, N., et al. (2017) Role of Early Onset Neutropenia in Development of Candidemia in Premature Infants. *Journal of Tropical Pediatrics,* **64** (1), 51-59.
RICHARDSON, J. P., et al. (2018) Processing of *Candida albicans* Ece1p Is Critical for Candidalysin Maturation and Fungal Virulence. *mBio,* **9** (1).
RICOTTA, E. E., et al. (2021) Invasive Candidiasis Species Distribution and Trends, United States, 2009–2017. *The Journal of Infectious Diseases*, **223** (7), 1295-1302.
ROBERTS, R. L., et al. (2000) Dynamics of rab5 activation in endocytosis and phagocytosis. *J Leukoc Biol,* **68** (5), 627-32.
ROBINSON, M. J., et al. (2009) Dectin-2 is a Syk-coupled pattern recognition receptor crucial for Th17 responses to fungal infection. *Journal of Experimental Medicine,* **206** (9), 2037-2051.
ROMANI, L. (2004) Immunity to fungal infections. *Nature Reviews Immunology,* **4** (1), 11-24.
ROMANI, L., et al. (1997) Initiation of T-helper cell immunity to *Candida albicans* by IL-12: the role of neutrophils. *Chemical immunology,* **68**, 110-135.
ROSELLETTI, E., et al. (2017) NLRP3 inflammasome is a key player in human vulvovaginal disease caused by *Candida albicans*. *Sci Rep,* **7** (1), 17877.

ROSENTUL, D. C., et al. (2014) Gene polymorphisms in pattern recognition receptors and susceptibility to idiopathic recurrent vulvovaginal candidiasis. *Front Microbiol,* **5**, 483.
RUSSO, A., et al. (2015) Risk factors and clinical outcomes of candidaemia in patients treated for Clostridium difficile infection. *Clin Microbiol Infect,* **21** (5), 493.e1-4.
SACCÀ, S. C., et al. (2018) The Eye, Oxidative Damage and Polyunsaturated Fatty Acids. *Nutrients,* **10** (6).
SAIMAN, L., et al. (2003) Azithromycin in patients with cystic fibrosis chronically infected with Pseudomonas aeruginosa: a randomized controlled trial. *Jama,* **290** (13), 1749-56.
SAKAMOTO, Y., et al. (2017) Vancomycin induces reactive oxygen species-dependent apoptosis via mitochondrial cardiolipin peroxidation in renal tubular epithelial cells. *Eur J Pharmacol,* **800**, 48-56.
SALIMI, A., et al. (2016) Toxicity of macrolide antibiotics on isolated heart mitochondria: a justification for their cardiotoxic adverse effect. *Xenobiotica,* **46** (1), 82-93.
SALINAS-MUÑOZ, L., et al. (2018) Estrogen Receptor-Alpha (ESR1) Governs the Lower Female Reproductive Tract Vulnerability to *Candida albicans*. *Front Immunol,* **9**, 1033.
SAVILLE, S. P., et al. (2003) Engineered control of cell morphology in vivo reveals distinct roles for yeast and filamentous forms of *Candida albicans* during infection. *Eukaryot Cell,* **2** (5), 1053-60.
SCAGLIOLA, A., et al. (2020) The Tricarboxylic Acid Cycle at the Crossroad Between Cancer and Immunity. *Antioxid Redox Signal,* **32** (12), 834-852.
SCHALLER, M., et al. (2003) The secreted aspartyl proteinases Sap1 and Sap2 cause tissue damage in an in vitro model of vaginal candidiasis based on reconstituted human vaginal epithelium. *Infect Immun,* **71** (6), 3227-34.
SCHALLER, M., et al. (2005) Hydrolytic enzymes as virulence factors of *Candida albicans*. *Mycoses,* **48** (6), 365-377.
SCHMIDT, S., et al. (2017) Natural Killer Cells in Antifungal Immunity. *Frontiers in immunology,* **8**, 1623-1623.
SCOTT, N. A., et al. (2018) Antibiotics induce sustained dysregulation of intestinal T cell immunity by perturbing macrophage homeostasis. *Science Translational Medicine,* **10** (464), eaao4755.
SEO, A. Y., et al. (2010) New insights into the role of mitochondria in aging: mitochondrial dynamics and more. *J Cell Sci,* **123** (Pt 15), 2533-42.
SHEPPARD, D. C., et al. (2004) Functional and structural diversity in the Als protein family of *Candida albicans*. *J Biol Chem,* **279** (29), 30480-9.
SHERRINGTON, S. L., et al. (2017) Adaptation of *Candida albicans* to environmental pH induces cell wall remodelling and enhances innate immune recognition. *PLoS Pathog,* **13** (5), e1006403.
SHOPOVA, I. A., et al. (2020) Human Neutrophils Produce Antifungal Extracellular Vesicles against Aspergillus fumigatus. *mBio,* **11** (2).
SIEDLAR, M., et al. (1997) Vancomycin down-regulates lipopolysaccharide-induced tumour necrosis factor alpha (TNFα) production and TNFa-mRNA accumulation in human blood monocytes. *Immunopharmacology,* **35** (3), 265-271.
SINGH, A., et al. (2014) Oral candidiasis: An overview. *J Oral Maxillofac Pathol,* **18** (Suppl 1), S81-5.
SMITH, P. D., et al. (2011) Intestinal macrophages and response to microbial encroachment. *Mucosal Immunology,* **4** (1), 31-42.
SOBEL, J. D. (2007) Vulvovaginal candidosis. *Lancet,* **369** (9577), 1961-71.
STAIB, P., et al. (2000) Differential activation of a *Candida albicans* virulence gene family during infection. *Proc Natl Acad Sci U S A,* **97** (11), 6102-7.

STANISZEWSKA, M., et al. (2013) Cell wall carbohydrates content of pathogenic *Candida albicans* strain morphological forms. *Med Dosw Mikrobiol,* **65** (2), 119-28.
STRICKLAND, A. B. and SHI, M. (2021) Mechanisms of fungal dissemination. *Cellular and Molecular Life Sciences,* **78** (7), 3219-3238.
STROLLO, S., et al. (2016) Epidemiology of Hospitalizations Associated with Invasive Candidiasis, United States, 2002-2012(1). *Emerg Infect Dis,* **23** (1), 7-13.
STUEHLER, C., et al. (2015) Immune Reconstitution After Allogeneic Hematopoietic Stem Cell Transplantation and Association With Occurrence and Outcome of Invasive Aspergillosis. *J Infect Dis,* **212** (6), 959-67.
SUÁREZ-RIVERO, J. M., et al. (2021) Mitochondria and Antibiotics: For Good or for Evil?) *Biomolecules.*
SUN, D., et al. (2019) Fungal dissemination is limited by liver macrophage filtration of the blood. *Nat Commun,* **10** (1), 4566.
SUN, N. S., C. ZHANG, L. WU, X. YU, Y. YANG, X.YANG, C. ZHONG, C. GAO, Z. MIAO, W. YANG, Z. GAO, W. HU, L. WILLIAM, K. LIU, C. CHANG, Y. AND GAO, Y. (2021) Hepatic Krüppel-like factor 16 (KLF16) targets PPARα to improve steatohepatitis and insulin resistance. *Gut,* **70** (11), 2183-2195.
SVOBODA, E., et al. (2015) Secreted aspartic protease 2 of *Candida albicans* inactivates factor H and the macrophage factor H-receptors CR3 (CD11b/CD18) and CR4 (CD11c/CD18). *Immunol Lett,* **168** (1), 13-21.
SWIDERGALL, M., et al. (2019) Candidalysin Is Required for Neutrophil Recruitment and Virulence During Systemic *Candida albicans* Infection. *J Infect Dis,* **220** (9), 1477-1488.
TALAPKO, J., et al. (2021) *Candida albicans*-The Virulence Factors and Clinical Manifestations of Infection. *J Fungi (Basel),* **7** (2).
TAM, X. H. A. K. (2017) Association of vancomycin with lipid vesicles. *ADMET,* **5** (Vol. 5 No. 3 (2017)).
TAN, S. T., et al. (2020) Emerging roles of lysophospholipids in health and disease. *Progress in Lipid Research,* **80**, 101068.
TANAKA, T., et al. (2001) Different cleavage specificities of the dual catalytic domains in chitinase from the hyperthermophilic archaeon Thermococcus kodakaraensis KOD1. *J Biol Chem,* **276** (38), 35629-35.
TAWFIK, A. F. (1991) Effects of Vancomycin, Teicoplanin, Daptomycin and Coumermycin on Normal Immune Capabilities. *Journal of Chemotherapy,* **3** (4), 226-231.
THOMPSON, H. L. and WILTON, J. M. (1992) Interaction and intracellular killing of *Candida albicans* blastospores by human polymorphonuclear leucocytes, monocytes and monocyte-derived macrophages in aerobic and anaerobic conditions. *Clinical and experimental immunology,* **87** (2), 316-321.
TODA, G., et al. (2021) Preparation and culture of bone marrow-derived macrophages from mice for functional analysis. *STAR Protoc,* **2** (1), 100246.
TOMISHIGE, N., et al. (2003) Mutations that are synthetically lethal with a gas1Δ allele cause defects in the cell wall of Saccharomyces cerevisiae. *Molecular Genetics and Genomics,* **269** (4), 562-573.
TSUI, C., et al. (2016) Pathogenesis of *Candida albicans* biofilm. *Pathog Dis,* **74** (4), ftw018.
TUCEY, T. M., et al. (2018) Glucose Homeostasis Is Important for Immune Cell Viability during Candida Challenge and Host Survival of Systemic Fungal Infection. *Cell Metab,* **27** (5), 988-1006.e7.
TURNER, S. A. and BUTLER, G. (2014) The *Candida* pathogenic species complex. *Cold Spring Harb Perspect Med,* **4** (9), a019778.

TURRENS, J. F. (2003) Mitochondrial formation of reactive oxygen species. *J Physiol,* **552** (Pt 2), 335-44.
TWIG, G., et al. (2008) Fission and selective fusion govern mitochondrial segregation and elimination by autophagy. *Embo j,* **27** (2), 433-46.
UK, A. R. (2018) So what would happen if our antibiotics stopped working?
UPPULURI, P., et al. (2010) Dispersion as an important step in the *Candida albicans* biofilm developmental cycle. *PLoS Pathog,* **6** (3), e1000828.
URBAN, C. F. and BACKMAN, E. (2020) Eradicating, retaining, balancing, swarming, shuttling and dumping: a myriad of tasks for neutrophils during fungal infection. *Current Opinion in Microbiology,* **58**, 106-115.
UWAMAHORO, N., et al. (2014) The pathogen *Candida albicans* hijacks pyroptosis for escape from macrophages. *mBio,* **5** (2), e00003-14.
VAN DER VEEN, J. N., et al. (2017) The critical role of phosphatidylcholine and phosphatidylethanolamine metabolism in health and disease. *Biochimica et Biophysica Acta (BBA) - Biomembranes,* **1859** (9, Part B), 1558-1572.
VAN OPSTAL, E., et al. (2016) Vancomycin Treatment Alters Humoral Immunity and Intestinal Microbiota in an Aged Mouse Model of Clostridium difficile Infection. *J Infect Dis,* **214** (1), 130-9.
VANCE, J. E. (2015) Phospholipid Synthesis and Transport in Mammalian Cells. *Traffic,* **16** (1), 1-18.
VIEIRA, O. V., et al. (2003) Modulation of Rab5 and Rab7 recruitment to phagosomes by phosphatidylinositol 3-kinase. *Mol Cell Biol,* **23** (7), 2501-14.
VOIGT, J., et al. (2013) Human Natural Killer Cells Acting as Phagocytes Against *Candida albicans* and Mounting an Inflammatory Response That Modulates Neutrophil Antifungal Activity. *The Journal of Infectious Diseases,* **209** (4), 616-626.
VYLKOVA, S., et al. (2011) The fungal pathogen Candida albicans autoinduces hyphal morphogenesis by raising extracellular pH. *mBio,* **2** (3), e00055-11.
VYLKOVA, S. and LORENZ, M. C. (2014) Modulation of phagosomal pH by *Candida albicans* promotes hyphal morphogenesis and requires Stp2p, a regulator of amino acid transport. *PLoS pathogens,* **10** (3), e1003995-e1003995.
VYLKOVA, S. and LORENZ, M. C. (2017) Phagosomal Neutralization by the Fungal Pathogen *Candida albicans* Induces Macrophage Pyroptosis. *Infect Immun,* **85** (2).
WÄCHTLER, B., et al. (2011) From attachment to damage: defined genes of *Candida albicans* mediate adhesion, invasion and damage during interaction with oral epithelial cells. *PLoS One,* **6** (2), e17046.
WAGENER, J., et al. (2017) *Candida albicans* Chitin Increases Arginase-1 Activity in Human Macrophages, with an Impact on Macrophage Antimicrobial Functions. *mBio,* **8** (1), e01820-16.
WAGENER, J., et al. (2014) Fungal chitin dampens inflammation through IL-10 induction mediated by NOD2 and TLR9 activation. *PLoS Pathog,* **10** (4), e1004050.
WALKER, L. A., et al. (2013) Elevated chitin content reduces the susceptibility of Candida species to caspofungin. *Antimicrob Agents Chemother,* **57** (1), 146-54.
WAN ISMAIL, W. N. A., et al. (2020) The Economic Burden of Candidemia and Invasive Candidiasis: A Systematic Review. *Value Health Reg Issues,* **21**, 53-58.
WANG, X., et al. (2015) Antibiotic use and abuse: a threat to mitochondria and chloroplasts with impact on research, health, and environment. *Bioessays,* **37** (10), 1045-53.
WANG, X., et al. (2018) Impaired Specific Antifungal Immunity in CARD9-Deficient Patients with Phaeohyphomycosis. *J Invest Dermatol,* **138** (3), 607-617.

WARD, T. L., et al. (2017) Infant fungal communities: current knowledge and research opportunities. *BMC Medicine,* **15** (1), 30.
WARRIS, A. and BALLOU, E. R. (2019) Oxidative responses and fungal infection biology. *Semin Cell Dev Biol,* **89**, 34-46.
WATANAKUNAKORN, C. (1984) Mode of action and in-vitro activity of vancomycin. *Journal of Antimicrobial Chemotherapy,* **14** (suppl_D), 7-18.
WEINGARDEN, A. R., et al. (2013) Microbiota transplantation restores normal fecal bile acid composition in recurrent Clostridium difficile infection. *American Journal of Physiology-Gastrointestinal and Liver Physiology,* **306** (4), G310-G319.
WELLINGTON, M., et al. (2014) *Candida albicans* triggers NLRP3-mediated pyroptosis in macrophages. *Eukaryot Cell,* **13** (2), 329-40.
WESTMAN, J., et al. (2018) Candida albicans Hyphal Expansion Causes Phagosomal Membrane Damage and Luminal Alkalinization. *mBio,* **9** (5).
WESTMAN, J., et al. (2020) Lysosome Fusion Maintains Phagosome Integrity during Fungal Infection. *Cell Host & Microbe*.
WHITE, M. H. (1996) Is vulvovaginal candidiasis an AIDS-related illness? *Clin Infect Dis,* **22 Suppl 2**, S124-7.
WHITNEY, P. G., et al. (2014) Syk signaling in dendritic cells orchestrates innate resistance to systemic fungal infection. *PLoS Pathog,* **10** (7), e1004276.
WILLIAMS, D. and LEWIS, M. (2011) Pathogenesis and treatment of oral candidosis. *J Oral Microbiol,* **3**.
WILLIAMS, N. C. and O'NEILL, L. A. J. (2018) A Role for the Krebs Cycle Intermediate Citrate in Metabolic Reprogramming in Innate Immunity and Inflammation. *Frontiers in Immunology,* **9**.
WILSON, R. B., et al. (1999) Rapid hypothesis testing with *Candida albicans* through gene disruption with short homology regions. *J Bacteriol,* **181** (6), 1868-74.
WISPLINGHOFF, H., et al. (2004) Nosocomial bloodstream infections in US hospitals: analysis of 24,179 cases from a prospective nationwide surveillance study. *Clin Infect Dis,* **39** (3), 309-17.
WU, S. Y., et al. (2019) *Candida albicans* triggers NADPH oxidase-independent neutrophil extracellular traps through dectin-2. *PLoS Pathog,* **15** (11), e1008096.
XIAO, Y., et al. (2019) Different influences on mitochondrial function, oxidative stress and cytotoxicity of antibiotics on primary human neuron and cell lines. *J Biochem Mol Toxicol,* **33** (4), e22277.
XU, S., et al. (2020) TLR4 promotes microglial pyroptosis via lncRNA-F630028O10Rik by activating PI3K/AKT pathway after spinal cord injury. *Cell Death & Disease,* **11** (8), 693.
YAMAMOTO, H., et al. (2016) Amla Enhances Mitochondrial Spare Respiratory Capacity by Increasing Mitochondrial Biogenesis and Antioxidant Systems in a Murine Skeletal Muscle Cell Line. *Oxid Med Cell Longev,* **2016**, 1735841.
YAMAMOTO, Y., et al. (1997) Involvement of mannose receptor in cytokine interleukin-1beta (IL-1beta), IL-6, and granulocyte-macrophage colony-stimulating factor responses, but not in chemokine macrophage inflammatory protein 1beta (MIP-1beta), MIP-2, and KC responses, caused by attachment of *Candida albicans* to macrophages. *Infect Immun,* **65** (3), 1077-82.
YANO, J., et al. (2017) Vaginal Heparan Sulfate Linked to Neutrophil Dysfunction in the Acute Inflammatory Response Associated with Experimental Vulvovaginal Candidiasis. *mBio,* **8** (2).
YANO, J., et al. (2018) Novel Mechanism behind the Immunopathogenesis of Vulvovaginal Candidiasis: "Neutrophil Anergy". *Infect Immun,* **86** (3).

ZHAI, B., et al. (2020) High-resolution mycobiota analysis reveals dynamic intestinal translocation preceding invasive candidiasis. *Nature Medicine,* **26** (1), 59-64.
ZHANG, J., et al. (2021) Influences of sex, rhythm and generation on the obesogenic potential of erythromycin to Drosophila melanogaster. *Science of The Total Environment,* **771**, 145315.
ZHOU, R., et al. (2010) Thioredoxin-interacting protein links oxidative stress to inflammasome activation. *Nature Immunology,* **11** (2), 136-140.
ZHU, W. and FILLER, S. G. (2010) Interactions of *Candida albicans* with epithelial cells. *Cellular microbiology,* **12** (3), 273-282.
ZHU, W., et al. (2012) EGFR and HER2 receptor kinase signaling mediate epithelial cell invasion by *Candida albicans* during oropharyngeal infection. *Proceedings of the National Academy of Sciences,* **109** (35), 14194-14199.
ZITVOGEL, L., et al. (2012) Inflammasomes in carcinogenesis and anticancer immune responses. *Nat Immunol,* **13** (4), 343-51.
ZOROVA, L. D., et al. (2018) Mitochondrial membrane potential. *Anal Biochem,* **552**, 50-59.

8 APPENDIX 1. LIST OF LIPID METABOLITES

Idx	Assay	p.value	Fold change		Post-hoc analysis p-value		Post-hoc analysis statistically significant (p<0.05)		compound_name
			V.Unstim / C.Unstim	V.Stim/ C.Stim	V.Unstim / C.Unstim	V.Stim/ C.Stim	V.Unstim / C.Unstim	V.Stim / C.Stim	
M659T24	HILIC negative	8.96E-05	0.74	4.89	0.219	0.000	Yes	No	Medicagenic acid 3-O-b-D-glucuronide; 26-Glucosyl-1,3,11,22-tetrahydroxyergosta-5,24-dien-26-oate
M315T263	HILIC positive	0.00043546	0.60	0.11	0.212	0.015	No	Yes	Decanoylcarnitine
M283T34	HILIC negative	0.0016981	0.70	1.01	0.026	0.938	Yes	No	hydroxyoctadecanal; Nonenol; 16-Methylheptadecanoic acid; Stearic acid
M947T478	Lipids negative	0.0019541	0.58	0.65	0.100	0.021	Yes	No	PC(40:6); PS(44:8)
M545T414	HILIC negative	0.0054257	6.10	0.86	0.000	0.906	Yes	No	Daidzein 4'-glucuronide-7-sulfate; Daidzein 7-glucuronide-4'-sulfate

M803T469	Lipids negative	0.0074405	1.89	0.75	0.088	0.294	No	No	PE(36:2); PE(36:1); PC(34:2); PS(37:1)
M251T40_1	HILIC negative	0.0098256	0.66	0.98	0.003	0.920	No	No	Methyl 2-propenyl pentasulfide
M205T557	HILIC positive	0.013766	2.28	1.32	0.031	0.037	Yes	Yes	6-Methylmercaptopurine
M526T122	Lipids negative	0.017044	0.54	0.66	0.014	0.124	Yes	No	LysoPC(15:0); LysoPC(14:0); LysoPE(18:0)
M394T24	HILIC negative	0.017263	0.70	1.79	0.103	0.102	No	No	Unidentified
M393T32	HILIC negative	0.017472	0.65	1.31	0.065	0.162	No	No	17-Hydroxypregnenolone sulfate
M166T392	HILIC negative	0.018932	1.11	2.17	0.405	0.128	Yes	No	2-Keto-glutaramic acid; Succinimide
M137T74	HILIC negative	0.020654	0.65	0.53	0.300	0.260	No	Yes	Nicotinamide N-oxide; Urocanic acid; etc.
M435T26	HILIC positive	0.021408	0.27	0.18	0.185	0.023	No	Yes	3a,7a,12a-Trihydroxy-5b-cholestan-26-al; etc.
M554T200	Lipids negative	0.023375	0.59	0.66	0.022	0.095	Yes	No	LysoPC(16:0); LysoPE(20:0); LysoPC(17:0)
M540T157	Lipids negative	0.024496	0.67	0.62	0.040	0.076	No	Yes	LysoPC(16:0); LysoPE(18:0); LysoPC(15:0)
M261T74	HILIC negative	0.025358	0.47	0.26	0.027	0.030	No	No	3-Methylazelaic acid; Heptylmalonic acid; Sebacic acid; etc.

M266T308	HILIC positive	0.025458	0.76	0.84	0.047	0.166	No	No	Benzoylcarnitine; ethyl indole-3-lactate; hexadienoic acid; etc.
M820T498	Lipids negative	0.026102	0.73	0.86	0.234	0.526	Yes	No	Hydroxytetradecanoyl carnitine; TG(47:5)
M747T438	Lipids negative	0.027352	0.64	0.88	0.004	0.403	No	No	PE(P-18:1/18:1); PE(P-16:0/20:2); PE(20:2/P-16:0); PE(18:2/P-18:0)
M253T37	HILIC positive	0.029174	1.76	0.89	0.393	0.372	No	No	6-hydroxyheptyl 4-hydroxybenzoate; Ethyl 2-benzylacetoacetate; Benzyl acetoacetate
M393T26_1	HILIC positive	0.029746	1.57	1.37	0.335	0.338	No	No	TG(47:4); DG(22:0); Tetracosatetraenoic acid; TG(45:1)
M351T442	HILIC positive	0.030045	3.52	1.05	0.022	0.906	No	No	Unidentified
M508T244	Lipids negative	0.032122	0.61	0.73	0.102	0.142	No	No	LysoPE(20:0); LysoPC(17:0)
M811T299	HILIC negative	0.033115	1.74	1.23	0.680	0.548	Yes	No	PS(38:4); PE(38:5); PE(37:5); PE(38:5); PS(36:1)
M609T157	Lipids negative	0.033232	0.57	0.74	0.025	0.094	No	No	Vitamin D2 3-glucuronide
M398T70	HILIC positive	0.034442	1.28	5.05	0.712	0.059	No	Yes	Behenoylglycine; hydroxydocosanoic acid; Alpha-Linoleoylcholine
M219T49	HILIC negative	0.03563	0.37	2.55	0.062	0.313	Yes	No	6-hydroxy-2H-1,3-benzodioxole-5-carboxylic acid; 2-(2,4-dihydroxyphenyl)-2-oxoacetic acid

M791T477	Lipids negative	0.036466	0.79	0.78	0.185	0.401	No	No	PC(32:1); PE(36:1); PE(35:1); PS(36:0)
M297T347	HILIC positive	0.038888	0.73	0.61	0.319	0.096	Yes	No	(R)-2,3-Dihydroxy-3-methylvalerate; Glycerol 1-propanoate; etc.
M880T478	Lipids negative	0.039029	0.60	0.85	0.062	0.214	No	No	SM(d18:1/23:0); SM(d17:1/24:0); TG(46:6)
M188T359	HILIC positive	0.039542	0.28	1.73	0.018	0.499	Yes	No	Triethanolamine; N-Methylethanolaminium phosphate; etc.
M287T29	HILIC negative	0.039865	1.16	0.37	0.866	0.149	Yes	No	dihydroxytridecadienoic acid; hexadiendiol; hydroxy-oxotridecenoic acid; etc.
M433T28_2	HILIC positive	0.041828	0.44	0.59	0.069	0.360	Yes	No	17-Hydroxyandrostane-3-glucuronide
M676T157	Lipids negative	0.042555	0.60	0.70	0.024	0.140	No	Yes	Unidentified
M858T496	Lipids negative	0.04265	0.69	0.73	0.147	0.032	No	No	TG(44:3); TG(50:7)
M469T24	HILIC negative	0.044078	0.54	0.25	0.434	0.238	No	No	Ceanothine C
M283T392_1	HILIC positive	0.045366	1.85	0.61	0.560	0.401	Yes	No	Glycerol tripropanoate; Folic acid; Ethyl acetoacetate; Oxohexanoic acid; etc.
M387T42	HILIC positive	0.046437	0.38	0.39	0.033	0.105	No	Yes	Unidentified
M336T554	HILIC positive	0.0057676	3.48	1.09	0.000	0.641	No	No	Unidentified

M93T281	HILIC negative	0.0082424	1.79	0.91	0.115	0.435	No	Yes	Dimethoxyflavone; 5-Hydroxy-7-methoxy-6-methylflavone; etc.
M250T40	HILIC negative	0.0083358	0.70	0.90	0.041	0.521	No	No	Unidentified
M298T32	HILIC negative	0.0089864	0.60	2.09	0.118	0.222	No	No	Isoleucyl-Tryptophan; Leucyl-Tryptophan
M1359T465	Lipids negative	0.0092117	0.80	0.97	0.246	0.874	Yes	Yes	Unidentified
M105T507_1	HILIC positive	0.010559	1.99	1.10	0.110	0.691	No	No	Unidentified
M451T41	HILIC positive	0.013129	0.51	0.16	0.098	0.115	No	No	Unidentified
M287T259	HILIC negative	0.013633	2.63	1.57	0.590	0.553	Yes	No	Unidentified
M186T384	HILIC negative	0.015346	1.91	1.92	0.068	0.028	No	No	Unidentified
M392T479	HILIC positive	0.016548	1.59	0.91	0.061	0.704	No	No	Unidentified
M1021T465	Lipids negative	0.016689	0.85	1.08	0.661	0.812	No	No	CDP-DG(36:4)
M295T25	HILIC negative	0.016978	0.49	2.72	0.123	0.109	No	No	Unidentified
M242T256	HILIC negative	0.017148	2.46	0.55	0.530	0.114	No	No	Unidentified

M1075T469	Lipids negative	0.018484	2.31	0.97	0.257	0.945	No	No	Unidentified
M297T40	HILIC negative	0.018549	0.61	1.07	0.041	0.722	No	No	Unidentified
M208T35	HILIC negative	0.019088	0.54	2.11	0.081	0.098	Yes	No	Unidentified
M283T25_2	HILIC negative	0.021588	0.58	2.39	0.109	0.070	Yes	No	Unidentified
M199T286	HILIC positive	0.022973	0.44	0.60	0.089	0.048	No	No	N-Acetylputrescine; Pregnenolone sulfate; etc.
M360T435	HILIC positive	0.022988	0.72	3.44	0.471	0.015	No	No	N-trans-p-Coumaroyloctopamine; N-cis-Caffeoyltyramine; Arginylcysteine
M179T37	HILIC positive	0.024574	0.49	0.97	0.110	0.805	No	Yes	5-Phenylvaleric acid; 4-(1-Methylethenyl)benzaldehyde; etc.
M444T27_1	HILIC positive	0.024702	0.51	0.35	0.166	0.116	Yes	No	Unidentified
M598T157	Lipids negative	0.024809	0.49	0.81	0.026	0.303	No	Yes	Unidentified
M569T244	Lipids negative	0.026144	0.66	0.66	0.023	0.087	No	No	DG(24:0)
M758T254	HILIC positive	0.02792	6.27	1.17	0.308	0.783	No	No	PG(34:0); PE(P-18:1/14:0); PE(14:1/P-18:0); PE(16:1/P-16:0)
M321T26	HILIC negative	0.03002	0.94	0.40	0.733	0.036	No	No	Unidentified

M352T27_1	HILIC positive	0.031086	0.63	1.04	0.440	0.912	Yes	No	13,14-dihydro-15-oxolipoxin A4; 8-isoprostaglandin E2; etc.
M134T49	HILIC negative	0.031193	0.45	1.40	0.081	0.272	No	No	Hypothiocyanite; 3-Sulfinoalanine
M772T244	Lipids negative	0.032086	0.56	0.73	0.027	0.176	Yes	No	Unidentified
M429T79	HILIC positive	0.03572	1.46	0.56	0.622	0.531	No	Yes	Arachisprenol 12
M298T494	HILIC positive	0.036888	1.22	0.70	0.228	0.315	Yes	No	1-Methyl-3-(2-thiazolyl)-1H-indole
M210T348	HILIC positive	0.037051	0.24	0.14	0.128	0.016	No	No	Benzenepropanenitrile; Benzyl thiocyanate; etc.
M418T31	HILIC negative	0.038641	0.51	2.82	0.143	0.142	No	No	Glaudine
M358T507	HILIC positive	0.040544	1.30	1.01	0.147	0.944	Yes	No	2,5-diamino-N-(2-sulfoethyl)-3-(sulfooxy)pentanimidic acid
M567T174	Lipids negative	0.040881	0.68	0.67	0.064	0.083	No	No	Unidentified
M246T40_1	HILIC negative	0.042458	0.63	0.61	0.069	0.354	No	No	Unidentified
M262T495	HILIC positive	0.042491	2.99	1.62	0.023	0.193	Yes	No	Nb-trans-p-Coumaroylserotonin glucoside; etc.
M634T174	Lipids negative	0.043	0.53	0.91	0.042	0.807	Yes	Yes	LysoPC(18:1)

M131T281	HILIC negative	0.043641	1.48	1.01	0.408	0.926	No	No	2-Thiophenecarboxaldehyde
M251T90	HILIC positive	0.045703	0.38	0.70	0.054	0.116	Yes	No	Methyl 3-(methylthio)propanoate; etc.
M238T52	HILIC positive	0.046926	0.41	0.44	0.107	0.060	No	Yes	Unidentified
M517T25_2	HILIC positive	0.049853	1.97	0.97	0.203	0.912	Yes	No	DG(31:1); Cholesteryl caproate
M377T256	HILIC negative	0.042051	0.55	0.56	0.072	0.185	No	No	Unidentified
M448T47	HILIC positive	0.0019992	0.23	0.79	0.029	0.090	Yes	No	N-Nonanoylglycine; PE(38:2)
M359T38	HILIC positive	0.040177	0.33	0.49	0.058	0.036	No	Yes	Unidentified
M1057T464	Lipids negative	0.035126	0.76	1.00	0.212	0.999	No	No	Unidentified
M393T524	HILIC positive	0.025126	2.36	1.00	0.043	0.992	Yes	No	Unidentified
M415T73	HILIC positive	0.03796	0.38	0.32	0.059	0.069	No	No	PGP(34:1)
M316T263	HILIC positive	0.011838	0.50	0.31	0.145	0.114	No	No	DG(35:1); DG(37:4)
M492T27	HILIC positive	0.027974	0.47	1.14	0.153	0.680	No	No	PGP(40:7); Dethiobiotin

M304T34	HILIC negative	0.029742	0.75	0.43	0.251	0.458	No	No	Unidentified
M104T350	HILIC positive	0.024423	0.54	0.29	0.273	0.058	No	No	Asparaginylglycine; Glycylglycylglycine
M259T63	HILIC positive	0.033163	0.02	1.10	0.184	0.874	No	No	gamma-L-Glutamyl-L-pipecolic acid; etc.
M576T313	HILIC positive	0.030288	2.32	1.18	0.464	0.775	No	No	DG(34:2); TG(34:0)
M615T361	Lipids negative	0.040034	0.63	0.75	0.118	0.569	No	No	Stercobilinogen
M625T413	Lipids negative	0.026958	0.77	0.81	0.405	0.256	No	No	Ganglioside GM3 (d18:0/23:0)
M306T68	HILIC negative	0.046028	1.14	0.31	0.819	0.290	No	No	Unidentified
M429T59	HILIC positive	0.0088829	0.18	2.18	0.299	0.082	No	No	Unidentified
M688T465	Lipids negative	0.043409	1.00	1.47	0.996	0.219	No	No	N-pentadecanoylsphingosine-1-phosphocholine; etc.
M367T23	HILIC negative	0.010463	0.63	3.00	0.311	0.098	No	No	Unidentified
M1001T22	HILIC positive	0.013764	0.70	3.05	0.523	0.135	No	No	Unidentified
M855T45	HILIC positive	0.0018765	0.65	22.51	0.585	0.074	No	No	Unidentified

M823T251	HILIC positive	0.011602	1.25	2.75	0.590	0.064	No	No	PE(22:4/P-18:1); PE(22:5/P-18:0); PE(P-18:0/22:5); PE(P-18:1/22:4)
M480T49	HILIC positive	0.031153	0.80	4.53	0.689	0.105	No	No	(sulfooxy)tetracosenoic acid; hydroxytridecadienoic acid; etc.
M479T421	Lipids negative	0.030001	0.82	0.83	0.436	0.197	No	No	TG(18:0); gamma-Tocopherol hydroquinone; etc.
M1002T22	HILIC positive	0.026683	0.68	3.30	0.523	0.122	No	No	3(S)-Hydroxy-2(S),6-dimethyl-heptanoyl-CoA; 3-Oxo-OPC4-CoA
M404T524	HILIC positive	0.0083755	2.88	0.81	0.189	0.551	No	No	3,5-Dihydroxyphenylvaleric acid glucuronide; etc.
M203T523	HILIC positive	0.038603	1.71	0.71	0.262	0.441	No	No	Asymmetric dimethylarginine; Symmetric dimethylarginine; Glycyl-Lysine
M735T451	Lipids negative	0.043683	0.92	1.14	0.324	0.681	No	No	PC(O-16:1/16:1); PC(14:0/P-18:1); PC(14:1/P-18:0); PC(16:1/P-16:0)
M503T51	HILIC positive	0.021903	0.93	4.68	0.886	0.096	No	No	Unidentified
M878T456	Lipids negative	0.029193	1.12	0.85	0.695	0.612	No	No	SM(d18:2/23:0); SM(d17:1/24:1)
M415T75	HILIC positive	0.042161	0.52	3.41	0.400	0.267	No	No	Quinine sulfate; (sulfooxy)tetradecanedioic acid; etc.
M1004T22	HILIC positive	0.047798	0.52	3.25	0.383	0.208	No	No	Undecanoyl-CoA
M1126T464	Lipids negative	0.046392	1.45	0.83	0.200	0.582	No	No	Unidentified

M209T247	HILIC negative	0.039264	2.22	1.77	0.647	0.415	No	No	Unidentified
M364T51	HILIC positive	0.012434	2.32	0.84	0.080	0.676	No	No	Unidentified
M553T410	HILIC negative	0.047851	0.53	2.15	0.256	0.311	No	No	Kaempferol 3-(2"-acetylrhamnoside); 6"-O-Acetylgenistin; etc.
M673T24	HILIC negative	0.045917	0.76	2.47	0.107	0.981	No	No	Allodesmosine; Ganglioside GT2 (d18:0/22:0)
M71T281	HILIC negative	0.045993	1.79	1.08	0.066	0.665	No	No	Chloride ion; Phosphine
M321T35	Lipids negative	0.008431	0.74	1.09	0.209	0.773	No	No	Unidentified
M755T251	HILIC positive	0.038234	0.71	1.63	0.411	0.651	No	No	DG(42:9); PE(P-18:1/18:4); PE(P-16:0/20:5); PE(37:4); PC(34:4); etc.
M412T24	HILIC negative	0.012635	0.58	4.13	0.310	0.506	No	No	Ochratoxin C
M292T558	HILIC positive	0.047295	1.99	1.10	0.093	0.712	No	No	Unidentified
M301T504	HILIC negative	0.042612	3.89	1.22	0.313	0.611	No	No	(S)-Pterosin K; {3-[(2-methylpropanoyl)oxy]-1-phenylpropoxy}sulfonic acid; etc.
M236T507	HILIC positive	0.046103	1.09	1.98	0.683	0.064	No	No	4-Hydroxy-1H-indole-3-acetonitrile; L-Histidine trimethylbetaine; etc.

M704T244	Lipids negative	0.039991	0.74	0.73	0.133	0.214	No	No	Unidentified
M172T271	HILIC positive	0.027613	0.34	0.26	0.053	0.203	No	No	Dimethylurea